2019-11

Minocycline treatment timing and its influence on serotonin expression following spinal cord injury

Flood, Jennifer Margaret

UNIVERSITY OF CALGARY

Minocycline treatment timing and its influence on serotonin expression following spinal cord injury

by

Jennifer Margaret Flood

A THESIS

SUBMITTED TO THE FACULTY OF GRADUATE STUDIES

IN PARTIAL FULFILLMENT OF THE REQUIREMENTS FOR THE

DEGREE OF MASTER OF SCIENCE

GRADUATE PROGRAM IN NEUROSCIENCE

CALGARY, ALBERTA

NOVEMBER, 2019

Abstract

The effects of incomplete traumatic spinal cord injury (SCI) can be partly reversed by the plasticity of local and spared descending projections. A promising window of plasticity occurs for a number of weeks following injury and involves the control of neuroinflammatory processes. The FDA-approved drug, minocycline, is a promising drug for treating SCI since it decreases microglia activity, reduces macrophage activity, and generally provides neuroprotective properties. In this thesis I established a timeline of injury, looking at both serotonin (5-HT) and microglia/macrophage (Iba-1) immunoreactivity (ir), and I targeted a time point before a significant reduction of descending serotonergic fibers, in the form of 5-HTir, took place (i.e. 1-week). I found that the administration of minocycline increased 5-HTir caudal and ipsilateral to the lesion, compared to shams and controls. Using the selected time point, 1-week post-SCI, I administered minocycline and found a decrease in lesion size and an increase of 5-HTir both caudal and ipsilateral to the injury as well as rostral and contralateral to the injury. In this thesis, I provide evidence that minocycline impacts 5-HT expression when administered acutely and one week following SCI. These data suggest that the timing of minocycline treatment influences the neuroprotective properties previously reported and also influences descending 5-HT expression post-SCI.

Acknowledgments

This thesis would not be possible without the guidance and support by everyone who provided me assistance during my graduate program.

I am grateful to my supervisor, Dr. Patrick Whelan, who has both guided and supported me throughout this project. The personal growth that I have experienced during my masters has not only promoted my confidence as a researcher but extends into every aspect of my life. I am thankful for the opportunity to work under Dr. Whelan and grateful for the countless hours spent working together. I would like to thank my committee members, Dr. Shalina Ousman and Dr. Tuan Trang, who generously made the time to accommodate my committee meetings and provided me with meaningful feedback, insight into my project and the support necessary to complete my project. I am also grateful for my external examiner, Dr. Steven Casha, who has taken the time to both read my thesis and take part in my defense. I would also like to thank Dr. Charlie Kwok for her instrumental input in project design, countless meetings, and support. This research could not be completed without the funding from Spinal Cord, Nerve Injury and Pain, the Hotchkiss Brain Institute and the Faculty of Veterinary Medicine at the University of Calgary.

Thank you to the current and past members of the Whelan lab, who have supported me throughout graduate school and who have been instrumental in my success. The support and friendship that has been extended to me is not unappreciated. I would like to specifically thank Michelle Tran for the friendship and support that went above and beyond. I want to extend my gratitude to Lesley Towill for her administrative support that does not go unnoticed. Lastly, I would like to thank my family and friends who continually support me and provide me with encouragement and backing throughout my studies.

Table of Contents

Abstract ii
Acknowledgments iii
Table of Contents iv
List of Figures and Illustrations vi
List of Symbols, Abbreviations and Nomenclature vii

CHAPTER 1: INTRODUCTION 1
Overview 1
1.1 Spinal cord 1
1.2 Spinal cord injury 2
1.3 Traumatic SCI 3
1.4 Serotonin 4
1.5 Serotonin receptors 5
1.6 Serotonin and SCI 7
1.7 Minocycline 8
1.8 Pathophysiological description of SCI 9
1.9 Microglia 11
1.10 Microglia and SCI 12
1.11 Research statement 13
1.12 Research objectives 14
1.13 Spinal cord injury time-course assessment and analysis of serotonin and microglia expression 14
1.14 Examine the role of minocycline treatment on 5-HTir and Iba-1ir 1-hour post-SCI 15
1.15 Examine the role of minocycline treatment on 5-HTir and Iba-1ir 7 days post-SCI and compare to 1-hour post-SCI administration 15

CHAPTER 2: METHODS 18
2.1 Animals 18
2.2 Spinal cord hemisection injury 18
2.3 Pharmacological treatment of animals day 21 post-SCI 19
2.4 Tissue processing 20
2.5 Analysis and statistics 21

CHAPTER 3: TIME-COURSE RESULTS 23
Overview 23
3.1 Spinal cord injury time-course assessment of serotonin immunoreactivity 23
3.2 Spinal cord injury time-course assessment of microglia/macrophage immunoreactivity 25
3.3 Spinal cord injury time-course summary of significant findings 28

CHAPTER 4: TREATMENT RESULTS 30
4.1 Minocycline treatment did not change 5-HT but reduced Iba-1 expression at the lesion site 30
4.2 Minocycline treatment results in a difference of 5-HT expression and reduces Iba-1

expression rostral and ipsilateral to the injury 33
4.3 Minocycline treatment increases caudal 5-HT and decreases Iba-1 mean expression intensity ipsilateral to injury 36
4.4 Expression of serotonin and microglia/macrophage surrounding motoneurons post-SCI after minocycline treatments 38
.
CHAPTER 5: DISCUSSION 59
5.1 Overview of findings 59
5.2 Changes in 5-HTir and Iba-1ir after SCI 60
5.3 Impact of minocycline treatment 1-hour post-SCI 62
5.4 Impact of minocycline treatment 7 days post-SCI 65
5.5 Potential impact of latent minocycline treatment 67
5.6 Significance 71

REFERENCES 73

List of Figures and Illustrations

Figure 1.1 Details of a transverse section of the spinal cord 16
Figure 1.2 Basic synthesis of serotonin (5-HT: 5-hydroxytryptamine) 17
Table 1.1 Serotonin (5-HT) family receptor subtypes, G-protein association, and effect or pathways 17
Figure 2.1 Timeline schematic of days selected for processing SCI timeline 22
Figure 2.2 Timeline schematic of treatment paradigms used to test 5-HTir changes after minocycline treatment 22
Figure 3.1 Serotonin and microglia/macrophage positive immunostaining in the brainstem 39
Figure 3.2 Serotonin decreases ipsilateral to the injury site when compared to shams 40
Figure 3.3 Serotonin expression is decreased at the lesion site following SCI 41
Figure 3.4 Microglia/macrophage expression is significantly changed ipsilateral and contralateral to the lesion 41
Figure 3.5 Serotonin expression decreases ipsilaterally and increases contralaterally rostral to the lesion site following SCI 42
Figure 3.6 Rostral to the injury, an increase of microglia/macrophage is observed ipsilaterally 43
Figure 3.7 Serotonin expression decreases caudal to the lesion site following SCI 44
Figure 3.8 Microglia/macrophage expression increases at the lesion site following SCI 45
Figure 3.9 Summary of significant time-course MPIA data for 5-HTir and Iba-1ir 46
Figure 4.1 Serotonin expression decreases and microglia/macrophage expression increases at the lesion when treated with minocycline 47
Figure 4.2 Serotonin and microglia/macrophage expression decreases at the lesion site 48
Figure 4.3 Microglia/macrophage and serotonin expression decreases rostral to the lesion site with minocycline treatment 49
Figure 4.4 Minocycline administration changes serotonin expression rostral to the injury decreasing microglia/microglia expression ipsilaterally 50
Figure 4.5 Serotonin expression increases caudal to the lesion site with minocycline 51
Figure 4.6 Minocycline administration increases expression of serotonin and reduces microglia/macrophage expression caudal to the lesion 52
Figure 4.7 Minocycline treatment reduces serotonin and microglia/macrophage expression surrounding motoneurons at the lesion site contralaterally 53
Figure 4.8 Minocycline treatment reduces microglia/macrophage expression surrounding motoneurons rostral to the lesion site 54
Figure 4.9 Minocycline treatment increases serotonin expression surrounding motoneurons caudal to the lesion site 55
Figure 4.10 Summary comparing minocycline treatment to saline treatment MPIA 56
Figure 4.11 Summary of minocycline administration 7 days versus 1-hour post-SCI 57
Figure 4.12 Lesion size determination analysis 58

List of Symbols, Abbreviations, and Nomenclature

Symbol	Definition
5-HT	five - hydroxytryptamine
5-HTP	five - hydroxytryptophan
α	alpha
AADC	amino acid decarboxylase
ANOVA	analysis of variance
ATP	adenosine triphosphate
β	beta
BBB	blood brain barrier
Ca PIC	calcium persistent inward currents
CNS	central nervous system
CX3CR1	chemokine receptor - one
CSF1R	colony stimulating factor - one - receptor
DAMPS	damage-associated molecular patterns
DNA	deoxyribonucleic acid
ELISA	enzyme - linked immunosorbent assay
FDA	food and drug administration
G-protein	guanine nucleotide - binding proteins
Iba-1	ionized calcium-binding adapter molecule - one
IL-β	interleukin - one - beta
IL-1	interleukin - one
IL-6	interleukin - six
IP	intraperitoneal injection
ir	immunoreactivity
L1	lumbar - one
L/min	litre per minute
mg/kg	milligram per kilogram
mL	millilitre
MPIA	mean pixel intensity per area
mRNA	messenger - ribonucleic acid
Na PIC	sodium persistent inward currents
NO	nitric oxide
PBS	phosphate - buffered saline
PBST	phosphate -buffered saline - triton
PFA	paraformaldehyde
PICs	persistent inward currents
PLX5622	brain-penetrant CSF1R inhibitor
RNA	ribonucleic acid
SCI	spinal cord injury
SD	standard deviation
SERT	serotonin transporter
T10	thoracic - ten
T11	thoracic - eleven

T12	thoracic - twelve
T-cell	thymus lymphocytes
TNF-α	tumor necrosis factor - alpha
VF	ventral funiculi
VLF	ventrolateral funiculi
µl	microliter
µm	micrometer

CHAPTER 1: INTRODUCTION

Overview

Traumatic spinal cord injury (SCI) has a devastating effect that influences neuronal networks, sensory input, and supraspinal connections that lead, for example, to impairment of motor function. After a traumatic incomplete SCI occurs, spontaneous recovery depends on spared descending connections to sprout and form new connections. This thesis focuses on the serotonergic descending fibers following injury, as serotonin (5-HT) is an important neuromodulator and neurotransmitter that influences network plasticity promoting sprouting after injury (Ballermann and Fouad, 2006, Weidner et al., 2001, Fouad et al., 2010). Previous studies have looked at different treatments that can be applied post-SCI to enhance recovery in patients (Kwon et al., 2011). One drug, in particular, is minocycline, which acts as an anti-inflammatory antibiotic, originally FDA-approved as an anti-acne medicine. Minocycline manipulates the activation of microglia and also influences macrophage activity, and has completed phase II clinical trials where it has been shown to promote recovery post-SCI (Casha et al., 2012). However, there remains a gap in knowledge regarding the effects of minocycline treatment on descending serotonergic fibres when applied shortly after injury versus one week later. My thesis examines how 5-HT immunoreactivity (ir) and microglia and macrophage (Iba-1ir) expression changes over two weeks post-SCI to target a treatment time-point to reverse 5-HTir reduction.

1.1 Spinal cord

The spinal cord is part of the central nervous system (CNS) controlling the voluntary muscles of the trunk and limbs and receives sensory information from both regions (Watson et al., 2008). Furthermore, the spinal cord controls most blood vessels and viscera of the thorax, abdomen, and pelvis (Watson et al., 2008). According to Watson et al. (2008), the spinal cord in

an adult is described as a continuous cylinder of central nervous tissue, and segmental components are derived from the pattern of spinal nerves (nerve rootlets arising from the cord bundled together forming one pair), which emerge from each segment. Within the vertebral canal, the spinal cord and meninges are found (composed of the dura, arachnoid, and pia mater) (Watson et al., 2008). A transverse section of the spinal cord contains the dorsal median sulcus, ventral medial fissure, central canal (surrounded by grey matter), ventrolateral sulcus, dorsolateral sulcus, three funiculi of the white matter (dorsal funiculus, lateral funiculus, and ventral funiculus), and the two horns of the grey matter (dorsal and ventral horn) as outlined in **Figure 1.1** (Watson et al., 2008). Within the mouse model, the spinal cord is made up of a total of 34 segments (8 cervical, 13 thoracic, 6 lumbar, 4 sacral, and 3 coccygeal) (Harrison et al., 2013). However, in contrast to the mouse, the human spinal cord contains only contains 31 segments (8 cervical, 12 thoracic, 5 lumbar, 5 sacral, and 1 coccygeal) (Watson et al., 2008).

1.2 Spinal cord injury

The spinal cord is the major conduit for both sensory and motor signals that pass between the brain and the periphery (Schwab and Bartholdi, 1996). The spinal cord is also a major processing center for autonomic, motor, and sensory functions (Schwab and Bartholdi, 1996). Therefore, it is not surprising that SCI is a devastating condition, which results in 4,259 new cases per year in Canada alone, and it is estimated that 42% is the result of traumatic SCI (INESS, 2010). Furthermore, 85,556 individuals are living with SCI in Canada, according to 2010 reports, with 51% suffering from traumatic SCI (INESS, 2010). According to the World Health Organization, males are most at risk overall (20-29; 70+ years old) for SCI, with a male-to-female ratio of at least 2:1 among adults (WHO, 2013). SCI causes a variety of disorders which include locomotor dysfunction, chronic pain, and spasticity (Raineteau and Schwab, 2001). Traumatic SCI takes

place when there is an external physical impact, in contrast to non-traumatic SCI associated with disease, infection, or tumor damage to the spinal cord (INESS, 2010). Traumatic SCI causes not only physical consequences but also financial and psychosocial stress for both patient and caregiver, costing from $1.1 to 4.6 million per patient (Ahuja et al., 2017) It is therefore, critical to improve long-term functional outcomes for patients with SCI.

1.3 Traumatic SCI

Traumatic SCI can be classified into two categories: complete or incomplete injury. Complete SCI generates a lack of both motor and sensory function below the injury site causing paralysis; although, it is rare for complete anatomical SCI in humans (Ghosh and Pearse, 2014). The incomplete injury involves the retention of some movement and sensation below the level of injury, which depends on the severity of the injury (Ghosh and Pearse, 2014). Trauma to the spinal cord causes the interruption of important dynamic interactions that take place in spinal neuronal networks, sensory input, and supraspinal connections that, altogether, causes impairment of locomotor function (Rossignol et al., 2006, Ghosh and Pearse, 2014). Furthermore, the damage caused by SCI results in the impairment of function at or below the injury site (Ghosh and Pearse, 2014). As a result, axons projecting from regions rostral to the lesion are compromised after SCI, which are important for neuromodulator transmission within the spinal cord (Fouad et al., 2010). Also, control over afferent input and local reflexes are compromised, leading to pathological motor output such as clonus and spasticity (Fouad et al., 2010). Neuromodulators are released from neurons that can be local, at synaptic sites affecting nearby neurons, or released in a paracrine fashion influencing other neurons, muscle cells, or effector cells binding to their corresponding receptors (Burrows, 1996). Neuromodulators often have long-lasting effects acting through G-

protein coupled receptors (Burrows, 1996). Neurons require neuromodulators to establish readiness for movement generation, which includes 5-HT transmission (Nardone et al., 2015).

1.4 Serotonin

5-HT is found within platelets, mast cells, enterochromaffin cells within the gastrointestinal tract and neurons (Li and Barres, 2018, Cooper et al., 2003). Only 1-2% of 5-HT is found within the brain, however, because it cannot cross the blood-brain barrier (BBB), 5-HT must be synthesized within brain cells (Cooper et al., 2003). Synthesis and supply of tryptophan, the primary substrate of 5-HT production, determines the levels of 5-HT within brain cells, which is further determined by plasma tryptophan levels derived primarily from the diet (Cooper et al., 2003). Large neutral amino acids, for example, aromatic amino acids (eg. phenylalanine), branched-chain amino acids (eg. isoleucine), and others (eg. histidine) compete for tryptophan, therefore altering tryptophan available to brain cells in addition to tryptophan plasma levels (Cooper et al., 2003). The first step to the synthetic synthesis of tryptophan to 5-HT is hydroxylation of tryptophan at the 5' position into 5-HTP by the enzyme tryptophan hydroxylase (**Figure 1.2**, Cooper et al., 2003). This enzymatic dependent breakdown of tryptophan is the rate-limiting step as tryptophan hydroxylase occurs in low concentrations in most tissues including brain tissues and is oxygen dependent (**Figure 1.2**, Cooper et al., 2003). 5-HTP is decarboxylated to yield serotonin almost immediately by amino acid decarboxylase (AADC) (**Figure 1.2**, Cooper et al., 2003). In addition, because decarboxylation of 5-HTP takes place rapidly, this is not a rate-limiting step (**Figure 1.2**, Cooper et al., 2003).

5-HT nerve terminals contain high-affinity uptake sites, which are important in maintaining transmitter homeostasis and terminating transmitter action (Cooper et al. 2003). Reuptake and release of 5-HT take place through a carrier located in the plasma membrane and works in both

directions, in and out of the cell, depending on the concentration gradient (Cooper et al., 2003). The monoamine transporter involved is part of a large gene family comprised of carriers for other transmitters, which includes serotonin transporter (SERT) (Cooper et al., 2003). SERT is found throughout the CNS along with nerve terminal projections of serotonergic neurons throughout the brain and spinal cord (Cooper et al., 2003). SERT mRNA expression is found to be localized almost exclusively within serotonergic cell bodies within the raphe nuclei, with high levels found specifically in both median and dorsal raphe (Cooper et al., 2003). Serotonergic neurons are restricted to clusters of cells lying near or within the midline, or raphe regions, of the upper brainstem and pons (Cooper et al., 2003, Fuxe 1965). Dahlstroem and Fuxe (1965), were the first to describe the nine 5-HT nuclei, with the more caudal groups projecting largely to the medulla and spinal cord (Cooper et al., 2003). These nuclei are further divided into three main regions, which include the medullary raphe pallidus, raphe magnus, and raphe obscurus (Azmitia, 1999). Serotonergic raphe spinal pathways from the raphe obscurus and pallidus are found to contribute to motor activity (Nardone et al., 2015). Furthermore, these nuclei project to the ventrolateral white matter, terminating in the ventral horn synapsing onto interneuron and motoneurons, and terminating in the intermediate gray through the ventral funiculi (VF) and ventrolateral funiculi (VLF) (Nardone et al., 2015). The axon terminals are found at all levels of the cord and a single raphe neuron can influence, for example, both cervical and lumbar cord by sending axon collaterals to both (Schmidt and Jordan, 2000).

1.5 Serotonin Receptors

According to Cooper et al. (2003), there are at least 15 molecularly identified 5-HT receptors, some containing isoforms from mRNA editing and some with splice variants. The majority of these receptors belong to a large family that interacts with G-proteins (guanine

nucleotide-binding proteins), with the exception of 5-HT_3 receptors which are ligand-gated ion channel receptors (**Table 1.1**, Cooper et al., 2003). G-proteins themselves can be classified into subfamilies based on their influence to stimulate (G_s) or inhibit ($G_{i/o}$) the activity of the intracellular pathway (Cooper et al., 2003). The G-protein receptor superfamily associated 5-HT receptors contain a characteristic seven-transmembrane domain and contain the ability to alter G-protein-dependent processes (**Table 1.1**, Cooper et al., 2003). This 5-HT receptor group can be further divided into families based upon amino acid sequence homology and coupling to secondary messengers (Cooper et al., 2003). The 5-HT_1 family (composed of 5-HT_{1A} and 5-HT_{1B}) has negatively coupled receptors to adenylyl cyclase (Cooper et al., 2003). The 5-HT_2 family (composed of 5-HT_{2A}, 5-HT_{2B}, and 5-HT_{2C}) contains three receptors with the same secondary messenger coupling, similar amino acid homology, and activation of phospholipase C (Cooper et al., 2003). Adenylyl cyclase is an enzyme that plays a regulatory role in essentially all cells and phospholipase C, a membrane-associated enzyme, known to cleave phospholipids important in signal transduction pathways (Cooper et al., 2003). In addition, 5-HT_1 receptors are found primarily in the dorsal horn and 5-HT_2 receptors in the ventral horn and medial-lateral nucleus (Schmidt and Jordan, 2000). Locomotor network activation and generation of locomotor-like movements have also been associated with 5-HT_{2A} receptors (Ung et al. 2008). In contrast to the ventral horn, most of the projections to the dorsal horn do not form synaptic contacts, suggesting volume (non-junctional) neurotransmission of 5-HT (Maxwell et al., 1983, Marlier et al., 1991, Schmidt and Jordan, 2000). The heterogenous positively-coupled 5-HT receptors to adenylyl cyclase include 5-HT_4, 5-HT_6, and 5-HT_7 subtypes (Cooper et al., 2003). The 5-HT_5 receptor type, which includes 5-HT_{5A} and 5-HT_{5B}, has an unknown coupling mechanism and is likely coupled to a different effector system (Cooper et al., 2003). 5-HT_3 directly activates a 5-HT gated ion channel

that depolarizes many different neurons (Cooper et al., 2003). 5-HT_3 receptors are present in both dorsal horn neurons and primary afferents likely involved in pain modulation. They are also found in the ventral horn, however, the role in spinal motor control is unknown (Schmidt and Jordan, 2000).

In motoneurons and many ventral-horn interneurons, 5-HT depolarizes motoneurons, facilitating low-voltage-gated persistent inward currents (PICs) which include both sodium (Na^+ PIC) and calcium (Ca^{2+} PIC) allowing for sustained depolarizations generating muscle contractions (Heckmann et al., 2005, Harvey et al., 2006). PICs are exhibited in spinal motoneurons that allow for sustained depolarizations, enhance synaptic input, and produce firing of neurons that will outlast stimulation (Bennett et al., 1998, Hounsgaard et al., 1988, Lee and Heckman, 1998, Li and Bennett, 2003). Brainstem derived 5-HT influences PICs and has been shown in studies looking at acute spinal cord transections where self-sustained firing and plateaus (sustained depolarizations) are largely eliminated (Hounsgaard, 2002, Harvey et al., 2006).

1.6 Serotonin and SCI

Following SCI, supraspinal serotonergic projections are severed, which results in a depletion of 5-HT (Carlsson et al., 1963). Because the release of 5-HT is important as a mediator for locomotion, it has been found to be a major limiting factor in the recovery of motor function (Hashimoto and Fukuda, 1991, Madriaga et al., 2004, Dai et al., 2005, Jordan et al., 2008). Pearlstein et al. (2005), found that when 5-HT levels were restored to a pre-SCI state, improvement in locomotor function was observed. In addition, during the regeneration of neurons, 5-HT is predicted to be important in network plasticity post-SCI, promoting locomotion (Ghosh and Pearse, 2014, Nardone et al., 2015). Furthermore, post-SCI motoneurons are classified as acutely unexcitable primarily due to the lack of brain-stem derived 5-HT depending on the degree of

injury, spasticity, and function (Nardone et al., 2015, Heckmann et al., 2005). This is strongly observed when SCI lesions the VLF and VF, which is responsible for most of the 5-HT innervating the ventral horn (Schmidt and Jordan, 2000). Spontaneous recovery of locomotor activity within an incomplete SCI utilizes the spared descending connections to help with recovery (Fouad et al., 2010). Descending axons sprout to form new connections post-SCI, and recovery is heavily influenced by brainstem regions with descending axons (Fouad et al., 2010). Recent work also supports the idea of supersensitivity of 5-HT following denervation (Bennett et al., 1998, Li and Bennett, 2003, Murray et al., 2010, Husch et al., 2012). Therefore, understanding and promoting plasticity post-SCI is important to find useful targets and time-points for developing new therapeutic interventions.

1.7 Minocycline

Minocycline has high lipophilic properties that can penetrate the blood-brain barrier (Lee et al., 2003). Furthermore, minocycline can be used to manipulate the activation of microglia (Yrjänheikki et al., 1998, Lee et al., 2003, Stirling et al., 2004, Ahuja et al., 2017). Minocycline was originally developed as an acne treatment because of its antibacterial properties (Wells et al., 2003, Lee et al., 2003, Stirling et al., 2004). As a bacteriostatic tetracycline synthetic antibiotic, it has been previously demonstrated that this drug has neuroprotective properties, which include inhibition of microglia activation, IL-1β (interleukin-1-beta), a cytokine that can be released by microglia, TNF-α (tumor necrosis factor-alpha), a cytokine cell signaling protein, and apoptosis (Wells et al., 2003). In addition, this drug also prevents nitric oxide synthase from producing NO (nitric oxide) which is toxic to cells at high levels (Amin et al., 1996), as well as caspases 1 and 3, that also contribute to IL-1 and apoptosis (Chen et al., 2000). As early as 1998, minocycline was shown to exhibit neuroprotective properties during the application of the drug in treating ischemic

stroke (Yrjänheikki et al., 1998). Since then, the neuroprotective properties of minocycline have been demonstrated in multiple sclerosis, traumatic brain injury, Parkinson's disease, and Huntington's disease (Plemel et al., 2014). In addition, minocycline has also been shown to treat animal model SCI (Lee et al., 2003, Wells et al., 2003, Stirling et al., 2004, Teng et al., 2004, Festoff et al., 2006, Yune et al., 2007). Although it has many applications including inhibition of microglia activation, it applies to many facets of the immune response post-SCI. Several measurable motor recovery improvements were also translated to human patients that received minocycline administration with cervical SCI, and overall findings pointed towards improvement in both functional and neurological outcomes when compared to placebo treatment (Casha et al., 2012). This project will review the timing of therapeutic treatment based on the secondary phase of SCI described below.

1.8 Pathophysiological description of SCI

The pathophysiological description of SCI is categorized into two separate phases: first, the primary phase involving the initial physical insult, and the secondary phase in the form of the response to this insult post-SCI (Schwab and Bartholdi, 1996, Ahuja et al., 2017). According to Schwab and Bartholdi (1996), this secondary phase of injury can be further divided into acute, subacute, and late phase. Although, the focus of this study is on microglia and macrophage response to SCI, with heavy emphasis on microglia, a brief overview of the events leading up to microglia activation and recruitment of macrophages is provided below.

The secondary post-SCI phase is both delayed and progressive over time (Ahuja et al., 2017). When an SCI takes place there is a disruption in blood vessel innervation and a significant reduction in the amount of blood flow thereby, causing a reduction of oxygen tension at the site of the injury (Schwab and Bartholdi, 1996, Beck et al., 2010). In addition, disrupted neuronal activity

as a result of SCI interrupts conduction and neuronal excitability. For example, SCI causes increases of calcium extracellularly which has been linked to negative cellular effects the activation of phospholipase C, as an example, breaking down cellular membranes leading to cellular death (Schwab and Bartholdi, 1996, Hounsgaard et al., 1988, Perrier and Hounsgaard, 2003). Overall, a hallmark of this phase is hemorrhagic necrosis leading to cell death (Schwab and Bartholdi, 1996). In response to this disruption of the blood-brain barrier, the subacute phase becomes active in the form of reactive gliosis involving both activated astrocytes and microglia (Schwab and Bartholdi, 1996, Ahuja et al., 2017). The inflammatory response begins within hours of the injury and peaks within several days (Schwab and Bartholdi, 1996). Inflammation is part of the immune system's first line of defense against infectious pathogens, relying primarily on the ability to recognize and respond to injury or pathogen entry (Alberts et al., 2002). These responses activate a cascade of signaling pathways, which includes activation of cytokine release that may, as an example, act as a chemoattractant recruiting other immune cells to help mount an effective defense (Alberts et al., 2002). Under normal conditions, there is a group of non-neuronal cells known as glia that help to both support and enable effective nervous system function (Gaudet and Fonken, 2018). When a traumatic insult to the spinal cord occurs, glia can be beneficial or can further amplify the secondary injury response. One of the major cell lines involved is microglia, which are the resident immune cells within the CNS (Gaudet and Fonken, 2018). Microglia cells take on an activated phenotype and will be discussed in detail below. Among other roles, resident microglia help recruit macrophages through the release of pro-inflammatory cytokines, for example, IL-1β, and TNF-α (David and Kroner, 2011, Gensel and Zhang, 2015). According to Blight (1992), macrophages aid in removing cellular debris allowing for an increase in blood vessel innervation, repair of the CNS, and clearing debris stimulates scar formation releasing factors

inducing proliferation of cellular components. However, delayed loss of axons has been linked to macrophage responses caused by cytotoxic products of activated phagocytes (Blight, 1992).

1.9 Microglia

Microglia represent 5-10% of the cell population within the CNS (Li and Barres, 2018). They were first described as *bodyguards* by del Rio-Hortega between 1920-1930, which is appropriate as these cells survey the CNS and help maintain homeostatic control (Li and Barres, 2018). Microglia also contribute to synaptic refinement to modify neuronal circuits during development using the complement system, which enhances antibodies and phagocytic cell lines to clear damaged cells or pathogens remaining non-adaptable (Stevens et al., 2007, Abbas et al., 2014, Paolicelli et al., 2011). The adaptive immune system produces antibodies that activate this complementary system to actively protect the host (Abbas et al., 2014). However, the primary role of microglia is to monitor the CNS through interactions of receptors and cell surface ligands expressed on the cell surface of neurons (Hoek et al., 2000, Ransohoff and Perry, 2009). Within a healthy CNS, microglia express a ramified morphological state with little expression of antigen-presenting machinery when compared to the active state (Ransohoff and Perry, 2009). Microglia projections extend into the extracellular space of the CNS where the presence of immunomodulatory factors is sensed through receptors that recognize DAMPS (damage-associated molecular patterns) (Gaudet and Fonken, 2018). DAMPS include proteins and metabolites that are upregulated in the extracellular matrix of the CNS such as, adenosine triphosphate (ATP), ribonucleic acid (RNA), or deoxyribonucleic acid (DNA). Alternatively, there may be factors actively secreted to help initiate inflammation (Gladwin and Ofori-Acquah, 2014, Bours et al., 2006). Some examples include toll-like receptors binding DAMPS, which activate microglia or cytokine upregulation after SCI (Kigerl et al., 2014, Noble and Wrathall, 1989).

1.10 Microglia and SCI

After SCI, microglia engage in upregulation of transcription factors, secreted factors, and immunomodulatory receptors, which cause an increase in inflammation (Noble, 2002, Gaudet and Fonken, 2018). The morphology of microglia is altered after SCI: instead of ramified and extensive long projections of fine processes, they retract their processes and, in a strongly activated state, become amoeboid (Gaudet and Fonken, 2018). In this state, they are mobile - migrating and proliferating at the lesion epicenter (Gaudet and Fonken, 2018). Studies have shown that within one week, the response shifts towards an anti-inflammatory response, important for regeneration, repair, and remodeling of tissue (Gensel and Zhang, 2015). Post-SCI, microglia, and macrophages encourage axon growth and have the ability to exert suppression or maintenance upon contact (McPhail et al., 2004, Horn et al., 2008). In addition, toll-like receptor 2, for example, increases post-SCI inflammation and reduces axon dieback (Stirling et al., 2004). Microglia and macrophages are found at the lesion epicenter starting between days 3-7 post-SCI (Jones et al., 2002). The environment itself has an influence on the morphology as well as the state and response of microglia and macrophages. According to Eggen et al. (2013), once microglia are stimulated, binding DAMPS as an example, they morphologically change and undergo molecular changes producing cytokine responses with phagocytic activity. In addition, microglia are responsible for early post-SCI phagocytosis within the first 3 days (Kigerl et al., 2009). By day 28 post-SCI, there is an expression shift from anti-inflammatory markers towards pro-inflammatory markers (Kigerl et al., 2009). This binary shift of anti- to pro-inflammatory dominated state is an oversimplification of the dynamic changes that immune cells can undergo to adapt within an injured environment.

Previous research has investigated the acute activity of inflammation in response to SCI and how inhibition dynamically changes the response to injury over time (Wells et al., 2003,

Stirling et al., 2004), Lee et al., 2003, Bellver-Landete et al., 2019). After SCI, there is an inflammatory response resulting from the release of cytokines as well as chemokines from inflammatory cells, which are proposed to cause further axonal damage (Bethea et al., 1999, Kigerl et al., 2009, and Stirling et al., 2004). As outlined above, one of the major cell lines involved in this response is microglia. Recently, a study conducted by Bellver-Landete et al., (2019) used a contusion model of SCI at vertebral level T9-10 to observe the role of microglia post-SCI and found that microglia activity was extensive during the first two weeks of injury. In addition, microglia were found to be influential in scar development post-SCI to protect neural tissues (Bellver-Landete et al., 2019). This project will focus on the role of microglia and their role in the changes in 5-HT expression following SCI. According to Mahé et al., (2005), once activated, microglia can influence neuronal function and serotonin transmission releasing cytokines, NO, glutamate as well as reactive oxygen species. It is also important to note is that microglia also contain serotonergic receptors, 5-HT_{2A}, 5-HT_{2B}, 5-HT_{3B}, 5-HT_{5A}, and 5-HT_{7} (Krabbe et al., 2012). The 5-HT_{2B} receptor has previously been associated with slowing disease progression in lateral sclerosis (El Oussini et al., 2017). Furthermore, microglial 5-HT7 receptors are coupled to G_s (stimulatory guanine nucleotide regulatory proteins) to generate IL-6, which is known to issue a warning signal to indicate an emergency and is strictly regulated (Mahé et al., 2005, Tanaka et al., 2014).

1.11 Research statement

In rodents, minocycline treatment prevents axonal dieback and further tissue degradation (neuroprotective properties), which is mediated through the prevention of microglia activation, reduction in IL-1β, TNF-α, NO, and decreases caspase 1 and 3 activity (Chen et al., 2000, Lee et al., 2003, Wang et al., 2003, Wells et al., 2003, Stirling et al., 2004). Here, I investigated the

outcome of a later minocycline treatment period of SCI in parallel with treatment within 12 hours for 7 days (Wells et al., 2003, Casha et al., 2012). I anatomically assess 5-HTir (immunoreactivity) changes during two treatment timelines with minocycline in conjunction with the expression of microglia immunoreactivity (Iba-1ir), to determine how treatments change 5-HTir post-SCI. Below, I will provide an overview of the key objectives and hypotheses that were tested for targeting SCI treatment.

1.12 Research objectives

1.13 Spinal cord injury time-course assessment and analysis of serotonin and microglia expression

First, I investigated the time-course of SCI to find a period of time that would be a target for the latent treatment with minocycline. Using male C57/BL6 mice 8 - 9 weeks old, I explored days 3, 7, 14, 21 and 28. Double-labeled immunohistochemistry was performed on the raphe obscurus localized in brainstem and spinal cord segments for post-SCI and sham, which included the lesion site (thoracic T12 spinal segment), rostral to the lesion (T10-T11, ~2.4mm from the injury), and caudal to the lesion (lumbar L1, ~2.6mm from the lesion site). I visually examined both 5-HTir and Iba-1ir and qualitatively examined the mean pixel intensity per area (MPIA) through image analysis, at each of the levels listed above and, in addition, separated ipsilateral and contralateral sides of each section of the cord evaluated (n = 4 per level, Two-way ANOVA, Holm-Sidak method). ***Hypothesis:*** **I predicted, based on previous literature, that Iba-1ir would be observed to peak around day 7 at the lesion site and 5-HTir would decrease ipsilateral to the lesion site at both the lesion site and caudal to the lesion site.**

I found that a significant reduction of 5-HTir was observed on day 14 caudal to the injury, and an increase was observed rostral and contralateral to the injury site. Peak expression of Iba-1ir was observed on day 7 at the lesion site and higher overall between days 3 through 14.

Therefore, I based my targeted treatment of minocycline starting day 7 post-SCI for treatment to fully take effect day 14.

1.14 Examine the role of minocycline treatment on 5-HTir and Iba-1ir 1-hour post-SCI

Before applying my targeted treatment, first I applied 1-hour post-SCI minocycline treatment to see how 5-HTir and Iba-1ir changed when using the same paradigm as Wells et al. 2003 (details in Chapter 2). ***Hypothesis:*** **I predicted that treatment with minocycline would increase 5-HTir ipsilateral and caudal to the injury itself relative to saline treatment, and that rostral to the lesion, an increase of 5-HTir contralaterally would no longer be observed.**

I observed a significant increase of 5-HTir caudal and ipsilateral to the injury relative to the saline control treatment. There was a reduction of Iba-1 expression rostral and caudal to the lesion site. Rostral to the lesion site there was a reduction in 5-HTir resulting in a similar level of expression observed in the sham. This suggests that minocycline treatment was effective at reducing Iba-1 expression and retaining close to sham levels of 5-HTir post-SCI.

1.15 Examine the role of minocycline treatment on 5-HTir and Iba-1ir 7 days post-SCI and compare to 1-hour post-SCI administration

I assessed the role of minocycline treatment on day 7. ***Hypothesis:*** **I predicted that treatment 7 days post-SCI would result in an increase of caudal and ipsilateral 5-HTir, a decrease of rostral contralateral 5-HTir, and an overall decrease of Iba-1ir relative to saline treatments.** Furthermore, I predicted that between the 1-hour post-SCI versus day 7 post-SCI treatments, 5-HTir would result in similar outcomes but with higher expression of 5-HTir overall in the day 7 start day treatment.

Instead, I observed significant retention or expression of 5-HTir compared to shams, and treatment with minocycline improved 5-HTir compared to saline treatments across the rostral and

caudal segments. Iba-1ir was reduced compared to saline; however, overall Iba-1ir and 5-HTir levels were more similar to non-treated SCI versus immediate 1-hour administration post-SCI. These results, although qualitative, indicated that 1-hour post-SCI treatment caused the most significant difference in the treatment paradigm and also resulted in 5-HTir more similar to shams when observing rostral and caudal to the lesion site. In addition, treatment 7 days post-SCI still had an effect on the expression of 5-HTir and Iba-1ir relative to the saline treatments overall.

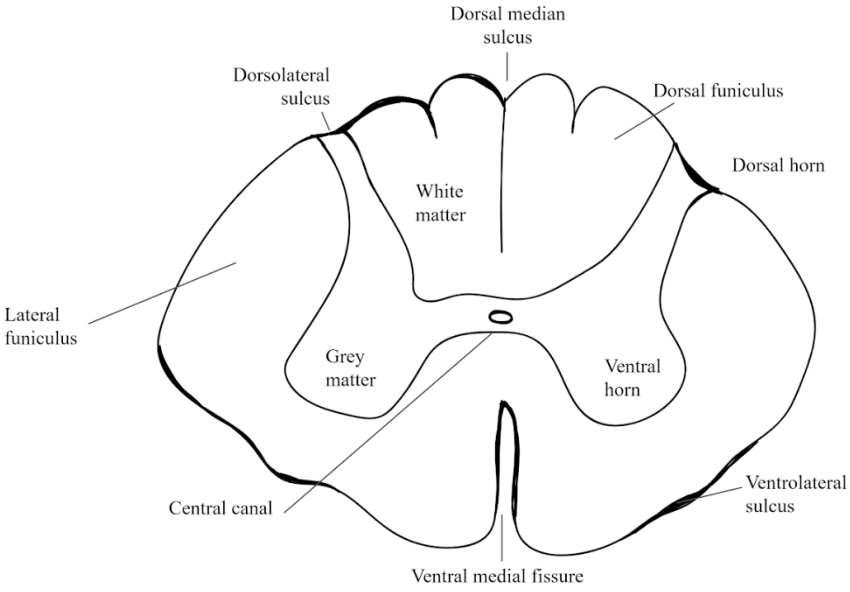

Figure 1.1 Details of a transverse section of the spinal cord. A transverse section of the spinal cord contains the dorsal median sulcus, ventral medial fissure, central canal (surrounded by grey matter), ventrolateral sulcus, dorsolateral sulcus, three funiculi of the white matter (dorsal funiculus, lateral funiculus, and ventral funiculus), and the two horns of the grey matter (dorsal and ventral horn) (Watson et al., 2008, Flood. J, 2019).

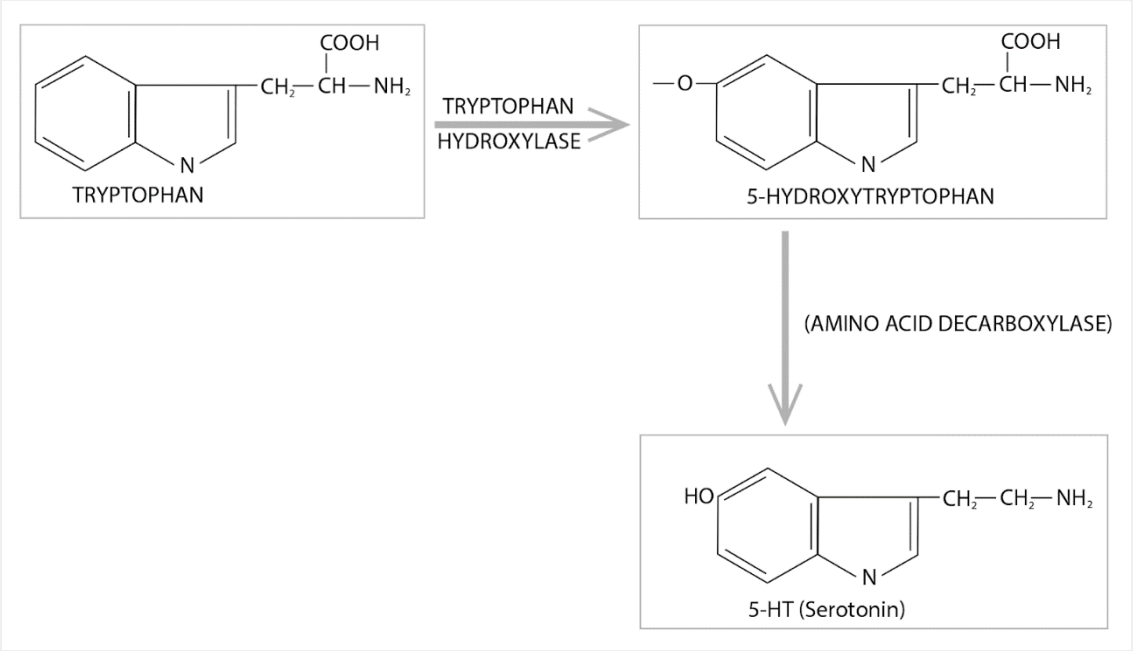

Figure 1.2 Basic synthesis of serotonin (5-HT: 5-hydroxytryptamine). Hydroxylation of tryptophan by the enzyme tryptophan hydroxylase, to produce 5-hydroxytryptophan as the rate-limiting step (Cooper et al., 2003). 5-hydroxytryptophan is further broken down by AADC (aromatic amino acid decarboxylase) to produce serotonin (Cooper et al., 2003).

Table 1.1 Serotonin (5-HT) family receptor subtypes, G-protein association, and effector pathways (Cooper et al., 2003).

Receptor Family	Receptor subtype	Effector Pathway	G Protein
5-HT$_1$	5-HT$_{1A}$	Inhibition: adenylate cyclase Opening: potassium channel Closing: calcium channel	G_i G_i G_o
5-HT$_1$	5-HT$_{1B-1E}$	Inhibition: adenylate cyclase	G_i
5-HT$_2$	5-HT$_{2A-2C}$	Hydrolysis: Phosphoinositide	G_q
Other	5-HT$_4$	Activation: adenylate cyclase	G_s
Others	5-HT$_{5A-B}$	Unknown: coupling mechanism	?
Others	5-HT$_6$	Activation: adenylate cyclase	G_s
Others	5-HT$_7$	Activation: adenylate cyclase	G_s
Ligand-gated ion channels	5-HT$_3$	Ligand-gated ion channel	None

CHAPTER 2: METHODS

2.1 Animals

Adult male C57/BL6 mice between the ages of 8 - 9 weeks old (Charles River © 2019) were used. All proposed animal experiments were approved by the University of Calgary Health Sciences Animal Care Committee (Protocol: AC15-0026), in accordance with guidelines published by the Canadian Council for Animal Care.

2.2 Spinal cord hemisection injury

All animal experiments were approved by the University of Calgary Health Sciences Animal Care Committee (Protocol: AC15-0016), following the Canadian Council for Animal Care guidelines. C57/B6J mice were initially anesthetized in an induction chamber using 1.75 mL of isoflurane administered on a piece of cloth in the bottom of the chamber. Animals were then transferred onto the surgery table and administered with an inhalant anesthetic of 1.0-1.5% isoflurane (SurgiVet Model 100 Vaporizer) with 0.4 L/min of oxygen (100% medical-grade, tank grade: 1072; Praxair) using a nose cone. The animals were shaved from the genitals to the rib cage bilaterally and sterilized using 5% iodine solution topically. The area was cleaned by using 95% ethanol to remove excess iodine.

The surgical area was shaved and disinfected with 2.5% iodine and 95% (vol/vol) isopropyl alcohol. The analgesic, buprenorphine, was administered (0.05 mg/kg) pre-surgically. Mice received a laminectomy at the T9-T10 vertebral level, which corresponds to the spinal segment of T11-T12 (Harrison et al. 2013). A longitudinal incision was made in the skin, followed by cutting the erector spinae along the vertebral column and then bluntly dissecting the muscle surrounding the T9-T10 segments. After stabilizing the vertebral column, the T9-10 vertebra was located using the last rib, which attaches to the rostral end of the T13 vertebrae. The T11-T12 spinal cord

segments (T9-T10 vertebral region) were hemisected with a 27 gauge needle inserted into the spinal cord and cut laterally. Sham animals received a durotomy, which involved the dura being cut without a lesion to the spinal cord. The muscle and skin were sutured closed using 6-0 vicryl dissolvable suture material provided by ETHICON ® and the recovery of the mice were visually monitored. Mice were monitored daily for the first week to ensure hydration (water intake) and their bladders' were manually expressed with control returning by day three. In addition, the Hydrogel™, provided by Clear H_2O®, was provided to all injured animals during the first-week post-SCI.

To establish a timeline of injury post-SCI. a total of 40 mice were used. 20 out of the 40 animals received an SCI and the remaining sham animals received only durotomies. Mice were further divided into days of interest SCI (n = 4) and SHAM (n = 4) for days 3, 7, 14, 21 and 28, respectively (**Figure 2.1**). For further investigation of day 21 post-SCI, a total of 31 mice were used. 16 out of the 31 animals received SCI and the remaining sham animals received laminectomies (**Figure 2.2**).

2.3 Pharmacological treatment of animals day 21 post-SCI

To further investigate day 21 post-SCI, mice (n = 31) were divided into two groups. Group 1 (n = 16) received either the saline or minocycline treatment starting 1 hour after injury containing both SCI (n = 8) and sham (n = 8) animals. The treatment was administered as an intraperitoneal injection (IP) of saline (SCI: n = 4, sham: n = 4) or 50 mg/kg minocycline (SCI: n = 4, sham n = 4, MilliporeSigma, St. Louis, MO, USA) similar to previous reports (Yrjänheikki et al. 1999; Sanchez Mejia et al. 2001; Brundula et al. 2002; Wells et al. 2003). 24 hours later, the second injection of minocycline (50 mg/kg) was administered. Administration of minocycline (25 mg/kg) continued every 24 hours for the remaining 5 days of treatment. Group 2 (n = 15) received the

treatment starting 7 days post-SCI containing, as before, both SCI (n = 8) and sham (n = 7) animals. Treatment was administered as an IP injection of saline (SCI: n = 4, sham: n = 3) or 50 mg/kg minocycline (SCI: n = 4, sham: n = 4). Similar to group 1, they received an injection of minocycline (50 mg/kg) 24 hours later and continued daily administration of minocycline (25 mg/kg) for 5 days. We used 25-50 mg/kg based on previous literature using the mouse. In addition, the half-life of minocycline in rodents is approximately 2-3 hours. Animal studies have previously used a single daily administration (Wells et al. 2003, Wang et al. 2003, Stirling et al. 2004).

2.4 Tissue processing

On respective days post-injury, animals were perfused with cold 4% paraformaldehyde (PFA). Brains and vertebral columns were extracted and immersed in 4% PFA overnight for post-fixation. 24 hours after perfusion, the brains were transferred to 30% sucrose for cryoprotection. Spinal cords were extracted 24 hours after post-fixation and placed back into 4% PFA for up to 4 hours, then transferred to 30% sucrose. The cryoprotected tissue, spinal cord and brainstem, were sectioned every 30 µm using a cryostat at -20°C, separated according to segments T12-T13 (lesion site), L1-L2 (caudal to the lesion), and T10-11 (rostral to the lesion), and stored in 1X PBS (phosphate buffer solution) until immunohistochemistry staining commenced. Tissue was washed using 1X PBS three times for ten minutes each, then placed in blocking solution (5% donkey serum diluted with 0.3% PBST (PBS and 0.3% of Triton) for one hour. The tissue was incubated overnight at room temperature on a shaker with the primary antibodies rabbit anti-Iba-1 (1:1000, Wako 19-19741, Lot PTN5930) and goat anti-5-HT (1:10,000, Immunostar 20079, Lot 1744001) diluted in blocking solution. The next day, tissue was washed in 1X PBS, three times, for 10 minutes each. Secondary antibodies Alexa Fluor 546 donkey anti-rabbit (1:1000, Life Technologies Inc. A10040, Lot 1946340) and Alexa Fluor 488 donkey anti-goat (1:1000, Life

Technologies Inc. A11055, Lot 1463163) were diluted in blocking solution and tissue was then incubated in the solution in the dark at room temperature for 2 hours. The tissue was washed in 1X PBS three times for 10 minutes each before mounting and coverslipping. For the negative controls, spinal cord tissue and brain tissue was stained with primary antibodies omitted. Confocal microscopy was performed with the Leica SP8 using 10X and 25X water objectives. The tissue was imaged using appropriate filter cubes (Alexa Fluor 488. Ex: 495 nm, Em: 519 nm and Alexa Fluor 546. Ex: 525 nm, Em: 600 nm). Images were taken from three main areas at the lesion site, rostral (2.6 mm) to the lesion, and caudal (2.4 mm) to the lesion (n = 4: sections each day for all n = 4 animals). A total of 4 sections from each area were taken and analyzed for each animal for a total of 4 animals for each time-point and treatment.

2.5 Analysis and statistics

Image analysis was performed using ImageJ software. Images were uploaded directly and converted to maximum intensity images for pixel intensity analysis. Each transverse spinal cord image was divided into ipsilateral and contralateral areas and mean pixel intensity per area (MPIA) was recorded for both 5-HT (green) and Iba-1 (magenta) channels. All statistical analyses were performed using SigmaPlot 14.0 software (Systat Software 2019, Version 13, San Jose, California). Negative control images were subtracted to control for immunohistochemistry intensity variation. Images were evaluated using two-way repeated-measures analysis of variance (ANOVA), between shams and injuries. If a significant difference was found, pairwise comparisons were completed using Holm-Sidak's post-hoc test method. A p-value of < 0.05 was considered statistically significant and all data were presented as mean +/- standard deviation. Lesion size determination was completed using the lesion site sections and counted, with 30 µm sections, and the size was determined. Analysis between saline treatments and

minocycline treatments were assessed using t-test statistics. Posthoc analysis was performed using SigmaPlot.

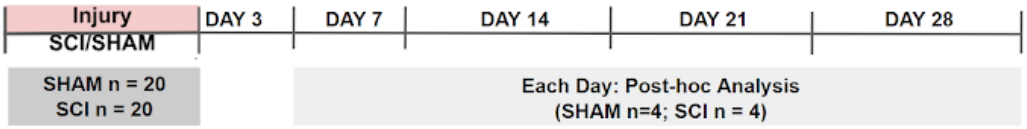

Figure 2.1 Timeline schematic of days selected for processing SCI timeline. Injury days 3, 7, 14, 21 and 28 were selected as days post-SCI, for both sham (n = 4) and SCI (n = 4), for analysis of 5-HTir and Iba-1ir visual and qualitative analysis.

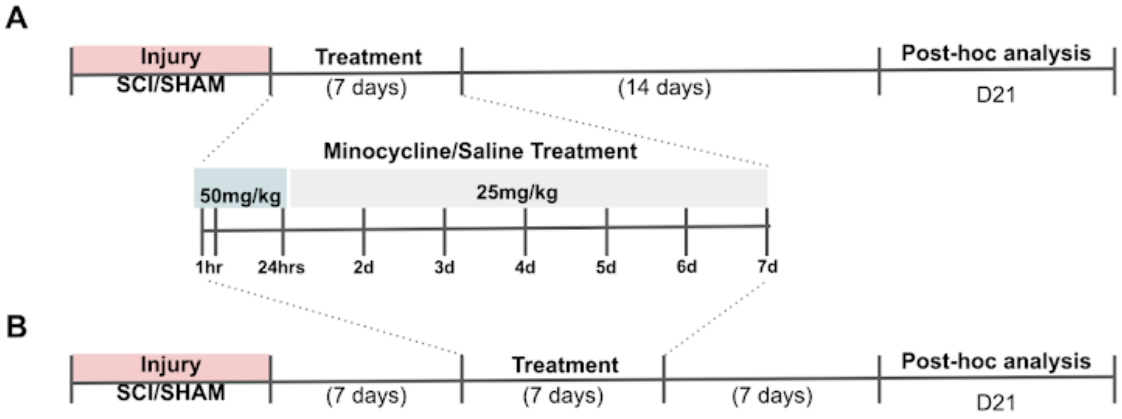

Figure 2.2 Timeline schematic of treatment paradigms used to test 5-HTir changes after minocycline treatment. **(A)** Treatment as outlined by (Wells et al. 2003): administration of minocycline or saline 1-hour post-SCI. First, two 24 hour treatments at 50 mg/kg of minocycline or saline and thereafter for 5 days 25 mg/kg for both sham (n = 4) and SCI (n = 4). **(B)** Treatment administration of minocycline or saline 7 days post-SCI. First, two treatments on day 7 and 8 post-SCI of minocycline or saline were administered at 50 mg/kg and thereafter for 5 days at 25 mg/kg for both sham (n = 4) and SCI (n = 4).

CHAPTER 3: TIME-COURSE RESULTS

Overview

First, I established a timeline for the expression of serotonin (5-HT) and microglia/macrophage (Iba-1) following spinal cord injury. Days 3, 7, 14, 21 and 28 post-SCI were selected (n = 4), and the dynamic changes of 5-HT and Iba-1 immunoreactivity (ir) post-SCI were analyzed. Double-labeled immunohistochemistry was performed on brainstem and spinal cord segments for post-SCI and sham, which included the lesion site (thoracic T12 spinal segment), caudal to the lesion (lumbar L1, ~2.6 mm from the lesion site), and rostral to lesion (T10 - T11, ~2.4 mm from the injury) (Harrison et al. 2013). 5-HTir (green) nuclei were found in the raphe obscurus of the brainstem in a typical triangular formation (**Figure 3.1**). Iba-1ir (magenta) cells were observed uniformly distributed within the brainstem (**Figure 3.1**). 5-HTir and Iba-1ir were quantitatively analyzed as outlined (see Chapter 2) at days 3, 7, 14, 21 and 28 post-injury (n = 4; **Figure 3.9**).

3.1 Spinal cord injury time-course assessment of serotonin immunoreactivity

Visual assessment of transverse sham spinal cord images showed widespread 5-HTir across all laminae of the transverse spinal cord, including the intermediolateral nuclei, central canal, and ventral horn at all segments examined. Contralateral to the lesion site (T12 spinal segment level), 5-HTir was visually similar to shams across all injury days (**Figure 3.2**). On the other hand, the ipsilateral expression of 5-HTir was reduced at the lesion site compared to all laminae that normally express 5-HTir (**Figure 3.2**). The intermediolateral nucleus and the ventral horn had the largest decrease in 5-HTir expression compared to the shams (**Figure 3.2**). Using the imaged data, I took the mean pixel intensity per area (MPIA) both ipsilateral and contralateral to the injury at the lesion site for qualitative analysis of 5-HTir expression changes (see Chapter 2). The 5-HTir

decreased ipsilaterally, at the lesion site for days 3, 7, 14, 21 and 28 for SCI versus sham ($P < 0.001$, **Figure 3.3**). Conversely, 5-HTir did not change contralateral to the injury at the lesion site ($P = 0.614$, **Figure 3.3**).

Rostral to the lesion site (T10-T11, ~2.4 mm from the injury), an increase of 5-HTir intensity was observed between days 3 and 21 (**Figure 3.5d**). 5-HTir within the ventral horn of the rostral sections increased when comparing day 3 to both days 14 and 21 contralateral to the lesion site (**Figure 3.5d**). The ventral horn, ipsilateral to the injury, showed a decrease in 5-HTir when comparing pairwise day 3 to both days 14 and 21, respectively (**Figure 3.5d**). The intermediolateral 5-HTir remained consistent across all days for the injuries ipsilateral and contralateral to the injury and compared to the sham expression (**Figure 3.5d**). Around the central canal, 5-HTir remained the same in both injury and sham animals (**Figure 3.5d**). Rostral to the lesion site, there was an observable difference in 5-HTir in the ventral horn (**Figure 3.5d**). Specifically, in the ipsilateral lamina VIII, there was reduced 5-HTir compared to contralateral segments (**Figure 3.5d**, bottom (I and II)). The MPIA rostral to the lesion site yielded a significant increase contralaterally in 5-HTir on days 21 ($P = 0.039$) and 28 ($P < 0.001$, **Figure 3.5b**). 5-HTir, ipsilateral to the lesion site, was decreased between days 3 and 21 ($P = 0.027$), and days 3 and 28 ($P = 0.049$). Rostral to the lesion, ipsilateral to the injury, there was a significant increase of 5-HTir between lesion versus sham animals ($P < 0.001$, **Figure 3.5a**). Statistically significant pairwise comparison between days 3 and 21 ($P = 0.012$) and days 3 and 28 ($P < 0.001$) was also observed (**Figure 3.5a**).

Caudal to the lesion site (lumbar L1, ~2.6 mm from the lesion site), sham animals had a similar 5-HTir compared to day 3, in the ventral horn, intermediolateral nuclei, and the central canal (**Figure 3.7d**). However, there was a visual decrease found post-injury in ipsilateral 5-HTir,

caudal to the injury (**Figure 3.7d**). Specifically, there was a significant decrease in 5-HTir in the ipsilateral ventral horn between day 3 and days 14 and 21 ($P < 0.01$; $P < 0.001$; **Figure 3.7a**). In addition, there was a pronounced decrease in 5-HTir within the intermediolateral nuclei and a moderate 5-HTir decrease around the central canal (**Figure 3.7a**). On the contralateral side, 5-HTir was expressed within the ventral horn, intermediolateral nuclei, and the central canal across all days within injuries and shams (**Figure 3.7b**). Ipsilateral MPIA was significantly decreased in 5-HTir on days 14, 21 and 28 post-SCI ($P < 0.001$, **Figure 3.7a**). In addition, 5-HTir was decreased across all days between sham and injury ($P < 0.001$, **Figure 3.7a**). However, contralateral and caudal to the injury, there was no difference found between sham and SCI tissue on days 3 ($P = 0.231$), 7 ($P = 0.783$), 14 ($P = 0.138$), 21 ($P = 0.693$) , and 28 ($P = 0.967$), and no difference found between days 7 ($P = 0.783$), 14 ($P = 0.138$) and 21 ($P = 0.399$), respectively (**Figure 3.7b**).

3.2 Spinal cord injury time-course assessment of microglia/macrophage immunoreactivity

Iba-1ir in sham animals tiled the tissue with concentrated expression around the edges of the white matter and within the ventral medial fissure. Iba-1ir at the lesion site was increased both ipsilateral and contralateral to the lesion across all days (**Figure 3.2**). Ipsilaterally, there was concentrated clumping of Iba-1ir cells, specifically within the gracile fasciculus, postsynaptic dorsal column, and dorsal corticospinal tract region of the white matter on both days 3 and 7 (**Figure 3.2**). Iba-1ir was also observed ipsilateral to the injury at the lesion site across all lamina, particularly around the central canal, ventral horn and within the ventral white matter (**Figure 3.2**). Expression of Iba-1ir was found to be higher on days 3 and 7 when compared to the other injury days, however, there was a peak expression of Iba-1 observed on day 7 (**Figure 3.2**). On days 3 through 28, there was a distinct ipsilateral lesion of the spinal cord, especially when looking at the dorsal horn of the injuries (**Figure 3.2**). Contralaterally, there was an observable increase of Iba-

1ir expression within the grey matter across all days (**Figure 3.2**). However, on day 7, there was also ventral white matter expression of Iba-1ir when compared to the other injuries (**Figure 3.2**). When looking across all injury days, there was a decrease of Iba-1ir by day 14 which decreased further by days 21 and 28 (**Figure 3.2**). MPIA Iba-1ir was increased ($P < 0.001$) between sham and SCI for days 3, 7, 14, 21, and 28 ipsilateral to the lesion site (**Figure 3.4**). Ipsilateral to the lesion site, an increase of Iba-1 MPIA was observed when comparing days 3 and 7 ($P < 0.001$, **Figure 3.4**). Furthermore, a significant injury effect was found with decreasing Iba-1ir between days 7 and 28 within SCI groups, respectively ($P < 0.001$, **Figure 3.4**). On the other hand, a significant increase in Iba-1ir was observed contralaterally, at the lesion site, for days 3, 7, 14, 21 and 28 when compared to sham ($P < 0.001$, $n = 4$, **Figure 3.4**).

When observing rostral to the lesion site (T10-T11, ~2.4 mm from the injury), an increase of Iba-1ir was observed between day 3 and days 14 and 21 (**Figure 3.5d**). A similar expression of Iba-1ir rostral to the injury was observed between sham and day 3 injury both contralateral and ipsilateral to the injury site (**Figure 3.5d**). Specifically, Iba-1ir tiled the tissue with a higher concentration around the tissue edge, within the white matter and within the ventromedial fissure (**Figure 3.5d**). However, by day 14, there was an increase of Iba-1ir within the white matter in these regions as well as within the grey matter ipsilateral to the injury (**Figure 3.5d**). The contralateral Iba-1ir on day 14 increased within the ventral white matter (ventral funiculus) (**Figure 3.5d**, bottom (I and II)). On day 21, Iba-1ir decreased within the grey matter when compared to day 14 (**Figure 3.5d**). An increase of Iba-1ir was observed on day 21 within the ventral funiculi bilaterally at the injury site (**Figure 3.5d**) There was an increase of Iba-1ir ipsilaterally within the lateral funiculi, gracile fasciculus, postsynaptic dorsal column pathway, and the dorsal corticospinal tract portion of the dorsal white matter (**Figure 3.5d**). Rostral to the lesion

and ipsilateral to the injury, a significant increase in MPIA of Iba-1ir was observed on days 3, 7, 14, 21 and 28 when comparing sham to injury ($P < 0.001$, $n = 4$, **Figure 3.6**). Conversely, contralaterally there was no significant difference in MPIA of Iba-1ir expression between sham and SCI spinal cord tissue rostral to the lesion site ($P = 0.672$, $n = 4$, **Figure 3.6**).

Caudal to the lesion site (lumbar L1, ~2.6 mm from the lesion site), shams had a similar expression of Iba-1ir with that of day 3, tiling the tissue with a higher concentration surrounding the edges of the white matter and the ventral medial fissure (**Figure 3.7d**). There was an increase of Iba-1ir observed within the ventral medial fissure on days 14 and 21, relative to the other injury days (**Figure 3.7d**). In addition, there was an increase of Iba-1ir ipsilateral to the injury within the levator scapulae motoneurons of lamina 5 through 9 (**Figure 3.7d**). Overall, the expression of Iba-1ir was notably higher ipsilateral to the injury compared to contralateral starting on day 14 (**Figure 3.7d**). This increase can also be observed in the bottom part of **Figure 3.7d**, where the bottom row expression (ipsilateral to the injury) is higher within the grey matter when compared to contralateral expression. Caudal to the lesion site, ipsilateral Iba-1ir was found to be increased for days 3, 7, 14, 21 and 28 relative to sham animals ($P < 0.001$, $n = 4$, **Figure 3.8**). However, contralaterally, no significant change in Iba-1ir was observed across all days ($P = 0.148$, $n = 4$, **Figure 3.8**). In addition, there was also an increase in Iba-1ir observed starting at day 14 caudal to the lesion site (**Figure 3.8**). Iba-1 immunostaining tiled the spinal cord tissue caudal to the lesion in both the shams and day 3 post-SCI, with a moderate increase in intensity around the tissue edges (**Figure 3.7d**). However, on days 14 and 21, the bilateral expression of Iba-1 differed, where an increase of Iba-1ir was observed ipsilateral to the injury (**Figure 3.7d**).

3.3 Spinal cord injury time-course summary of significant findings

At the lesion site (T12 segment), across all days, there was a reduction in ipsilateral 5-HTir within the intermediolateral positive nuclei and the ventral horn compared to the shams (**Figure 3.2**). This also corresponded with a significant decrease ipsilateral to the injury observed at the lesion site for days 3, 7, 14, 21 and 28 for SCI versus sham ($P < 0.001$, **Figure 3.3**). Iba-1ir at the lesion site significantly increased in expression bilaterally to the injury itself across all days (**Figure 3.4**). Expression of Iba-1ir was higher on days 3 and 7, however, there was a peak expression of Iba-1ir observed on day 7 (**Figure 3.4**). Contralaterally, there was an increase of Iba-1ir within the laminae across all days (**Figure 3.2**). This also corresponded with the qualitative data where Iba-1ir MPIA was found to increase ($P < 0.001$) between sham and SCI across all days (**Figure 3.4**).

Rostral to the injury (T10-T11, ~2.4 mm from the injury) on day 14, there was a difference in the ventral horn 5-HTir ipsilateral versus contralateral to the injury and shams (**Figure 3.5d**). These data also corresponded with the qualitative analysis of the images where there was a significant increase of MPIA contralaterally in 5-HTir on day 14 ($P < 0.001$), day 21 ($P = 0.0039$), and on day 28 ($P < 0.001$, **Figure 3.5b**). In addition, a statistically significant decrease pairwise comparison of 5-HTir MPIA between days 3 and 21 ($P = 0.027$), and days 3 and 28 ($P = 0.049$) was observed (**Figure 3.5b**). Iba-1ir was observed to increase across all days ($P < 0.001$, **Figure 3.5d**). By day 14, there was an increase of Iba-1ir expression within the white matter, the ventromedial fissure, and grey matter ipsilateral to the injury (**Figure 3.5d**). Contralateral expression of Iba-1ir increased within the ventral white matter (ventral funiculus) on day 14 (**Figure 3.5d**, bottom (I and II). These data corresponded with qualitative analysis where a

significant increase in expression of MPIA Iba-1ir observed on days 3, 7, 14, 21 and 28 when comparing injury to sham ($P < 0.001$, $n = 4$, **Figure 3.6**).

I was interested in targeting day 7 as the treatment to observe minocycline and its contribution to 5-HT expression because I quantitatively observed a reduction in the expression of 5-HT on that day (**Figure 3.9**). I was also interested in possible delayed effects of minocycline and therefore started minocycline treatment starting day 7, with treatment effect day 14, and sacrifice of the animal on day 21. Minocycline and saline were applied to both SCI ($n = 4$) and sham ($n = 4$) animals for each treatment. The first treatment of minocycline (see Chapter 2) or saline was applied 1-hour after injury (**Figure 3.4a**) and the second treatment was applied 7 days after injury (**Figures 3.4b,** and **3.9**).

CHAPTER 4: TREATMENT RESULTS

4.1 Minocycline treatment did not change 5-HTir but reduced Iba-1ir at the lesion site.

There was a similar expression of 5-HTir within the intermediolateral nuclei, ventral horns, and surrounding the central canal when visually observing the differences in shams treated with minocycline, or saline controls, for both treatments 1-hour post-SCI (**Figure 4.1a**) and 7 days post-SCI (**Figure 4.1b**) at the lesion site. The mean lesion size was 2.04 mm (+/- 0.05 SEM) for the control saline 1-hour post-SCI and 1.47 mm (+/- 0.06 SEM) for the minocycline 1-hour post-SCI (**Figure 4.12**) cohorts. A significant reduction in the lesion size in minocycline treatment versus saline treatment when administered 1-hour post-SCI (t-test; $P < 0.001$, **Figure 4.12**) was found. The mean lesion size was found to be 2.13 mm (+/- 0.06 SEM) for the control saline 7 days post-SCI cohort and a mean of 1.77 mm (+/- 0.0574 SEM) for the minocycline administration 7 days post-SCI cohort (**Figure 4.12**). There was a significant reduction in the lesion size with minocycline treatment versus saline 7 days post-SCI ($P = 0.029$, **Figure 4.12**). When comparing the two control saline treatments there was no significant difference observed ($P = 0.28$, Student's t-test, $n = 4$, **Figure 4.12**). However, there was a significant decrease in lesion size with minocycline administration 1-hour post-SCI versus 7 days post-SCI ($P = 0.010$, **Figure 4.12**).

Reduced 5-HTir was observed when visually comparing control saline-treated 1-hour post-SCI to the shams ipsilateral to the injury, notably, in the intermediolateral nuclei, ventral horn, and surrounding the central canal (**Figure 4.1a**). Contralateral to the injury, at the lesion site, there was similar 5-HTir between shams when assessed visually (**Figure 4.1a**). Minocycline administration 1-hour post-SCI resulted in a reduction in 5-HTir ipsilateral to the injury within the ventral horn, intermediolateral nuclei, and surrounding the central canal compared to saline controls (**Figure 4.1a** and **4.10**). Contralateral to the injury, however, 5-HTir was similar to the control saline

treatment and shams (**Figure 4.1.a** and **4.10**). Qualitative analysis of minocycline treatment directly 1-hour post-SCI ($P = 0.081$) found no significant increase or decrease of 5-HTir MPIA when compared to control saline treatments ipsilateral to the lesion at the lesion site (**Figure 4.2a**). Visually comparing control saline-treated tissue 7 days post-SCI with shams showed decreased 5-HTir expression ipsilateral to the injury in the intermediolateral nuclei, ventral horn, and surrounding the central canal (**Figure 4.1b** and **4.10**). There was also a spread of 5-HTir outside of the normal expression from lamina I through VII (**Figure 4.1b**). Contralateral to the injury at the lesion site, 5-HTir remained consistent relative to both shams (**Figure 4.1b**). Visually comparing minocycline administration 7 days post-SCI with control saline treatment showed a reduction of 5-HTir ipsilateral to the injury within the ventral horn, intermediolateral nuclei, and surrounding the central canal (**Figure 4.1a**). Contralateral to the injury, 5-HTir was similar to the control saline treatment and shams (**Figure 4.1.a**).

Minocycline treatments 1-hour post-SCI versus 7 days post-SCI showed similar expression of 5-HTir both ipsilateral and contralateral to the injury (**Figure 4.1**and **4.11**). However, there was greater 5-HT expression within the dorsal horn, specifically lamina I through V when treated with minocycline 7 days post-SCI (**Figure 4.1**). Qualitatively, (Chapter 3), a significant decrease of ipsilateral 5-HTir MPIA between sham and SCI in both 1-hour post-SCI treatment ($P < 0.001$) and 7 days post-SCI treatment ($P < 0.001$) was observed at the lesion site (**Figure 4.2a** and **4.11**). Furthermore, when comparing treatments, there was no difference in 5-HTir MPIA ipsilateral to the injury at the injury site ($P = 0.363$, **Figure 4.2a**). In addition, 5-HTir MPIA was similar contralateral to the injury at the lesion site when mice were treated 7 days post-SCI ($P = 0.063$, **Figure 4.2b** and **4.11**).

Iba-1ir was similar to what was reported in Chapter 3 for both shams in **Figure 3.2** (**Figure 4.1**). When comparing control saline-treated 1-hour post-SCI with shams, there was an increase of Iba-1ir ipsilateral to the injury at the lesion site (**Figure 4.1a**). In addition, there was a concentration of Iba-1ir across lamina I through VII, and within the ventral funiculus, lateral funiculus, and ventral horn (**Figure 4.1a**). Contralaterally, however, there was less observable Iba-1ir, except for the ventral funiculus surrounding the ventral medial fissure, ventromedial lateral nuclei, and ventral horn (**Figure 4.1a**). Visual assessment of 1-hour post-SCI mice, when comparing minocycline treatment versus control saline treatment, showed an increase of Iba-1ir ipsilateral to the injury (**Figure 4.1a**). In minocycline treated animals at the lesion site and contralateral to the injury, there was an increase of Iba-1ir with concentrations around the intermediolateral nuclei, the edges of the tissue, as well as within the ventral funiculus especially close to the ventral medial fissure (**Figure 4.1a** and **4.10**). Visual comparison of the minocycline with control saline-treated mice 7 days post-SCI injury to shams resulted in an increase of Iba-1ir ipsilateral to the injury at the lesion site (**Figure 4.1b** and **4.10**). Contralaterally, Iba-1ir was less intense and tiled the tissue especially surrounding the ventromedial lateral nuclei and ventral funiculus surrounding the ventral medial fissure (**Figure 4.1b**). Treatment with minocycline 7 days post-SCI when compared to control saline treatment resulted in an increase of Iba-1ir ipsilateral to the injury which was concentrated within the white matter especially surrounding the injury site, the ventral medial fissure, and surrounding the ventral funiculus (**Figure 4.1b**). Contralateral to the injury, in mice treated with minocycline, there was an increase of Iba-1ir perilesionally concentrated around the intermediolateral nuclei, the edges of the tissue, as well as within the ventral funiculus especially close to the ventral medial fissure (**Figure 4.1a** and **4.10**).

Visual comparison of Iba-1ir in mice treated 1-hour and 7 days post-SCI with minocycline showed similar expression, however, there was more Iba-1ir cells surrounding the intermediolateral nuclei (**Figure 4.1**). Through qualitative analysis, it was found that ipsilateral to the lesion and at the lesion site there was an increase of Iba-1ir MPIA when comparing SCI to sham across all treatments ($P < 0.001$, **Figure 4.2c**). There was a significant reduction in the expression of Iba-1ir MPIA in both 1-hour and 7-day minocycline treated mice compared to saline controls ($P < 0.001$, **Figure 4.2c** and **4.11**). Interestingly, there was no effect due to the day of minocycline treatment ($P = 0.574$), or as expected, in the saline controls ($P = 0.902$, **Figure 4.2c** and **4.11**). Contralateral to the lesion and at the lesion site, there was a significant increase of Iba-1ir MPIA when comparing SCI to sham ($P < 0.001$, **Figure 4.2d** and **4.11**). There was no significance between treatment 1-hour post-SCI and treatment 7 days post-SCI ($P = 0.443$), or saline and minocycline treatments ($P = 0.077$, **Figure 4.2d** and **4.11**).

4.2 Minocycline treatment results in a difference of 5-HT expression and reduces Iba-1 expression rostral and ipsilateral to the injury

Visual observation of the shams treated with minocycline or saline 1-hour and 7 days post-SCI rostral to the lesion site showed similar 5-HTir within the intermediolateral nuclei, ventral horn, and surrounding the central canal (**Figure 4.3**). Iba-1ir was observed to be similar (see also Chapter 3; **Figure 4.3**).

In control saline SCI animals (administered 1-hour post-SCI), there was a decrease in 5-HTir ipsilateral and rostral to the injury within the ventral horn (**Figure 4.3a**). However, within the intermediolateral nuclei, 5-HTir appeared the same in both shams and control saline mice treated 1-hour post-SCI (**Figure 4.3a**). Comparing control saline treatment of SCI (administered 1-hour post-SCI) to the shams, there was a significant reduction in 5-HTir ($P < 0.01$, **Figure 4.4**).

Contralateral to the injury, there was an increase in 5-HTir within the ventral horn when comparing control saline treatment administration to 1-hour post-SCI treated mice ($P < 0.001$, **Figures 4.3a** and **4.4**). Comparing minocycline treatment administered 1-hour post-SCI with sham mice ipsilaterally, there was no visual change in 5-HTir within the ventral horn, surrounding the central canal, and within the intermediolateral nuclei ($P = 0.397$, **Figure 4.3a**; **Figure 4.4**). In addition, there was no difference in 5-HTir within the ventral horn, intermediolateral nuclei or surrounding the central canal (**Figure 4.3a**) which was confirmed by measuring MPIA ($P = 0.700$, **Figure 4.5**). 7-day post-SCI minocycline treatment showed a decrease in ipsilateral 5-HTir within the ventral horn (**Figure 4.3b**) compared to shams. Expression of 5-HTir surrounding the central canal, within the intermediolateral nuclei rostral to the lesion, and both ipsilateral and contralateral to the injury, were similar (**Figure 4.3b**). MPIA analysis confirmed these findings ($P < 0.001$, **Figure 4.4b** and **4.10**). Contralateral to the injury, there was an increase in 5-HTir within the ventral horn (**Figure 4.3b**). Qualitatively, this resulted in a significant increase of 5-HTir ($P < 0.001$, **Figure 4.4b** and **4.10**). Minocycline administration 7 days post-SCI produced a decrease in 5-HTir ipsilateral and rostral to the injury site within the ventral horn (**Figure 4.3b**). This resulted in a significant decrease in the 5-HTir ($P < 0.001$, **Figure 4.4a** and **4.10**). However, contralateral to the injury, there was an increase of 5-HTir within the ventral horn when minocycline was administered 7 days post-SCI relative to sham mice ($P < 0.001$, **Figures 4.3b**, **4.4b** and **4.10**).

Comparing minocycline treatments, there was an observable difference between treatments. First, 5-HTir decreased when SCI was treated with minocycline 7 days post-SCI compared to 1-hour post-SCI ipsilateral to the injury (**Figure 4.3**). This was visually apparent within the ventral horn (**Figure 4.3** and **4.4c**). In addition, the contralateral 5-HTir increased in 7-day compared to 1-hour treated mice (MPIA, $P < 0.001$, **Figures 4.3**, **4.4d** and **4.11**).

Rostral and ipsilateral to the injury site, there was a visual increase in Iba-1ir within the lateral funiculus as well as ventral funiculus saline-treated SCI (1-hour post-SCI) and sham mice (MPIA, $P < 0.001$, **Figures 4.3a** and **4.4c**). Contralateral to the injury, there was a modest increase of Iba-1ir compared to ipsilateral to injury (**Figure 4.3a**), but this was not statistically significant ($P = 0.895$, **Figure 4.4d** and **4.10**). There was an increase in Iba-1ir rostral and ipsilateral to the injury in mice treated 1-hour post-SCI with minocycline compared to shams (MPIA, $P < 0.001$, **Figures 4.3a**, **4.4c** and **4.10**). Contralateral to the injury, there was Iba-1ir within the ventral funiculus surrounding the ventral lateral fissure and the central canal (MPIA, $P = 0.509$, **Figures 4.3a**, **4.4d** and **4.10**). Comparing control saline treatment 7 days post-SCI with both shams, there was an increase of Iba-1ir ipsilateral and rostral to the injury (**Figure 4.3b**). Contralaterally, Iba-1ir increased overall relative to shams and expression (**Figure 4.3b**). However, significant changes of Iba-1ir were found contralateral and rostral to the injury ($P = 0.895$, **Figure 4.4d** and **4.10**).

Iba-1ir was reduced, treated with minocycline both 1-hour post-SCI and 7 days post-SCI ipsilateral, rostral to the injury (MPIA, $P < 0.001$, **Figures 4.3b**, **4.4c** and **4.11**). Iba-1ir was similar in both treatments rostral to the injury (**Figure 4.3**) with an increase of Iba-1ir ipsilateral and contralateral to the injury within the white matter surrounding the ventral medial fissure being observed (**Figure 4.3**). No significance was found between treatments 1-hour and 7 days post-SCI within saline (MPIA, $P = 0.509$) or within minocycline (MPIA, $P = 0.390$) administration (**Figure 4.4d**) contralaterally.

4.3 Minocycline treatment increases caudal 5-HT and decreases Iba-1 mean expression intensity ipsilateral to injury.

Similar expression of 5-HTir within the intermediolateral nuclei, the ventral horns, and surrounding the central canal was observed in both 1-hour and 7-day shams (**Figure 4.5**). Iba-1ir was found to have a tiled expression (**Figure 4.5**).

Caudal to the injury, comparing treatment with saline 1-hour post-SCI to the shams showed a significant decrease in the expression of 5-HTir ipsilateral to the injury within lamina VII and VIII and within the ventral horn (MPIA, $P < 0.001$, **Figures 4.5a** and **4.6a**). Contralateral to the injury and caudal to the lesion site, there was a similar expression of 5-HTir relative to both shams (MPIA, $P = 0.542$, **Figures 4.5a** and **4.6b**). Comparing minocycline administration 1-hour post-SCI with control saline treatment, there was more 5-HTir ipsilateral to the injury within the ventral horn (**Figure 4.5a**). Contralateral expression of 5-HTir remained similar in both minocycline and control saline administration 1-hour post-SCI mice (**Figure 4.5a**). There was a significant decrease in the expression of 5-HTir ipsilateral to the injury, notably in the ventral horn, in 7-day post-SCI saline-treated animals compared to shams (**Figure 4.5b**). Caudal and ipsilateral to the lesion site, there was a significant decrease in 5-HTir between shams and 7-day post-SCI administration of control saline ($P < 0.001$, **Figure 4.6a** and **4.10**). Contralateral to the injury and caudal to the lesion site, there was a similar expression of 5-HT relative to both shams when visually assessed (MPIA, $P = 0.997$, **Figure 4.6b** and **4.10**). Comparing minocycline administration 7 days post-SCI with saline treatment SCI, there was an increase of 5-HTir ipsilateral to the injury within the ventral horn (**Figure 4.5b**). Contralateral to the injury, however, 5-HTir was similar in both saline-treated and sham mice (**Figure 4.5b**).

Minocycline administration in the 1-hour post-SCI versus 7-day post-SCI mice resulted in an increase of 5-HTir in the earlier treatment ipsilateral to the lesion site which was prominent within lamina VIII (**Figure 4.7**). Contralateral expression of 5-HTir remained similar in both treatments (**Figure 4.7**). There was an increase of 5-HTir MPIA when comparing injuries in both treatment 1-hour post-SCI ($P < 0.001$) and 7-days post-SCI treatment ($P < 0.001$, **Figure 4.6b** and **4.11**). In addition, there was also an increase of 5-HTir MPIA when 1-hour post-SCI minocycline was applied compared to day 7 post-SCI ($P < 0.001$, **Figure 4.6b** and **4.11**).

Treatment with saline 1-hour post-SCI resulted in an increase of Iba-1ir tiled expression (MPIA, $P < 0.001$, **Figures 4.5a** and **4.6**). On the other hand, when 1-hour post-SCI minocycline treatment was compared to control saline treatment, there was still an expression of Iba-1ir tiling the section (**Figure 4.5a**). This increase was also observed ipsilateral to the injury with minocycline treatment ($P < 0.001$, **Figure 4.6c** and **4.10**). Minocycline treatment delivered 7 days post-SCI resulted in an increase of Iba-1ir ipsilateral to the injury concentrated within the white matter (**Figure 4.5b**). Contralateral and caudal to the injury in minocycline treated mice, there was an increase of Iba-1ir expression compared to shams (**Figure 4.5b**). Treatment with saline 7 days post-SCI injury compared to the sham expression resulted in a decrease of Iba-1ir ipsilateral and caudal to the injury(**Figure 4.5b**). Contralateral to the lesion site, Iba-1ir was decreased when treated with saline 7 days post-SCI (**Figure 4.5b**).

Visual comparison of 1-hour post-SCI versus 7-days post-SCI minocycline treated mice showed similar Iba-1ir contralateral to the injury site (**Figure 4.5**). Overall, there was a significant reduction in Iba-1ir MPIA in both saline and minocycline treated mice ($P < 0.001$, **Figure 4.6** and **4.11**). When comparing 1-hour post-SCI with 7-days post-SCI saline-treated mice, no differences

were found in Iba-1ir (P = 0.0621, saline; P = 0.689, minocycline, **Figure 4.6**). Contralateral and caudal to the injury, there was no significant change of Iba-1ir (P = 0.601, **Figure 4.6d**).

4.4 Expression of serotonin and microglia/macrophage surrounding motoneurons post-SCI after minocycline treatments

I next examined the motoneurons at the lesion site, contralaterally, rostral to the lesion site and caudal to the lesion site. Bilaterally to the injury, each region was imaged (**Figures 4.7 - 4.9**). At the lesion site contralaterally, there was no difference between the treatments (**Figure 4.7**). When minocycline was delivered at 7 days post-SCI, there was higher Iba-1ir compared to when minocycline was delivered 1-hour post-SCI (**Figure 4.7**). Rostral to the injury, there was no difference in 5-HTir between treatments surrounding motoneurons (**Figure 4.8**). There was an observable difference in 5-HTir between saline and minocycline treatment overall when observing expression surrounding motoneurons (**Figure 4.8**). However, there was an increase in Iba-1ir cells surrounding the motoneurons in minocycline treated animals (**Figure 4.8**). No differences in time of minocycline treatment and Iba-1ir were found (**Figure 4.8**). Caudal and ipsilateral to the lesion site, there was a reduction in 5-HTir surrounding motoneurons (**Figure 4.9**). Iba-1ir decreased when minocycline was administered compared to saline controls (**Figure 4.9**). Treatment 1-hour post-SCI with minocycline resulted in more 5-HTir around motoneurons caudal to the lesion (**Figure 4.9**). Contralateral to the injury, there was more 5-HTir for all treatments when compared to ipsilateral expression (**Figure 4.9**). There was less Iba-1ir when treated with minocycline 1-hour post-SCI versus other treatments (**Figure 4.9**).

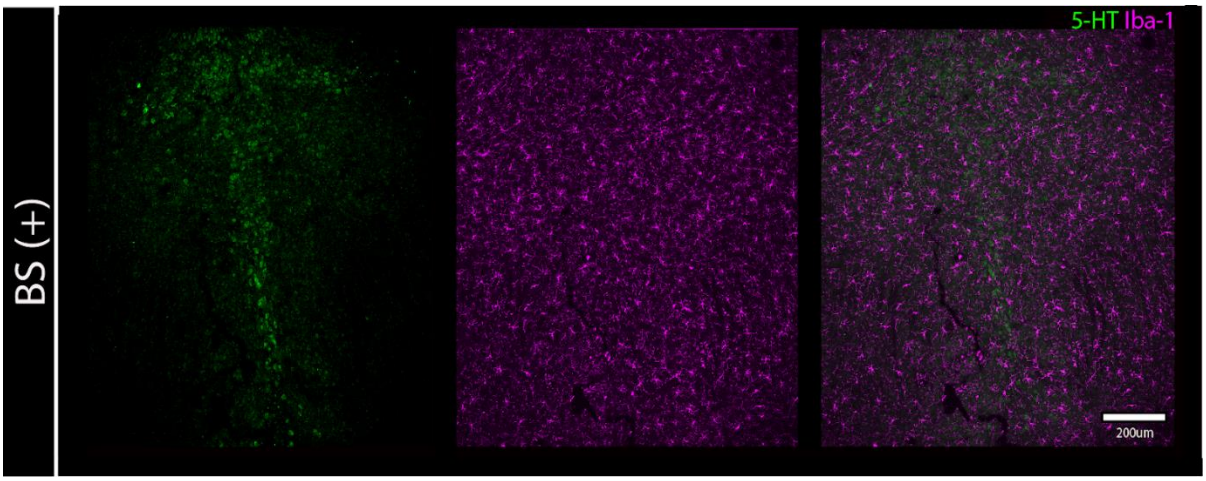

Figure 3.1: Serotonin and microglia/macrophage positive immunostaining in the brainstem. Brainstem showing expression of 5-HT (green) and microglial/macrophage Iba-1 (magenta) in the raphe obscurus nuclei (positive control, Bregma -5.02 mm). Raphe nuclei, 5-HT positive, are organized into a triangular shape within the brainstem and project down into the spinal cord innervating all levels. The raphe nuclei are a positive control for immunostaining. Iba-1ir in this region was observed to tile the brainstem (scale: 200 µm).

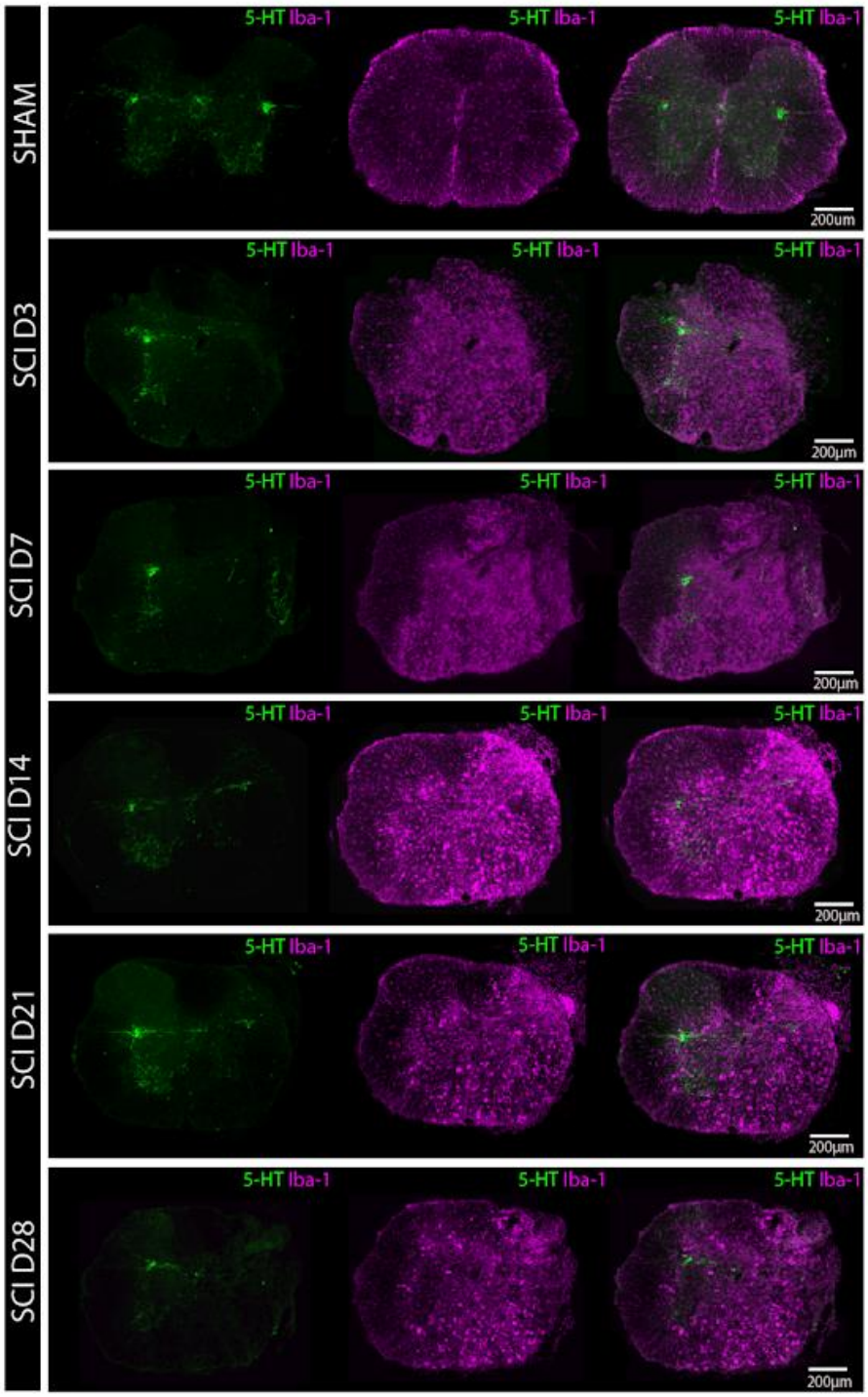

Figure 3.2: Serotonin decreases ipsilateral to the injury site when compared to shams. Immunostaining results comparing the difference between days 3, 7, 14, 21 and 28 (n = 4) injuries to shams (n = 20), at the lesion site. Spinal cord injuries are to the right of all images. 5-HTir (green) staining was found to decrease ipsilateral to the injury and contralateral remained similar to sham expression. Microglia/macrophage staining (Iba-1ir: magenta) remained uniform, tiling the spinal cord sections in the shams. Iba-1ir increased starting on day 3 through day 14 relative to the shams and days 21 and 28.

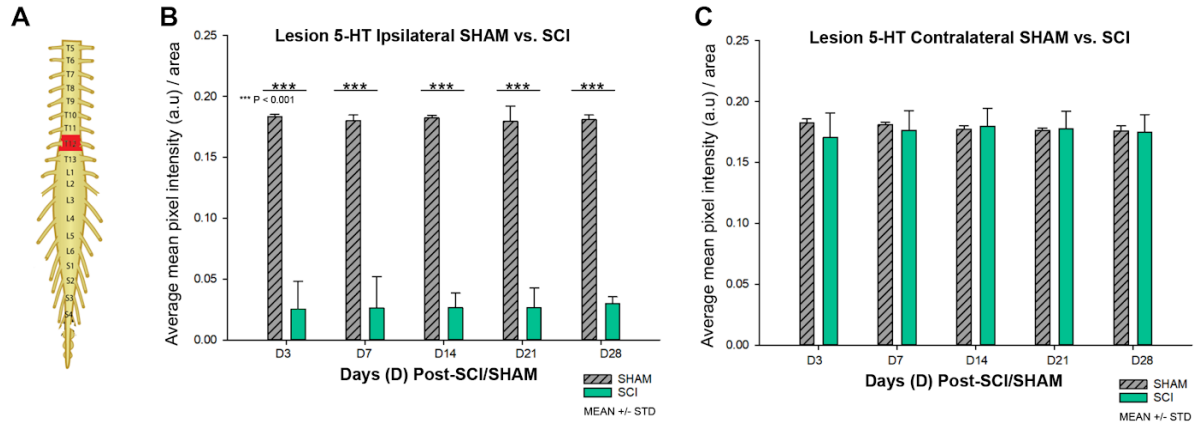

Figure 3.3: Serotonin expression is decreased at the lesion site following SCI. 5-HT MPIA significantly decreased ipsilaterally but not contralaterally. **(A)** Schematic showing lesion site at T12. **(B)** 5-HTir decreased ipsilaterally in SCI compared to sham animals ($P < 0.001$, Two-way-ANOVA, Holm-Sidak method, $n = 4$). **(C)** No change in 5-HTir MPIA was observed contralaterally ($P = 0.614$, $n = 4$).

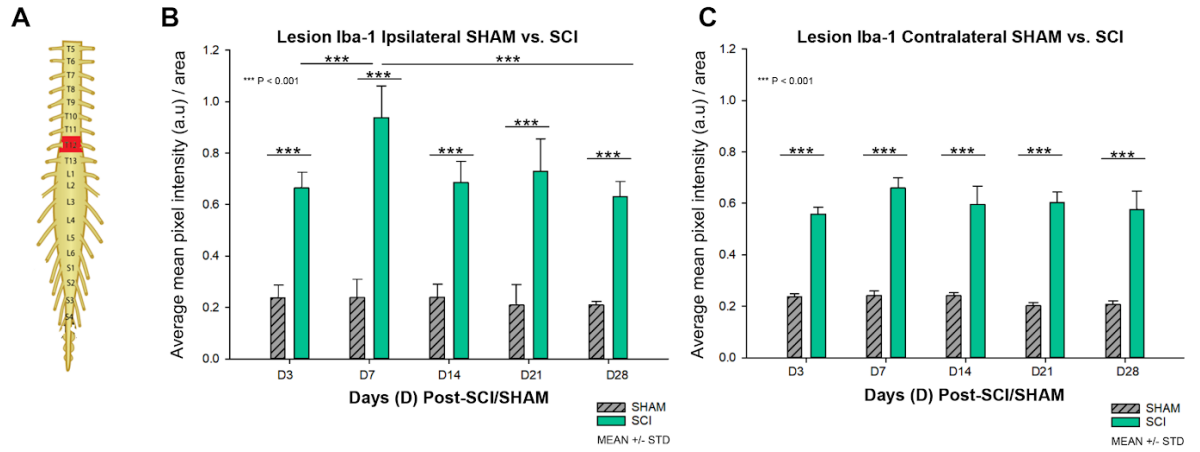

Figure 3.4: Microglia/macrophage expression is significantly changed ipsilateral and contralateral to the lesion. **(A)** Schematic showing the lesion site at T12. **(B)** Iba-1ir levels were quantified using ImageJ analysis of mean pixel intensity per area (MPIA) selected (ipsilateral to injury, $n = 4$). There was a significant increase in Iba-1 MPIA when compared to sham for all days ($P < 0.001$, Two-way ANOVA). There was also a notable peak of Iba-1 MPIA at day 7 relative to both days 3 and 28 ($P < 0.001$, Holm-Sadak method). **(C)** Contralateral to the lesion site, Iba-1 MPIA was found to increase significantly compared to expression in shams across all days ($P < 0.001$, Two-way ANOVA, Holm-Sadak method, $n = 4$).

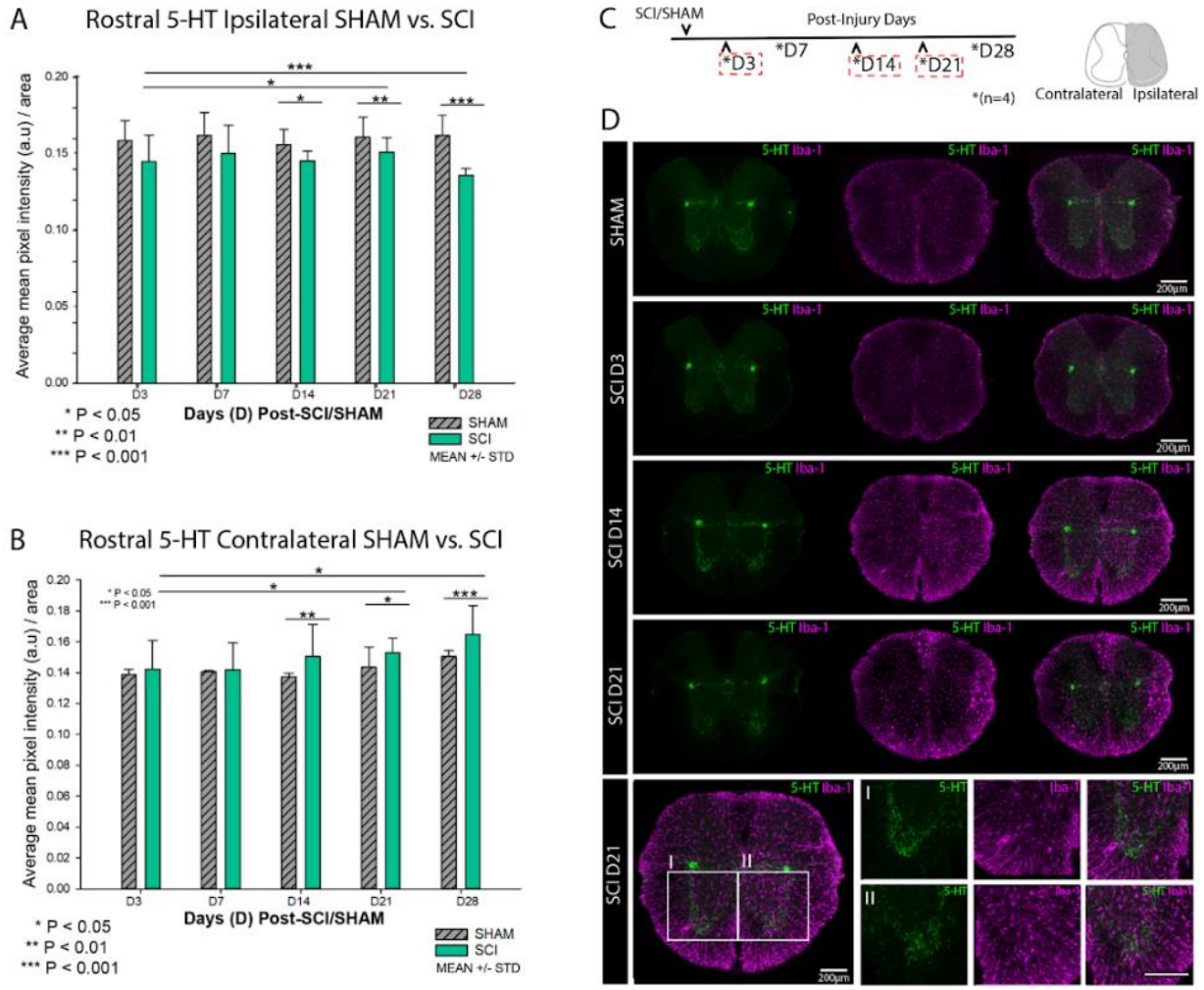

Figure 3.5: Serotonin expression decreases ipsilaterally and increases contralaterally rostral to the lesion site following SCI. **(A)** Ipsilateral to the injury, 5-HT MPIA showed a significant decrease at D14 ($P < 0.05$), 21 ($P < 0.01$), and 28 ($P < 0.001$) between sham and SCI (Two-way ANOVA, Holm-Sidak method, n = 4). In addition, there was pairwise significance between days 3 and 21 ($P < 0.01$) and days 3 and 28 ($P < 0.001$, Two-way ANOVA). **(B)** Contralateral to the lesion site, 5-HT MPIA was observed to increase between sham and SCI at days 14 ($P < 0.001$), 21 ($P < 0.05$), and 28 ($P < 0.001$, Two-way ANOVA, Holm-Sidak method). In addition, there was significance pairwise observed between days 3 and 21 as well as days 3 and 28 ($P < 0.005$, Two-way-ANOVA, n = 4). **(C)** Schematic diagram showing the post-injury data collection over days 3, 7, 14, 21 and 28 (n = 4 each) with days 3, 14, and 21 highlighted for comparison. Spinal cord legend indicates ipsilateral to injury is on the right of all images. **(D)** Immunostaining results comparing the difference between days 3, 14, and 21 (n = 4) between shams and injuries, rostral (2.4 mm) to the lesion site. 5-HTir increased rostral and contralateral to the lesion in injury versus sham and between days 3, 14, and 21. 5-HTir decreased ipsilaterally day 14 and 21 (n = 4). Iba-1ir remained uniformly tiling the spinal cord sections in the shams and day 3 post-SCI. Iba-1ir increased ipsilateral on day 3 and 14 relative to the shams. In addition, when comparing day 14 ipsilateral (B, bottom row) versus contralateral (A, bottom row), there was higher 5-HTir and of Iba-ir ipsilateral to the injury site (n = 4, scale: 200 µm).

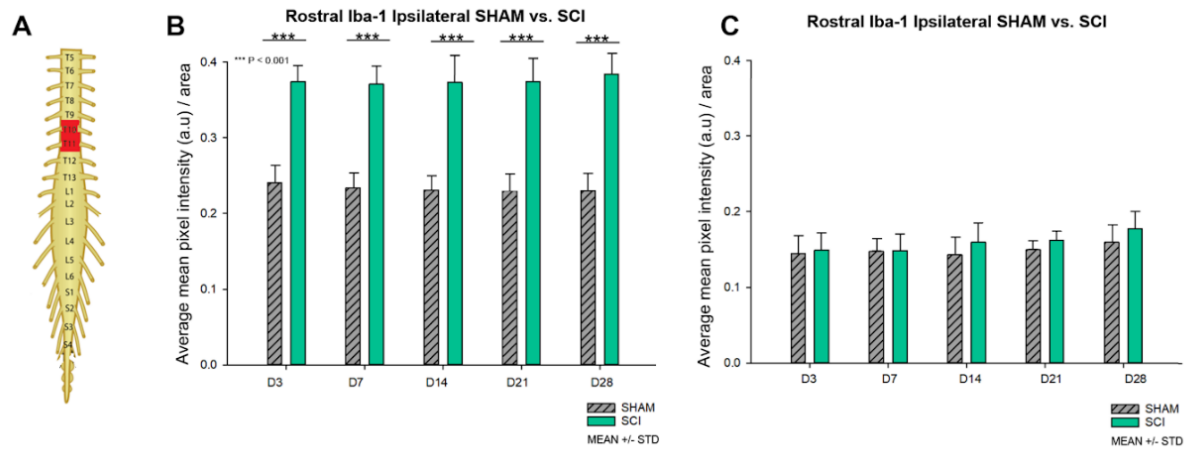

Figure 3.6: Rostral to the injury, an increase of microglia/macrophage is observed ipsilaterally. **(A)** Schematic showing the area rostral to the lesion at T10-T11. **(B)** Iba-1 MPIA ipsilateral to injury was observed to increase significantly relative to sham expression of Iba-1 ($P < 0.001$, Two-way ANOVA, $n = 4$). **(C)** Iba-1 MPIA contralateral to injury was found to have no statistically significant difference of expression between sham and SCI or between days ($P = 0.519$, Two-way ANOVA, Holm-Sidak method, $n = 4$).

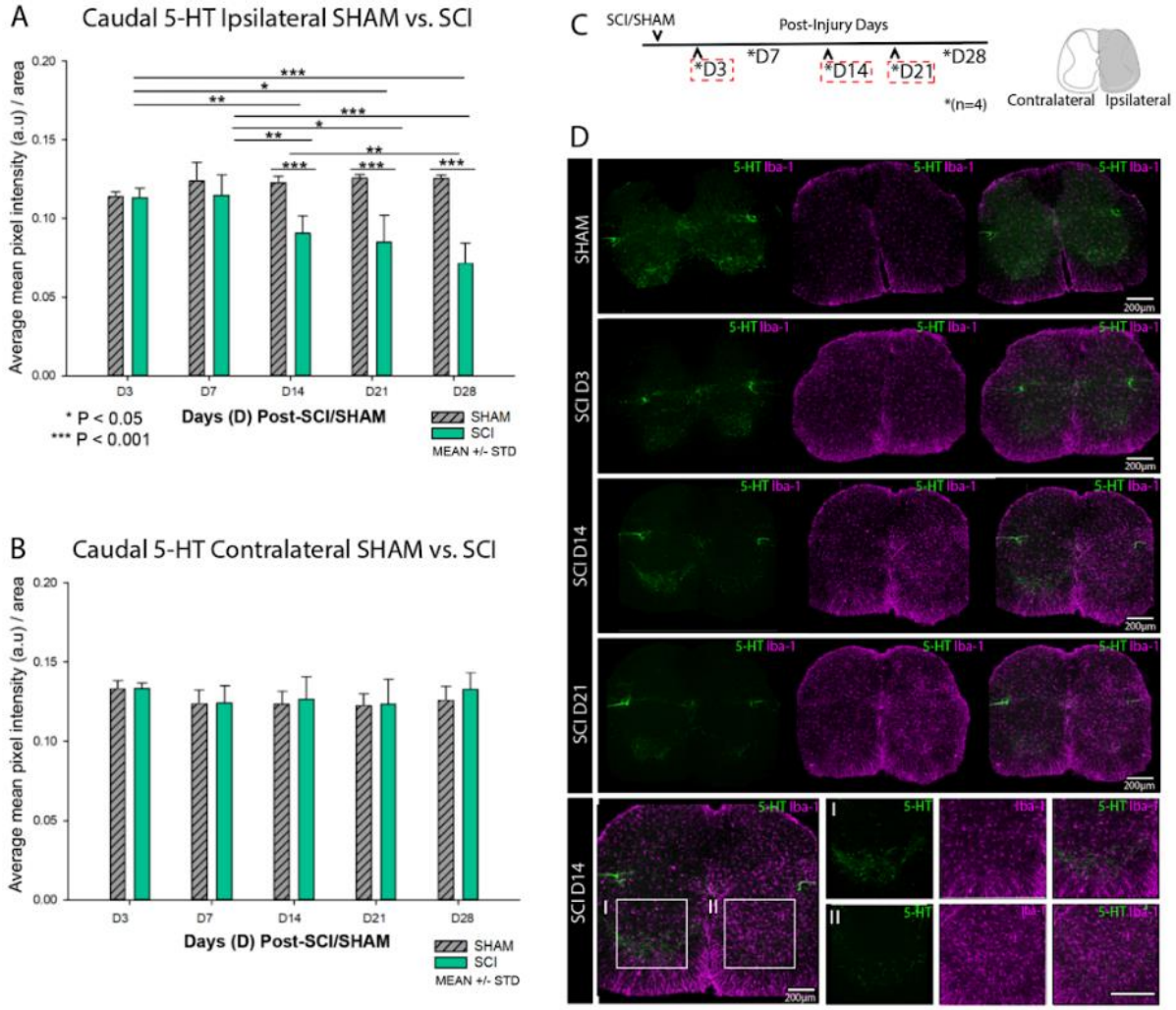

Figure 3.7: Serotonin expression decreases caudal to the lesion site following SCI. Caudal to the lesion site, a significant decrease in 5-HT MPIA was observed ipsilaterally but not contralaterally. **(A)** 5-HT MPIA significantly decreased between sham and SCI days 14, 21 and 28 ($P < 0.001$, Holm-Sidak method, $n = 4$). It was also observed that there was a significant decrease of 5-HT MPIA between injury day 3 versus 21, day 3 versus 28, day 7 versus 21, and day 7 versus 28 ($P < 0.05$). **(B)** Contralateral to the lesion site, significant decrease between sham and injury on days 3 ($P < 0.001$) and 28 ($P = 0.002$). Otherwise, there was no significant change in 5-HT MPIA for days 7 ($P = 0.783$), 14 ($P = 0.138$) or 21 ($P = 0.693$, $n = 4$). **(C)** Schematic diagram showing the post-injury data collection over days 3, 7, 14, 21 and 28 ($n = 4$ each) with days 3, 14, and 21 highlighted for comparison. Spinal cord legend indicates ipsilateral to injury is on the right of all images. **(D)** Immunostaining results comparing the difference between days 3, 14, and 21 ($n = 4$) between sham and injuries caudal (2.6 mm) to the lesion site. 5-HTir decreased caudal and ipsilateral to the lesion in injury versus sham, and between days 3, 14, and 21. Iba-1ir remained uniform tiling the center of the spinal cord sections and higher expression observed around the edges in the shams and day 3. On days 14 and 21, Iba-1ir intensified ipsilateral to the injury site. 5-HTir decreased (bottom row) ipsilateral to the injury relative to a contralateral and higher level of Iba-1ir ipsilateral to the injury site ($n = 4$, scale: 200 µm).

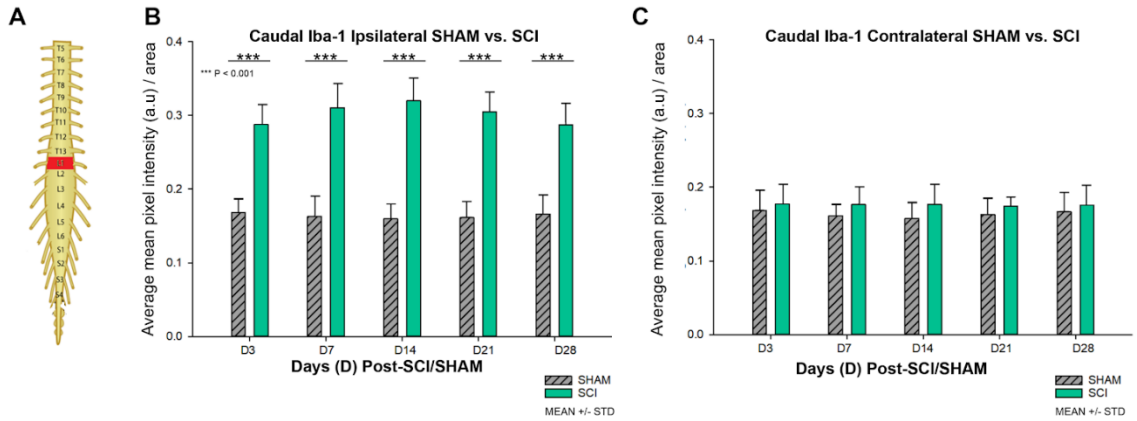

Figure 3.8: Microglia expression increases at the lesion site following SCI. A significant increase of Iba-1 MPIA was observed ipsilaterally but not contralaterally caudal to the lesion. **(A)** Schematic showing area caudal to the lesion site at L1. **(B)** A significant increase of Iba-1 MPIA was observed across all days comparing sham to SCI ($P < 0.001$). In addition, Iba-1 MPIA was found to peak at day 7 when comparing injury days 3 and 7 as well as days 7 and 28 ($P < 0.001$, Two-way ANOVA, n=4). **(C)** Contralateral to the lesion site, there was an observable difference of expression between sham and injury for all days, respectively ($P < 0.001$, Two-way ANOVA, n = 4).

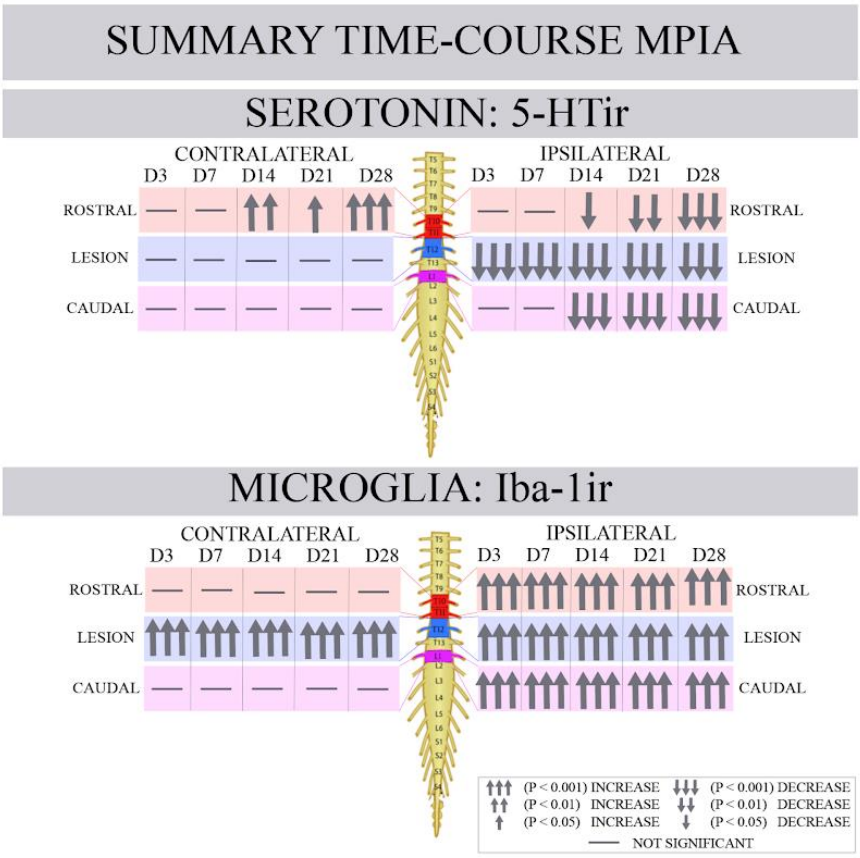

Figure 3.9: Summary of significant time-course MPIA data for 5-HTir and Iba-1ir. When comparing 5-HTir expression SCI versus sham, we observed a significant decrease ipsilateral to the injury at the lesion site across all days, caudal starting day 14, and rostral, contralateral to the lesion starting day 14. Rostrally and ipsilaterally, there was an increase of 5-HTir observed starting day 14 post-SCI. When looking at Iba-1ir, there was a significant increase across all days ipsilateral to the injury as well as contralateral to the lesion alone.

.

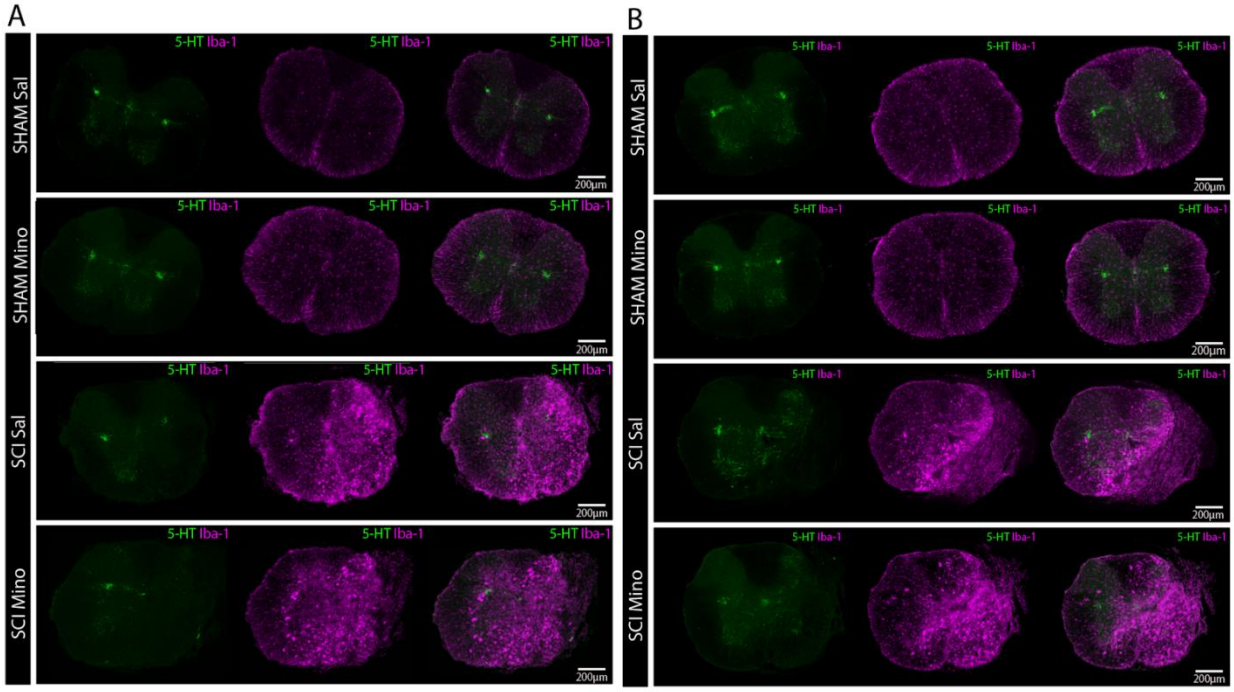

Figure 4.1: Serotonin expression decreased and microglia/macrophage expression increased at the lesion when treated with minocycline. **(A)** Immunostaining results comparing the difference of shams (n = 4) and treatments with control saline injections and minocycline injections 1-hour post-SCI at the lesion site. Shams (n = 4) for both saline and minocycline are similar in serotonin (5-HTir: green) staining and microglia/macrophage (Iba-1ir: magenta) staining. Injuries resulted in a decrease of 5-HTir and increased Iba-1ir ipsilateral to injury for both treatments. **(B)** Immunostaining results comparing the difference of shams (n = 4) and treatments with control saline injections and minocycline injections 7 days post SCI at the lesion site. Shams (n = 4) for both saline and minocycline are similar in 5-HTir and Iba-1ir. Injuries resulted in a decrease of 5-HTir and increased Iba-1ir ipsilateral to injury for both treatments. In addition, there was no visual change in expression between treatments at the lesion site (n = 4, scale: 200 µm).

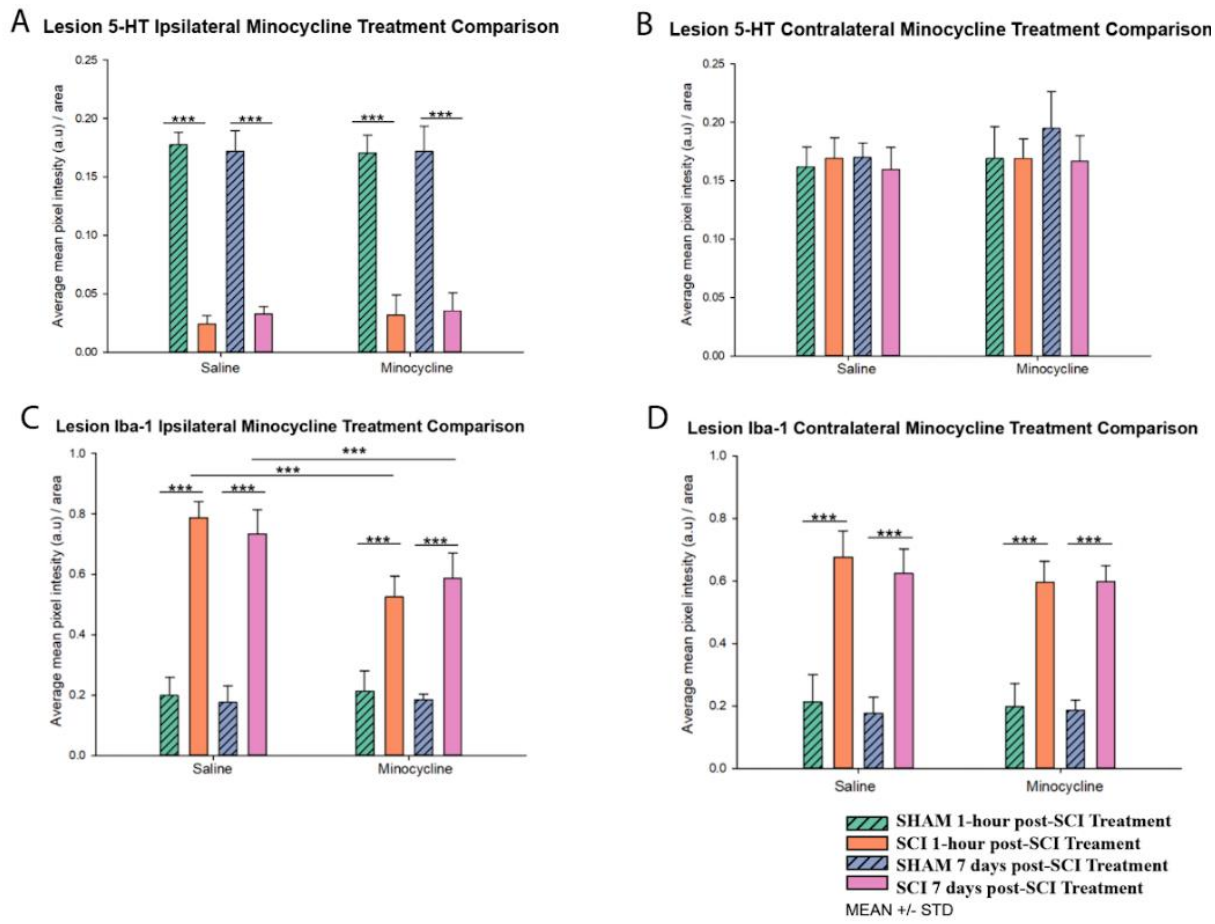

Figure 4.2 Serotonin and microglia/macrophage expression decreased at the lesion site. A significant reduction in the amount of 5-HT MPIA was observed ipsilaterally, but not contralateral to the injury when minocycline was administered post-SCI on day 21. **(A)** A significant reduction of 5-HT MPIA was observed when comparing sham versus SCI across all treatments ($P < 0.001$, Two-way ANOVA, $n = 4$), respectively, ipsilateral to the injury at the lesion site. **(B)** Contralateral to the injury at the lesion site, there was no significant change in 5-HT MPIA between sham and SCI or between treatments ($P = 0.738$, Two-way ANOVA, Holm-Sidak method, $n = 4$). **(C)** Ipsilateral to the lesion at the lesion site, there was a significant increase Iba-1 MPIA sham versus SCI across all treatments ($P < 0.001$, Two-way ANOVA, Holm-Sidak method, $n = 4$). There was also a significant decrease of Iba-1 MPIA between saline and minocycline treatments ($P < 0.001$) and a significant reduction in the amount of Iba-1 MPIA when treated 1-hour post-SCI with minocycline as opposed to 7 days post-SCI ($P < 0.001$, Two-way ANOVA, Holm-Sidak method, $n = 4$). **(D)** Contralateral to the lesion site at the lesion site, there was a significant increase of Iba-1 MPIA sham versus SCI across all treatments ($P < 0.001$, Two-way ANOVA, Holm-Sidak method, $n = 4$).

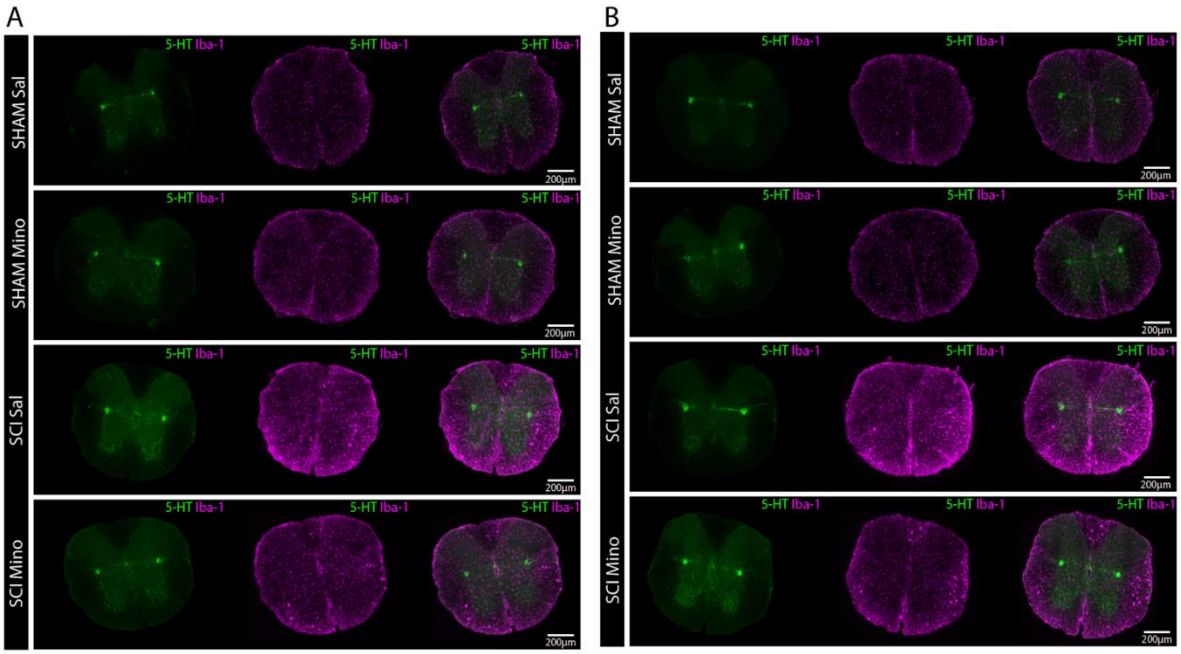

Figure 4.3: Microglia/macrophage and serotonin expression decreased rostral to the lesion site when SCI was treated with minocycline treatment. **(A)** Immunostaining results comparing the difference of shams (n = 4) and treatments with control saline injections and minocycline injections 1-hour post-SCI rostral (2.4 mm) to the lesion site. Shams (n = 4) for both saline and minocycline are similar in serotonin (5-HTir: green) and microglia/macrophage (Iba-1ir: magenta). Injuries resulted in an increase of 5-HTir and Iba-1ir, ipsilateral to injury for saline control treatments. However, a reduction in expression for both 5-HTir and Iba-1ir with the administration of minocycline was apparent. **(B)** Immunostaining results comparing the difference of shams (n = 4) and treatments with control saline injections and minocycline injections 7 days post-SCI rostral. Shams (n = 4) for both saline and minocycline were similar in 5-HTir and Iba-1ir. Injuries resulted in an increase of 5-HTir and Iba-1ir ipsilateral to injury for saline control treatments. There was a reduction in the expression of Iba-1ir with the administration of minocycline 7 days post-SCI. However, there was increased Iba-1ir and 5-HTir in the delayed treatment condition when you compare minocycline treatment 1-hour post-SCI (A) with 7 days post-SCI, (n = 4, scale: 200 µm).

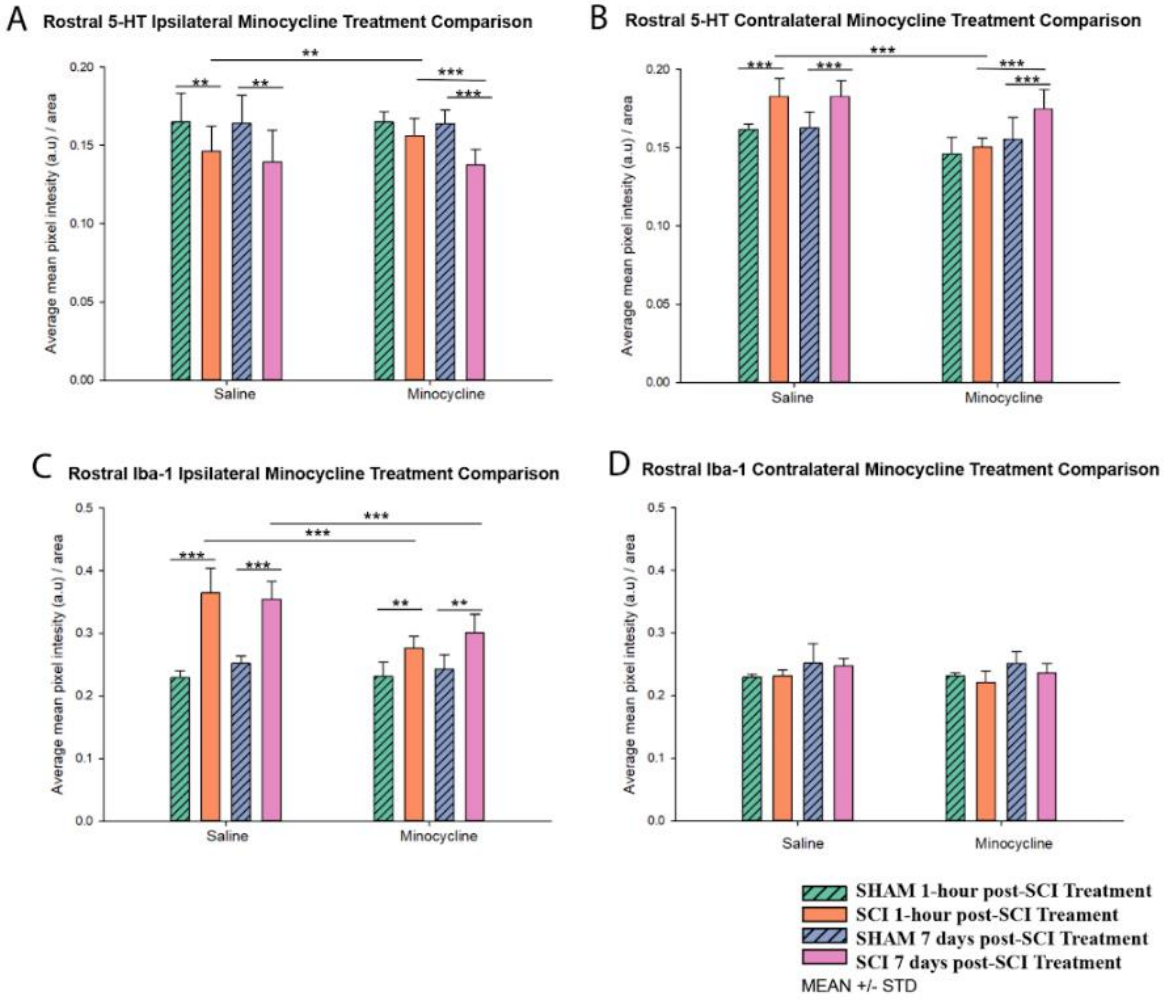

Figure 4.4: Minocycline administration changed serotonin expression rostral to the injury and decreased microglia/macrophage expression ipsilaterally. Rostral to the injury, a significant effect of minocycline on 5-HT MPIA was observed ipsilaterally and contralaterally on day 21, reducing microglia/macrophage MPIA rostral and ipsilateral to the lesion site. **(A)** Ipsilateral and rostral to the injury, there was a significant decrease in the amount of 5-HT MPIA comparing sham versus SCI in saline treatment 1-hour post-SCI, saline treatment 7 days post-SCI, and minocycline treatment 7 days post-SCI ($P < 0.01$, Two-way ANOVA, $n = 4$). A significant increase of 5-HTir minocycline administered 1-hour post-SCI was observed when compared to saline treatment ($P < 0.001$) as well as a significant increase comparing treatment 1-hour post-SCI versus 7 days post-SCI ($P < 0.001$, Two-way ANOVA, Holm-Sidak method, $n = 4$). **(B)** Contralateral and rostral to the injury, there was a significant increase of 5-HT MPIA when comparing sham versus SCI for saline treatments 1-hour and 7 days ($P < 0.001$, Two-way ANOVA, $n = 4$) as well as minocycline treatment 7 days post-SCI ($P < 0.05$, Two-way ANOVA, $n = 4$). There was a significant decrease in the 5-HT MPIA within minocycline treatment 1-hour post-SCI and a significant decrease when comparing minocycline treatment 1-hour post-SCI with 7 days post-SCI ($P < 0.001$, Two-way ANOVA, Holm-Sidak method, $n = 4$). **(C)** Ipsilateral and rostral to the lesion, there was a significant increase of Iba-1 MPIA between sham and SCI in the saline control treatment ($P < 0.001$) and minocycline treated injuries ($P < 0.01$, Two-way ANOVA, $n = 4$). Overall, there was a significant reduction of Iba-1 MPIA when comparing saline control treatment versus minocycline treatments ($P < 0.001$, Two-way ANOVA, Holm-Sidak method, $n = 4$). **(D)** Contralateral and rostral to the lesion, there was no significant change of Iba-1 MPIA ($P = 0.693$, Two-way ANOVA, Holm-Sidak method, $n= 4$).

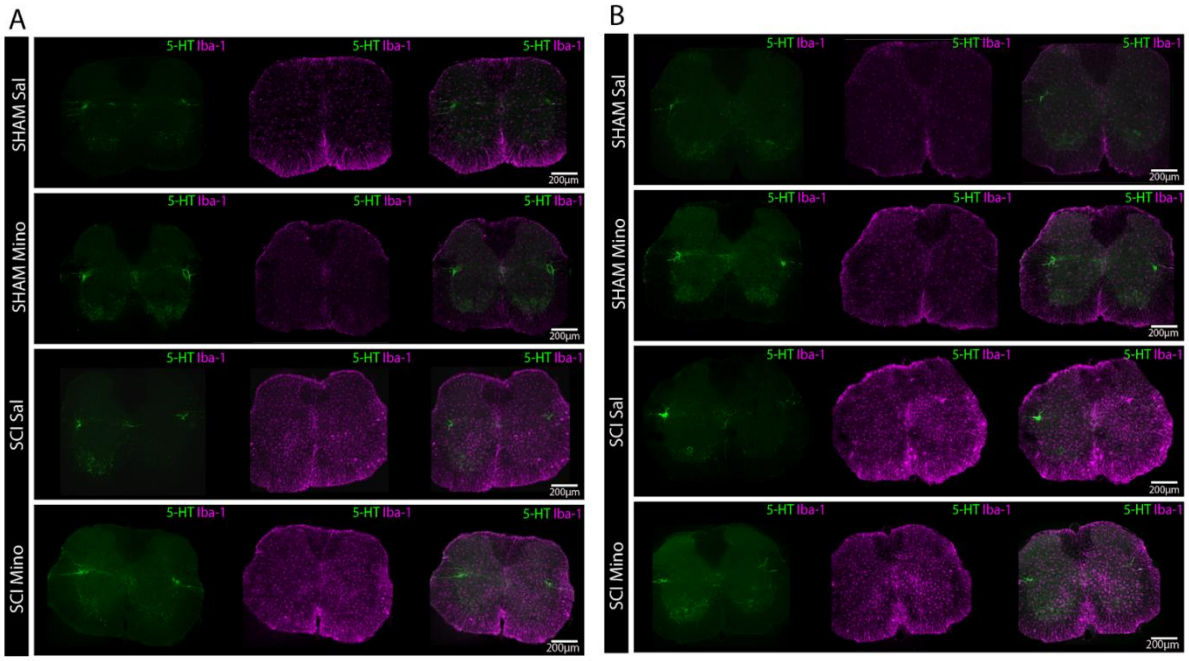

Figure 4.5: Serotonin expression increases caudal to the lesion site with minocycline. 5-HTir increased caudal and ipsilateral to the lesion site when SCI is treated with minocycline. **(A)** Immunostaining results comparing the difference of shams (n = 4) and treatments with control saline injections and minocycline injections 1-hour post-SCI caudal (2.6 mm) to the lesion site. Shams (n = 4) for both saline and minocycline were similar in 5-HTir and Iba-1ir staining generally having an outline of positive Iba-1ir around the tissue. Injuries resulted in a decrease of 5-HTir ipsilateral to the injury for both injuries. However, more 5-HTir was retained when minocycline treatment is applied. Iba-1ir appears to be similar visually when comparing saline to minocycline treatment. **(B)** Immunostaining results comparing the difference of shams (n = 4) and treatments with control saline injections and minocycline injections 7 days post-SCI caudal (2.6 mm) to the lesion site. Shams (n = 4) for both saline and minocycline were similar in 5-HTir and Iba-1ir, generally having an outline of positive Iba-1ir around the tissue. Injuries resulted in a decrease of 5-HTir ipsilateral to the injury for both injuries. 5-HTir has higher expression when minocycline treatment was applied. No differences in Iba-1ir when comparing saline to minocycline treatment were evident. When comparing treatment 1-hour post-SCI versus day 7 post-SCI there was increased 5-HTir and reduced Iba-1ir at 1-hour administration (n = 4, scale: 200 µm).

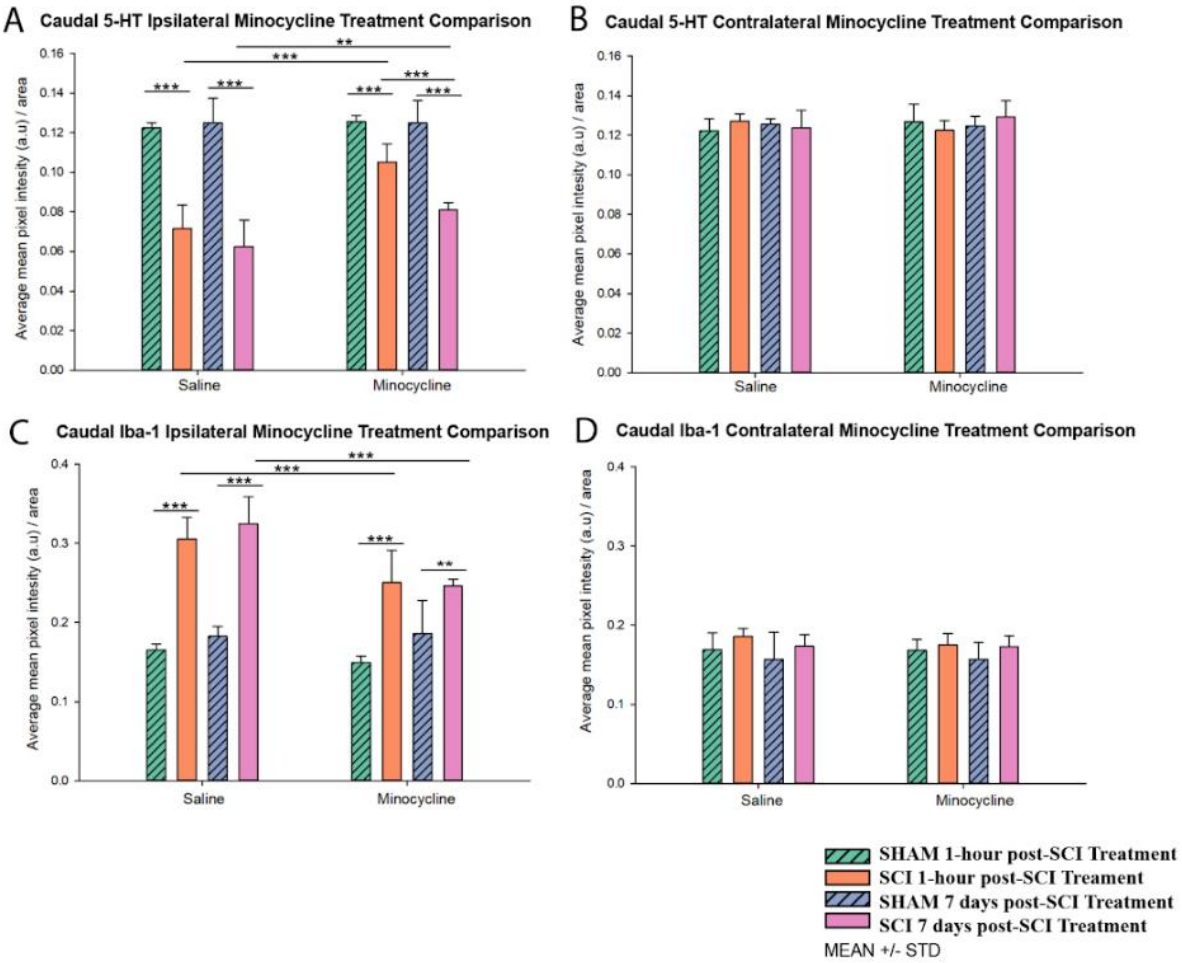

Figure 4.6: Minocycline administration increased expression of serotonin and reduced microglial expression caudal to the lesion. Caudal to the injury, a significant effect of treatment with minocycline on 5-HT MPIA is observed ipsilaterally and no significance observed contralaterally on day 21. **(A)** Ipsilateral and caudal to the injury, a significant decrease in the amount of 5-HT MPIA comparing sham to SCI across all treatments ($P < 0.001$, Two-way ANOVA, Holm-Sidak method, $n = 4$). In addition, it was found that there was a significant increase of 5-HT MPIA when comparing minocycline 1-hour post-SCI administration to saline ($P < 0.001$) and treatment 7 days post-SCI ($P < 0.01$, Two-way ANOVA, $n = 4$). Treatment with minocycline 7 days post-SCI caused 5-HT MPIA to significantly increase compared to saline treatment ($P < 0.001$, Two-way ANOVA, Holm-Sidak method, $n = 4$). **(B)** Contralateral and caudal to the injury, there was no significant change observed in 5-HT MPIA ($P = 0.932$, Two-way ANOVA, Holm-Sidak method, $n = 4$). **(C)** Ipsilateral and caudal to the lesion site, there was a significant increase of Iba-1 MPIA between sham and injury across all treatments ($P < 0.001$ for all but minocycline treated 7 days post-SCI $P < 0.01$, Two-way ANOVA, $n = 4$). In addition, there was a decrease observed between treatment with control saline and minocycline treatments ($P < 0.001$, Two-way ANOVA, Holm-Sidak method, $n = 4$). **(D)** Contralateral and caudal to the lesion site, there was no significant change of Iba-1 MPIA ($P = 0.928$, Two-way ANOVA, Holm-Sidak method, $n = 4$).

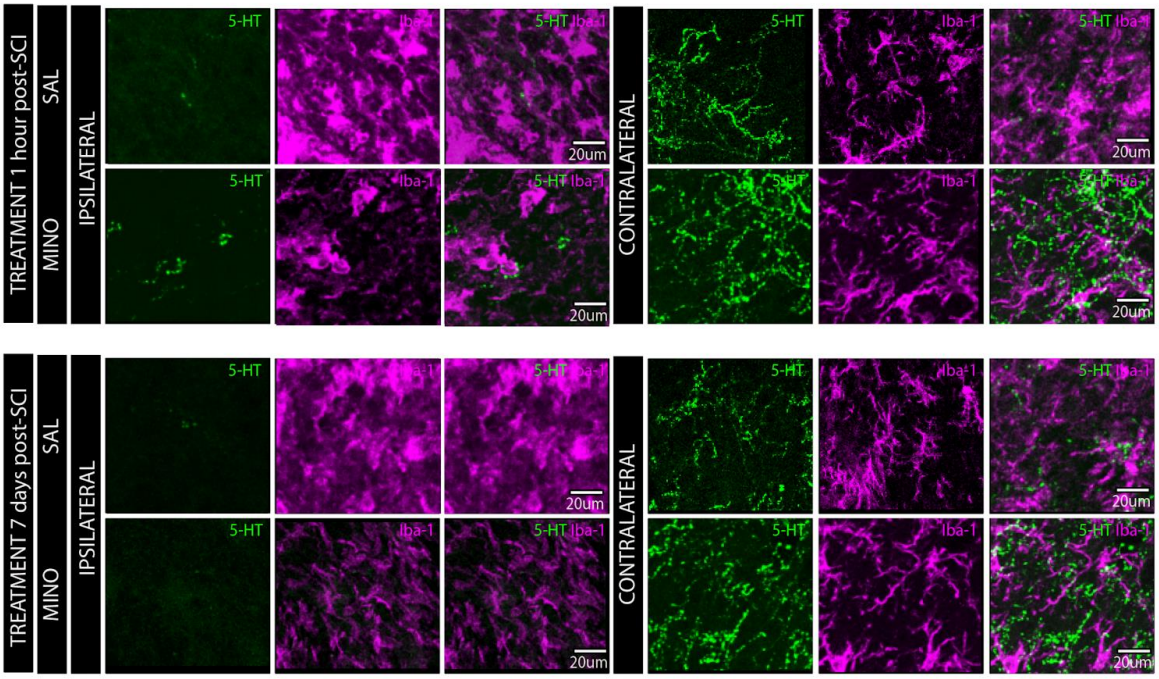

Figure 4.7: Minocycline treatment reduced serotonin and microglia/macrophage expression surrounding motoneurons at the lesion site contralaterally. There was reduced serotonin expression at the lesion site ipsilaterally and reduced microglia/macrophage expression when treated with minocycline. 5-HTir (green) staining and Iba-1ir (magenta) staining around motoneurons show that there was a reduction in Iba-1ir expression when minocycline treatment was applied to SCI. However, when looking at 5-HT expression at the lesion site, there was still little expression. Contralateral to the lesion site, visually there was no difference between saline control treatment and minocycline treatments in terms of 5-HTir or Iba-1ir, respectively (n = 4, scale: 20 µm).

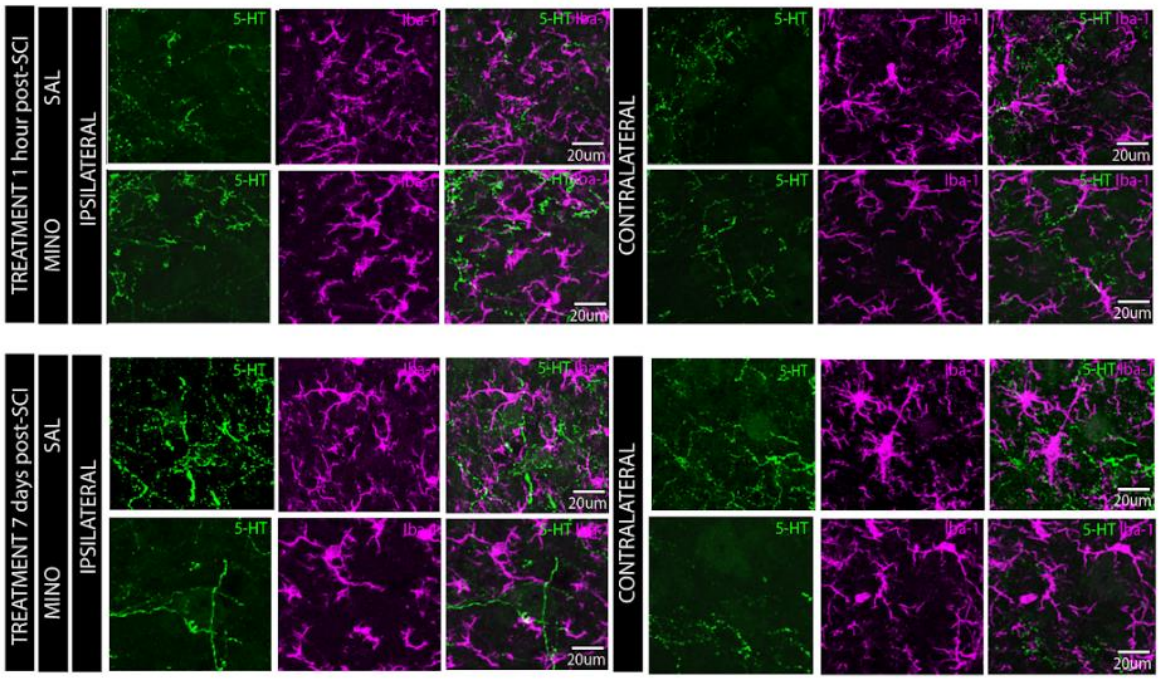

Figure 4.8: Minocycline treatment reduced microglia expression surrounding motoneurons rostral to the lesion site. Iba-1 expression decreased surrounding motoneurons rostral to the lesion site when SCI is treated with minocycline. 5-HTir (green) and Iba-1ir (magenta) around motoneurons showed that there was a reduction in Iba-1ir when minocycline treatment is applied to SCI rostral (2.4 mm) to the lesion site. There was an overall higher expression of Iba-1 ipsilateral to the injury versus contralateral. No differences in 5-HTir were visually apparent (n = 4, scale: 20 μm).

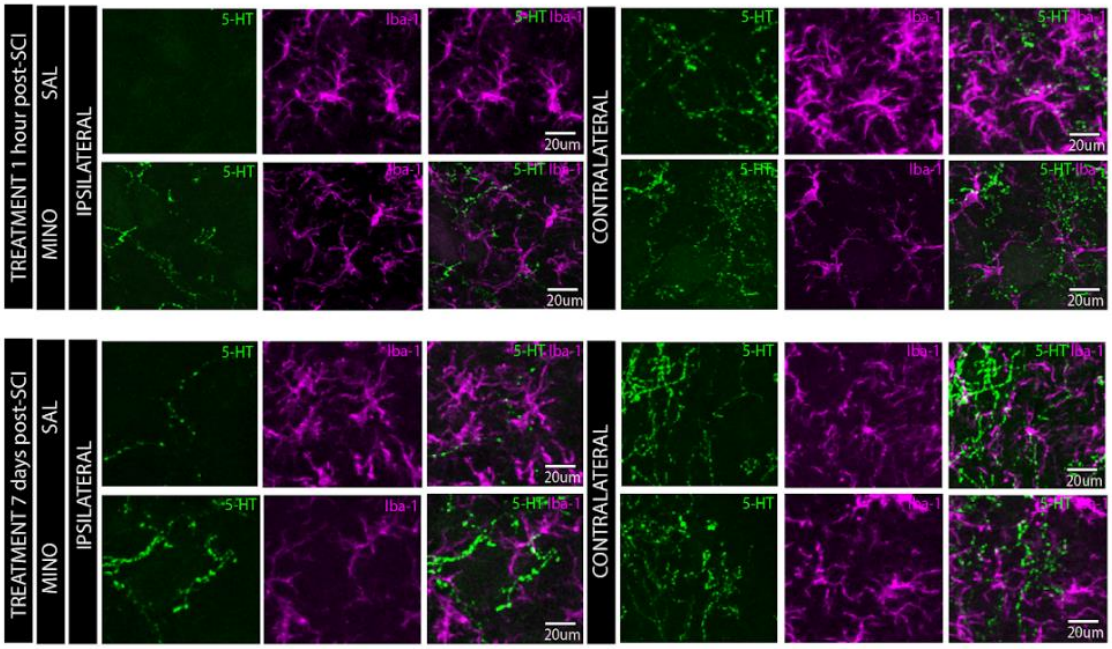

Figure 4.9: Minocycline treatment increased serotonin expression surrounding motoneurons caudal to the lesion site. 5-HTir increased caudal and ipsilateral to the lesion site surrounding motoneurons when SCI is treated with minocycline. Ipsilateral and caudal (2.6 mm) to the lesion site there was an increase in 5-HTir (green) surrounding motoneurons when comparing control saline treatments to minocycline treatment. In addition, there was more 5-HTir when treatment of minocycline is applied 1-hour post-SCI versus 7 days post-SCI, ipsilateral to the injury. Contralateral to the injury there appears to be more Iba-1ir (magenta) expression in saline control treatments versus minocycline treatments (n = 4, scale: 20 µm).

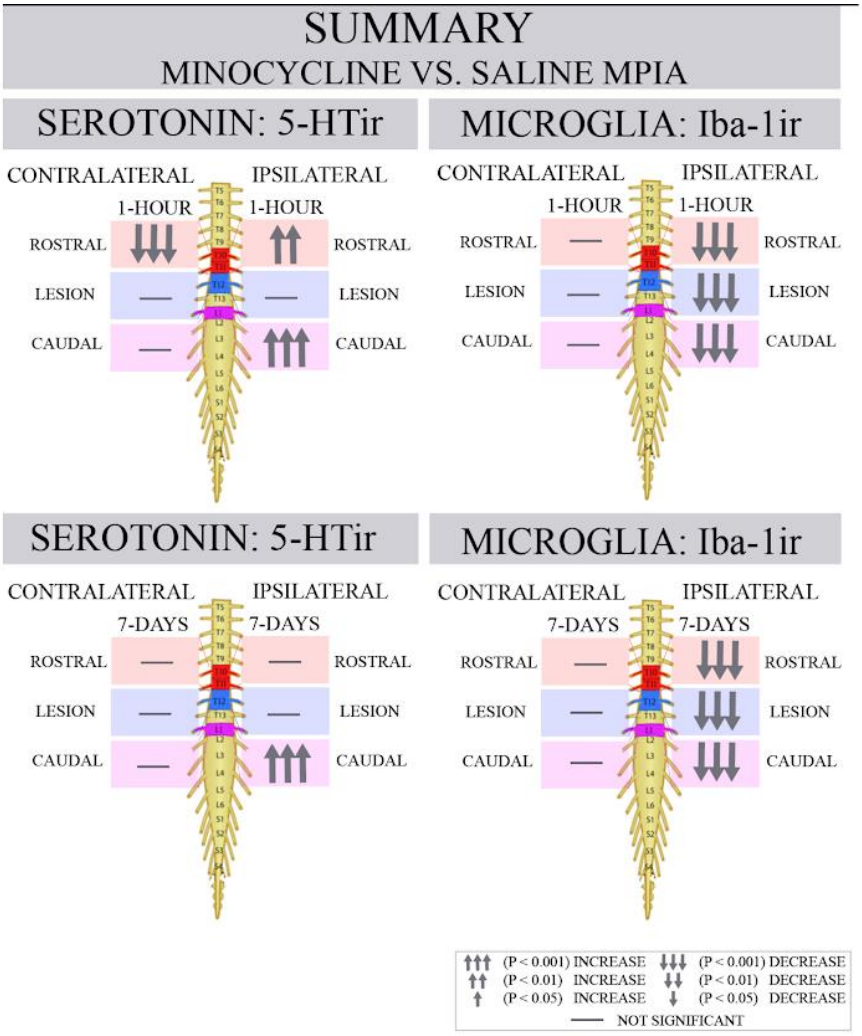

Figure 4.10: Summary comparing minocycline treatment to saline treatment MPIA. **1-hour** post-SCI administration of minocycline resulted in increased 5-HTir ipsilateral to the injury both rostral and caudal to the lesion compared to saline. In addition, a reduction of 5-HTir was observed contralateral and rostral to the lesion. Iba-1 expression decreased ipsilaterally across all regions. **7-days** post-SCI administration of minocycline resulted in an increase of 5-HTir rostral and caudal, ipsilateral to the injury. Iba-1ir decreased at all levels when compared to saline treatment.

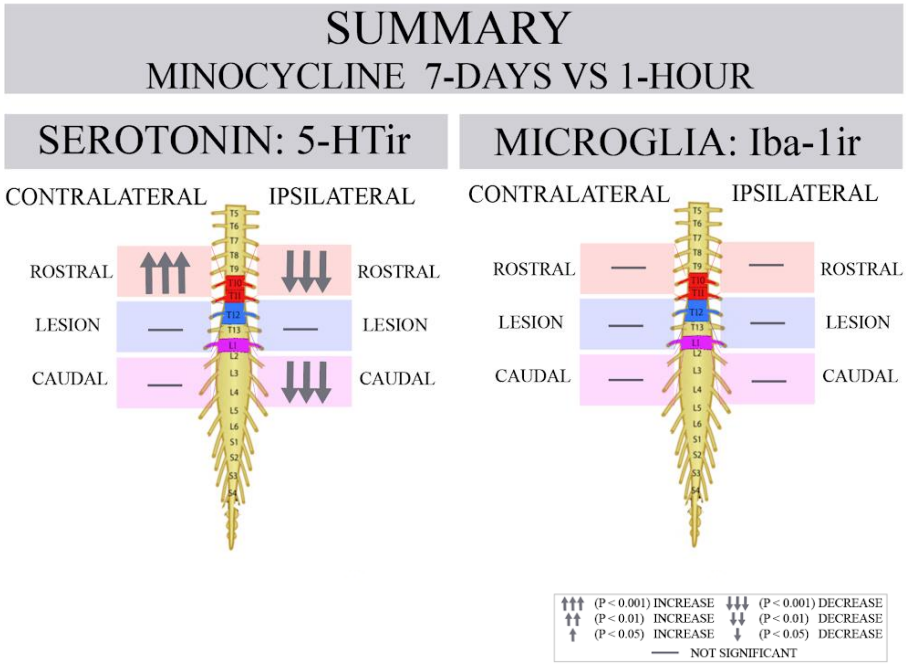

Figure 4.11: Summary of minocycline administration 7 days versus 1-hour post-SCI. When comparing 7-days post-SCI administration of minocycline compared to 1-hour post-SCI, there was a decrease in 5-HTir both rostral and contralateral to the injury as well as caudal and ipsilateral to the injury. However, an increase rostrally and ipsilaterally was observed. Iba-1ir, however, was not different when comparing treatments.

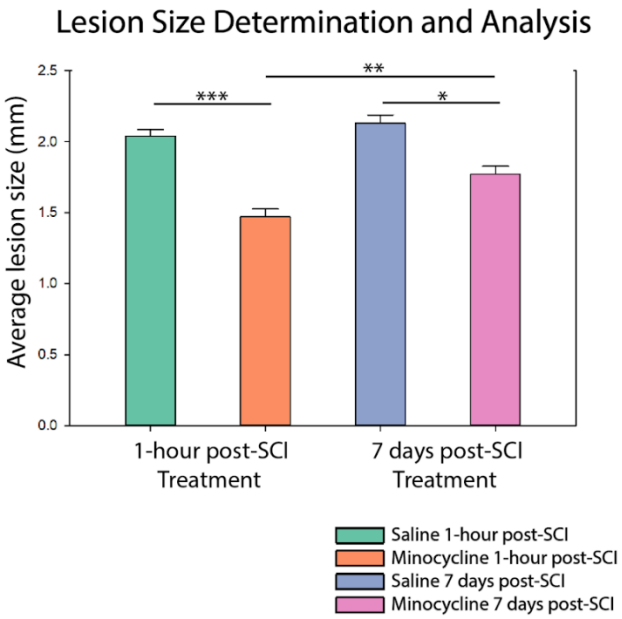

Figure 4.12: Lesion size determination analysis. Lesion size was determined using lesion sections obtained as outlined in chapter 2. Comparison between 1-hour post-SCI saline and minocycline ($P < 0.001$), 7 days post-SCI saline and minocycline ($P = 0.029$), and 1-hour post-SCI minocycline and 7 days post-SCI minocycline ($P = 0.010$) resulted in a significant difference in lesion size (Student's t-test, $n = 4$). Comparison between 1-hour post-SCI saline and 7 days post-SCI saline ($P = 0.279$) resulted in no significant difference (Student's t-test, $n=4$).

CHAPTER 5: DISCUSSION

5.1 Overview of findings

The goal of my thesis was to determine if delayed administration of minocycline would cause an increase of 5-HTir post-SCI and be comparable, if not more effective, when compared to immediate administration. To accomplish this, my thesis was divided into three aims. The first aim was to acquire a time-line (Chapter 2) to observe both 5-HTir and Iba-1ir following a hemisection of the spinal cord. The second aim was to administer minocycline 1-hour post-SCI (Wells et al. 2003) to test effects on both 5-HTir and Iba-1ir. The third aim, based upon my findings in the first and second, was to administer minocycline (Chapter 2) at day 7 post-SCI to examine the changes in 5-HTir and Iba-1ir. In my first aim, I found that a marked decrease in 5-HTir took place on day 14, caudal to the lesion, where I also observed an increase in Iba-1ir. In my third aim, the administration of minocycline increased 5-HTir and decreased Iba-1ir (**Figures 4.5 - 4.6** and **4.10**), caudal to the lesion, by day 14. What I did not anticipate was that 5-HTir decreased ipsilaterally, and increased contralateral and rostral to the lesion (**Figures 3.5** and **4.3 - 4.4** and **4.10**). Additionally, there was no difference in the effects of minocycline rostrally on 5-HTir when administered 7 days later. In aim 3, 5-HTir was increased and Iba-1ir decreased, ipsilateral and caudal to the lesion, and comparatively greater effects were observed when minocycline was administered 1-hour post-SCI (**Figures 4.5, 4.6,** and **4.10**). Overall, this thesis has demonstrated that minocycline treatment increased 5-HTir levels and decreased Iba-1ir levels post-SCI, and is more effective at increasing 5-HTir when administered immediately post-SCI versus 1-week post-SCI. When looking at motoneuron association with Iba-1ir cells, there was an increased expression in control-saline versus minocycline treated SCI. Interestingly, we observed an increase in Iba-1ir caudal and ipsilateral to the lesion in association with increased 5-HTir. Therefore, my data suggest

that day 7 post-SCI treatment may be an alternative treatment time-point based upon the location and severity of the injury. But this will need further work to assess behavior.

5.2 Changes in 5-HTir and Iba-1ir after SCI

Incomplete traumatic SCI is a dynamic process involving temporary or complete loss of function below the injury. In uninjured rodents, 5-HTir is found within the intermediolateral nuclei, surrounding the central canal, within the dorsal horn and within lamina I and II (Watson C., Paxinos G., and Kayaliglu G., 2009). The spinal cord is innervated by numerous 5-HT fibers along the whole length of the spinal cord, particularly in the ventral horn (Murray et al., 2010), which correlates with the sham data that I collected (**Figures 3.2 - 3.8**; **4.1 - 4.6**). Interruption of supraspinal axons that control voluntary movements and axons that provide neuromodulators, like 5-HT, leads to loss of motor control (Jordan et al., 2008, Heckmann et al., 2005, Carlsson et al. 1963). I confirmed these findings when I found a significant decrease of 5-HTir ipsilaterally at and caudal to the lesion, particularly within the ventral horn (**Figures 3.2** and **3.3**; Carlsson et al. 1963, Hashimoto and Fukuda 1991, Fouad et al., 2005, Jordan et al. 2008, Ghosh et al. 2009, Martinez and Rossignol 2011, Rossignol and Frigon, 2011, El Manira, 2014, Filli et al., 2014). These spared descending connections can also sprout below the injury site, which, in animal models has been linked to recovery (Ballermann and Fouad, 2006, Weidner et al., 2001, Fouad et al., 2010). Rostral to the lesion, 5-HTir increased contralaterally and decreased ipsilaterally to the injury starting on day 14 in the ventral horn (**Figure 3.5**). Rostral compensation of 5-HT has been reported previously, and lesioned axons sprout above the lesion site forming new connections and utilize the spared pathways to relay input (Bareyre et al., 2004, Courtine et al., 2007, Vavrek et al., 2006, Fouad et al., 2010).

Early activation of resident microglia around the lesion site occurs post-SCI, followed by the infiltration of macrophages (Popovich at al.,1998). This correlates with my results where Iba-1ir increased bilaterally at and caudal to the lesion site, and ipsilaterally and rostral to the lesion as early as day 3 (**Figures 3.2** and **3.4**; **3.5 - 3.8**). In addition, Iba-1 MPIA peaked on day 7 bilaterally at the lesion site (**Figures 3.2** and **3.4**; Giulian and Robertson, 1990, Blight, 1992, Popovich at al., 1998, Popovich et al., 1999, Bellver-Landete et al., 2019). After SCI, resident microglia is one of the first cell lines to respond (see Chapter 1), releasing cytokines and chemokines to recruit more microglia and macrophages to the site of injury (Li and Barres, 2018). There are beneficial roles in microglia activation after traumatic SCI, for example, clearing the site of injury of debris through phagocytosis, recruiting other microglia and macrophages to the injury site through the release of pro-inflammatory cytokines, and the release of anti-inflammatory cytokines (Prewitt et al., 1997, Rabchevsky and Streit, 1997, Hauben et al., 2000, Kigerl et al., 2009, Stirling and Yong, 2008, Bellver-Landete et al., 2019). Approaches to SCI treatment include reducing secondary injury processes that occur over days to weeks and promoting regeneration (Wells et al., 2003, Thomas and Gorassini, 2005, Ballermann and Fouad, 2006, Stirling and Yong, 2008). Only 10% of spinal cord regenerated axons are required to significantly improve functional recovery (Blight, 1983, Fehlings and Tator, 1995, Wells et al., 2003). Wells et al., (2003) found that minocycline administration 1-hour post-SCI increased long-term recovery in mice suffering from SCI and prevented axonal degeneration. I manipulated microglia activity post-SCI and targeted a time-point at which 5-HTir was reduced at and caudal to the lesion site. Because I observed a change rostrally in 5-HTir, I examined the effects of minocycline administration based on this change. Spontaneous recovery following incomplete SCI can lead to functional improvements in motor function in both humans and animal models (Barbeau et al., 2002, Lee et al., 2003, Wells et al.,

2003, Teng et al., 2004, Stirling et al., 2004, Thomas and Gorassini, 2005, Ballermann and Fouad, 2006, Festoff et al., 2006, Fouad et al., 2010). Minocycline as a treatment for SCI is considered to be of use in human patients and has completed phase II clinical trials (Kwon et al., 2011, Casha et al., 2012). It decreases microglia and macrophage activity, therefore sparing white and grey matter and decreasing apoptosis, and has applications in human SCI patient treatment (Kwon et al., 2011, Casha et al., 2012). Minocycline has widespread effects in the CNS limiting pathology of diseases including multiple sclerosis (Brundula et al., 2002, Wells et al.. 2003, Stirling et al., 2004, Silver et al., 2014). Previous work found that minocycline administration in patients, compared to the placebo group, resulted in those patients experiencing greater motor recovery (Casha et al., 2012). Minocycline antagonizes specific parts of the immune system's response to SCI allowing for a more targeted influence without global depletion of inflammatory cells, which would render the patient immunocompromised. Based on these previous studies, and the impact that minocycline has on treating SCI, I examined differences in Iba-1ir and 5-HTir immediately and 1-week post-SCI (Chapters 2, 3, and 4).

5.3 Impact of minocycline treatment 1-hour post-SCI

Minocycline treatment reduces proliferation and activation of microglia and macrophages, which correlates with the data that I obtained in this thesis. Administration of minocycline 1-hour post-SCI (details in Chapter 2), significantly reduced Iba-1ir at the lesion site, and ipsilaterally in both the rostral and caudal directions (**Figures 4.1 - 4.6** and **4.10**; Yrjänheikki et al., 1998, Tikka and Koistinaho, 2001, Stirling et al., 2004). There are several reasons for this: a decrease in apoptosis would be expected as a decrease in caspase-dependent cell death (Chen et al., 2000, Wang et al., 2003), which may account for the increase in 5-HTir caudal and ipsilateral to the lesion when minocycline was applied (**Figures 4.5**, **4.6** and **4.10**; Lee et al., 2003, Stirling et al.,

2004). Administration of minocycline may decrease lesion size by lowering activation of caspase-3 which has been linked to apoptotic cell death post-SCI (Springer et al., 1999, Lee et al., 2003, Stirling et al., 2004). We observed a significant decrease in lesion size with treatment with minocycline (**Figure 4.12**). The neuroprotective properties of minocycline treatment preventing axonal dieback and further tissue degradation would explain the observed increase in caudal expression of 5-HTir (**Figures 4.5** and **4.6**; Wells et al., 2003, Stirling et al., 2004). Inhibition of microglia and macrophage response may have prevented axonal dieback by inhibiting phagocytosis of the axonal growth cones or by reducing their activity, in turn reducing the release of axonal repellant or cytotoxic factors (Stirling et al., 2004). Minocycline reduces macrophage production of nitric oxide that can also attribute to axonal dieback (Amin et al., 1996, He et al., 2002, Stirling et al., 2004). I found no increase in 5-HTir expression at the lesion site, ipsilateral to the injury (**Figures 4.1**, **4.2** and **4.10**). However, it is previously reported that the lesion site is reduced in size when minocycline treatment is applied, due to its attenuation of the inflammatory response, where microglia rapidly accumulate around the site of SCI (Bethea et al., 1999, Oudega et al., 1999, Popovich et al., 1999, Lee et al., 2003, Wells et al., 2003, Bellver-Landete et al., 2019). From work presented in Chapter 3, I expected to see a change in rostral expression in 5-HTir, but I was surprised to see that the magnitude of the effect was dissimilar when applying minocycline 1-hour versus 1-week post-SCI (**Figures 4.3**, **4.4** and **4.11**). Stirling et al. (2004), found that there was progressive dieback that occurred not only caudal to the lesion site but also rostral to the injury. Caspase-3-positive apoptotic profiles were located at regions remote to the lesion site, which included rostral to the lesion (Stirling et al., 2004). This secondary degenerative response spreading from the lesion is what I also found both caudal as well as rostral, ipsilateral to the injury and helps to explain why I saw rostral increases of Iba-1ir in SCI with saline treatment (**Figures**

4.3, **4.4** and **4.10**). In addition, minocycline treatment significantly attenuates the number of these apoptotic profiles reducing secondary damage associated with SCI (Stirling et al., 2004). Reduction in the activity of microglia and macrophages post-SCI can reduce scarring and promote functional recovery along with axonal growth (Kotaka et al., 2017). Furthermore, Kigerl et al., (2009) found that at the lesion site, microglia display both pro- and anti-inflammatory markers and by day 28, predominantly pro-inflammatory markers. A prolonged pro-inflammatory response impedes tissue repair due to sustained activation of microglia or macrophages, in turn producing cytotoxic factors (Beck et al., 2010, Pajoohesh-Ganji and Byrnes, 2011, Prüss et al., 2011, Gaudet and Fonken, 2018, Kigerl et al., 2006). When microglia switch to an anti-inflammatory role, there is an improvement in neuroprotection, locomotor recovery, and phagocytosis (Francos-Quijorna et al., 2017). Long term activation of microglia, especially the switch to a dominantly pro-inflammatory response, has been found to improve anatomical connectivity and function. Therapeutic interventions that promote sprouting can be dependent on when they are administered but are crucially dependent on the intervention used (Houle and Ye, 1999). My goal was to investigate how delayed intervention with minocycline impacted the recovery of normal 5-HTir levels. 5-HTir caudal and ipsilateral to the lesion site was reduced (**Figure 4.4**). Hashimoto and Fukuda (1991), found that depletion of 5-HT in the lumbar cord distal to the injury site was observed 14 days after injury (c.f. Faden et al., 1988). I also observed a decrease ipsilateral and an increase contralateral to the injury at this time point (**Figures 4.3 - 4.4** and **4.10**). Microglia and macrophages secrete factors that help with neuroregeneration or neuroprotection post-SCI (Guth et al., 1994, Rapalino et al., 1998, Lee et al., 1999, Moalem et al., 1999, Hauben et al., 2000, Crutcher et al., 2006, Yin et al., 2006, Beck et al., 2010). In the study by Beck et al. (2010), they looked at phases involved in cellular inflammation, with macrophage and microglia activity

peaking at day 7, and reported that their influence, along with T-cells and neutrophils, lasted for 180 days post-SCI. Based upon the 5-HTir results, I administered minocycline 7 days post-SCI in order to have an effect on day 14 (Yrjänheikki et al., 1998, Sanchez Mejia et al., 2001, Brundula et al., 2002, Wells et al., 2003).

5.4 Impact of minocycline treatment 7 days post-SCI

I hypothesized that applying minocycline treatment would reduce Iba-1ir significantly when administered 7 days post-SCI (Yrjänheikki et al., 1998, Tikka and Koistinaho, 2001, Stirling et al., 2004). The associated peak of Iba-1ir occurs 7 days later, and therefore, I targeted day 14 post-SCI (Giulian and Robertson, 1990, Blight, 1992, Popovich et al., 1998, Popovich et al., 1999, Bellver-Landete et al., 2019). Bellver-Landete et al., (2019), showed that elimination of microglia leads to a reduction in growth factor production, glial scar formation, increased neuronal and oligodendrocyte death, and a reduction in locomotor performance. On the other hand, prolonged inflammation or excessive microglial activity can be detrimental to recovery (Serhan, 2007, David and Kroner, 2011). What I observed in this study was an increase of 5-HTir caudal to the injury, ipsilateral to the lesion, when compared to control-saline treated SCI (**Figures 4.4**, **4.5** and **4.10**). However, 5-HTir increased rostrally, ipsilateral to the lesion, and decreased contralateral to the lesion (**Figure 3.5**). These results indicate that treatment with minocycline impacts axonal degeneration or at the very least 5-HT levels, even 7-days post-SCI (**Figure 4.4**, **4.5** and **4.10**). However, it did not have as much of an effect as 1-hour post-SCI administration caudal as well as rostral to the lesion (**Figures 4.4**, **4.6** and **4.10**). Without further studies looking into behavioral output, it is difficult to state whether delayed treatment is still beneficial. In early studies, serotonin was found to be implicated in speed, gait, and postural shifts (Hashimoto and Fukuda, 1991, Veasey et al., 1995, Madriaga et al., 2004, Pearlstein et al., 2005, Dai et al., 2005, Jordan et al.,

2008). Therefore, future studies should review different behavioral tests such as open field, ladder rung, and the Basso mouse scale (Basso et al., 2006). Fouad et al. (2010), found that 5-HT fibre sprouting at or above the injury was directly required for locomotion. Indeed, the nulled effect observed in 1-hour administration of minocycline is also not necessarily linked to aiding or hindering locomotion either (**Figures 4.5** and **4.6**). It is important to note that the rostral findings were not predicted to be observed in this thesis, and as a result of these data, although statistically significant may not be biologically significant due to the small differences, and future studies will be required to address this.

5-HT can influence functions in innate and adaptive immunity stimulating monocytes and, indirectly, the secretion of cytokines (Dürk et al., 2005). Krabbe et al. (2012), found mRNA expression of 5-HT_{2A}, 5-HT_{2B}, 5-HT_{3B}, 5-HT_{5A} and 5-HT_{7} within brain microglia. Microglia are important for containing the lesion site in acute injuries (Hines et al., 2009), by surrounding the lesion site itself (Bellver-Landete et al., 2019). Protracted activation of microglia distal to the lesion can cause pain and impede function, in part due to chemokine release (Tan et al., 2008, Hansen et al., 2013, Freria et al., 2017). In the study by Freria et al. (2017), they deleted CX3CR1 gene and found that microglia in CX3XR1-/- mice promoted endogenous repair at and distal to the lesion site. Wildtype microglia and macrophages, once activated with inflammatory stimuli, were less supportive of repair and became more neurotoxic (Kigerl et al., 2009, Gensel et al., 2009, Miron et al., 2013, Kroner et al., 2014, Freria et al., 2017). 5-HT axons sprout, bypassing the lesion site, repopulating gray matter distal from the injury, and are implicated in the spontaneous recovery of locomotor function post-SCI (Schmidt and Jordan, 2000, Murray et al., 2010, Leech et al., 2014, Freria et al., 2017). There is an increase of 5-HT axons around lumbar motor neurons, that arise from local cues that regulate regrowth of 5-HT however, axons post-SCI are inhibited

downstream by signaling of CX3CR1 gene, mentioned above, expression in microglia (Freria et al., 2017). Therefore, I also examined the relative expression of Iba-1ir to motoneurons (Chapter 4). I observed multiple interactions (**Figures 4.7 - 4.9**), which may indicate the influence of Iba-1 positive microglia or macrophages in motoneuronal plasticity post-SCI. Although, the focus of this study surrounded the influence of minocycline treatment on microglia and macrophage activity post-SCI there are other cellular components influenced by the drug. Mast cells commonly found at close contact with the external environment (e.g skin) produce histamine, serotonin, and cytokines like IL-1β and TNF-α among other factors (Skaper and Facci, 2012). Post-SCI astrocytes become reactive through the upregulation of glial fibrillary acidic protein (GFAP), increasing the number of intermediate filaments, appearing larger with more processes (Schwab and Bartholdi, 1996). Within the first week there is an accumulated amount of reactive astrocytes peaking at day 14 post-SCI, still present at day 28, and are responsible for the formation of the scar within the late phase (Schwab and Bartholdi, 1996). Previous studies have shown that inhibition of microglia reduces damage to oligodendrocytes, responsible for remyelination, inhibits axonal dieback, changing the formation of the glial scar itself, suppresses mast cells, improving locomotor function (Stirling et al., 2004, Festoff et al., 2006, Yune et al., 2007, Joks and Durkin, 2011, Zhou et al., 2014). Although the exact mechanism responsible for the increase of 5-HTir observed after treatment with minocycline in this study, likely what is taking place is that the multifaceted minocycline treatment targets many factors, which is not limited to microglia and macrophage activity post-SCI.

5.5 Potential impact of latent minocycline treatment

Neuroinflammation can influence sensory, motor, and autonomic outputs following SCI. Many studies show both the beneficial and detrimental influence of macrophage and microglia

activity (David and Kroner, 2011). Application of macrophages or microglia at the lesion site promotes repair post-SCI (Franzen et al., 1998, Prewitt et al., 1997). Macrophage depletion or inactivation post-SCI has been suggested to increase neuroprotection, and improve motor, sensory, and autonomic function due to increased regeneration (Popovich et al., 1999, McPhail et al., 2004, Stirling et al., 2004). Modification of microglia and macrophage activation appears to be the best approach for treatment post-SCI (Blight, 1992, Jones et al., 2002). Minocycline allows for a more targeted influence on SCI, reducing microglial activation, IL-1β (interleukin-1-beta), and TNF-α, without global depletion of inflammatory cells (Yrjänheikki et al., 1998, Lee et al., 2003, Wells et al., 2003, Stirling et al., 2004, Ahuja et al., 2017). Delayed treatment 7-days post-SCI within this study, cannot be classified as more or less beneficial than 1-hour post-SCI administration based upon my results. We did observe a significant reduction of lesion size when comparing minocycline treatment to control saline administration 7 days post SCI (**Figure 4.12**). However, there was a significant reduction of the lesion size when comparing 1-hour administration of minocycline to 7 days post-SCI (**Figure 4.12**). What can be stated is that treatment 7 days post-SCI still influences 5-HTir caudal to the injury. In addition, axons sprout above the lesion site, forming new connections and utilizing the spared pathways to relay input, which may account for the rostral changes observed in SCI as well as in administration 7 days post-SCI (**Figures 4.3 - 4.4** and **4.10 - 4.11**; Fouad et al., 2001, Bareyre et al., 2004, Vavrek et al., 2006, Courtine et al., 2007, Fouad et al., 2010). I focus on possible motor outputs because of descending serotonergic fiber connections from the raphe obscurus, but dorsal horn innervation by 5-HT on afferent fibres is also affected by SCI. 5-HT receptors are localized on nociceptive primary afferents, while superficial dorsal horn is the principal target for descending serotonergic projections (laminae I and II), the deeper dorsal horn (laminae III-V), is the integration site is for mechanosensory

information as well as the point where input is received from the projections (Millan, 2002). Cragg et al. (2010), found that depletion of spinal 5-HT can, in the case of primary afferent terminals, relieve the descending inhibitory effect, increasing recovery through increased transmission from mechanosensory afferents. In addition, their findings pointed towards a complex role for 5-HT circuits in modulating both sensory and motor function, which may be mediated by intervening molecules and glial cells (Cragg et al., 2010). Furthermore, sensitivity to 5-HT takes place post-SCI. Spasms can result from residual 5-HT within the spinal cord and these levels are important in developing spasticity post-SCI (Harvey et al., 2006, Murray et al., 2010, D'Amico et al., 2014). Furthermore, endogenous 5-HT exposure to motoneurons can lead to intense, prolonged muscle contractions (D'Amico et al., 2014). Therefore, motoneuron and glial cell 5-HT receptor mechanistic interactions are important and must be considered in future studies when minocycline treatments are administered.

What I found is that treatment with minocycline impacts axonal dieback, or at the very least, 5-HT levels, even 7-days post-SCI to a significant extent compared with no treatment (**Figures 4.7**, **4.6** and **4.10**). However, it did not have as much of an effect as 1-hour post-SCI administration caudal and rostral to the lesion (**Figures 4.7**, **4.8** and **4.11**). Therefore, a future study must look into behavioral output, as SCI treatment impacts not only motor output (Schmidt and Jordan, 2000, Murray et al., 2010, Leech et al., 2014), but also sensory relay and pain pathways (Tan et al., 2008, Hansen et al., 2013, Cragg et al., 2010, Freria et al., 2017). In addition, pain, for example, is interpreted differently between males and females (Mogil, 2012). When dealing with drug development studies another important aspect is sexual dimorphism as studies continue to provide insight into these differences as studies incorporate both sexes (Mogil, 2012). We acknowledge that within this study we tailored our SCI model to reportings that males are most at

risk overall (20-29; 70+ years old) for SCI, with a male-to-female ratio of at least 2:1 among adults (WHO, 2013). However, there are categories for sex differences in pain such as toleration of pain, modulation of pain, neurochemical differences and cytokine expression as some examples, which were not addressed within this study (Mogil, 2012). At this point, the mechanism responsible for the observable difference between saline and minocycline treatment is not fully understood.

Further work could examine 5-HTir and Iba-1ir levels using ELISA, for example. Axons sprout above and below the lesion site forming new connections and utilize the spared pathways to relay input, (Carlsson et al., 1963, Hashimoto and Fukuda, 1991, Fouad et al., 2005, Vavrek et al., 2006, Fouad et al., 2010, Jordan et al., 2008, Ghosh et al., 2009, Martinez and Rossignol, 2011, El Manira, 2014, and Filli et al., 2014). We observed a significant reduction in lesion size when comparing treatment of minocycline to saline treatments, which may impact the sprouting above and below the injury site itself. Future work could examine how much recovery is related to 5-HT remodeling while monitoring the lesion size. In addition, by examining Iba-1 levels, in conjunction with CD11b, the role of microglia may be understood better. Macrophages could not be excluded as an inflammatory responder in our SCI model as current Iba-1 markers do not discriminate between microglia and macrophage. 5-HT receptors are localized on nociceptive primary afferents as well as the microglia themselves (Millan, 2002, Hines et al., 2009). Microglial response to 5-HT and fiber changes could also help understand the treatment application paradigm of minocycline post-SCI. There are limitations to staining a neuromodulator as they are localized within vesicles, transported, and bind to receptors as some examples (Schwab and Bartholdi, 1996). There are also limitations to fixing tissue using formaldehyde can affect amino acids, which do not include tryptophan or serotonin (Howat and Wilson, 2014). As discussed earlier these receptors are not limited to neuronal expression, but also glial expression. 5-HT_{2B} receptors, found

on microglia, have been associated with slowing disease progression in lateral sclerosis (El Oussini et al., 2017), 5-HT$_7$ receptors coupled to G$_s$ generates IL-6 (Mahé et al., 2005, Tanaka et al., 2014). Additional analysis looking at protein expression of receptor types present using western blots, targeting Iba-1, Cd11b (microglia), GFAP (astrocyte), OLIG2 or OLIG1 (oligodendrocyte progenitor) expression, would be useful to address how these populations change in conjunction with 5-HT expression. Future experiments could examine tracers in combination with 5-HT immunolabeling to see the double-labeled population and how this dynamically changes post-SCI. Conditional knockdown of receptor subtypes or blockers of serotonin can provide more insight into the connection between increased 5-HTir with minocycline treatment and decrease in Iba-1ir. In addition, there are mouse models, for example, the novel Tmem119-tdTomato reporter mouse for studying microglia in the CNS post-SCI, which is more specific than Iba-1 staining (Ruan et al., 2019), would provide further insight into the role that microglia specifically play within this treatment paradigm. Minocycline will affect more than microglial activity as it reduces the activity of caspases 1 and 3, prevents the synthesis of NO, and reduces glutamate excitotoxicity (Wang et al., 2000, Díaz-Ruiz et al., 2002, Wells et al., 2003).

5.6 Significance

SCI is a devastating condition resulting in 4,259 new cases per year in Canada (INESS, 2010). Descending axons sprout forming new connections post-SCI, and recovery has been linked to brainstem descending axons and corticospinal neurons (Fouad et al., 2005). Following SCI, supraspinal serotonergic projections are severed, resulting in the depletion of 5-HT (Carlsson et al., 1963). 5-HT raphespinal is projections are important as a mediator for locomotion and have been linked to improved recovery of motor function and functional network plasticity (Hashimoto and Fukuda, 1991, Pearlstein et al., 2005, Ghosh and Pearse, 2014, Nardone et al., 2015). Reducing

inflammation has been observed to reduce scarring and promote axonal growth and functional recovery post-SCI (Kotaka et al., 2017). Post-SCI, microglia engage in the upregulation of transcription factors, secreted factors, and immunomodulatory receptors, which causes an increase in inflammation (Noble, 2002, Gaudet and Fonken, 2018). Previous research conducted by Wells et al. (2003), concluded that administration of minocycline 1-hour after injury and thereafter for a total of 7 days caused an increase of motor output, hindlimb function, and strength, and contributed in axonal sparing and reduced the lesion site. By characterizing the role of microglia on neurons post-SCI based upon the established timeline of aim 1, I have supported previous findings that at the lesion site and caudal to the injury, there is a significant reduction of descending fibre 5-HTir (Hashimoto and Fukuda, 1991, Carlsson et al., 1963, Fouad et al., 2005, Jordan et al., 2008, Ghosh and Pearse, 2014). The results from this study in aim 2 and 3, suggest that minocycline administered 1-hour post-SCI and as late as 7 days post-SCI impacts 5-HTir. I observed an increase of 5-HTir in both treatments, with more treatment effects associated with early administration. Increased sprouting can indicate increase motor output, sprouting to form new connections and connectivity improving patient locomotion. What is more likely is that activated microglia exacerbate injury or promote repair depending on the time post-SCI, the lesion severity (ie. contusion, incomplete, hemisection), and location relative to the injury site (Freria et al., 2017).

REFERENCES

Abbas, A. K., Lichtman, A. H. H., & Pillai, S. (2014). *Cellular and Molecular Immunology E-Book*. Elsevier Health Sciences.

Ahuja, C. S., Nori, S., Tetreault, L., Wilson, J., Kwon, B., Harrop, J., … Fehlings, M. G. (2017). Traumatic Spinal Cord Injury-Repair and Regeneration. *Neurosurgery*, *80*(3S), S9–S22.

Alberts, B., Johnson, A., Lewis, J., Raff, M., Roberts, K., & Walter, P. (2002). *Innate Immunity*. Garland Science.

Amin, A. R., Attur, M. G., Thakker, G. D., Patel, P. D., Vyas, P. R., Patel, R. N., … Abramson, S. B. (1996). A novel mechanism of action of tetracyclines: effects on nitric oxide synthases. *Proceedings of the National Academy of Sciences of the United States of America*, *93*(24), 14014–14019.

Azmitia, E. C. (1999). Serotonin neurons, neuroplasticity, and homeostasis of neural tissue. *Neuropsychopharmacology: Official Publication of the American College of Neuropsychopharmacology*, *21*(2 Suppl), 33S – 45S.

Ballermann, M., & Fouad, K. (2006). Spontaneous locomotor recovery in spinal cord injured rats is accompanied by anatomical plasticity of reticulospinal fibers. *The European Journal of Neuroscience*, *23*(8), 1988–1996.

Barbeau, H., Ladouceur, M., Mirbagheri, M. M., & Kearney, R. E. (2002). The effect of locomotor training combined with functional electrical stimulation in chronic spinal cord injured subjects: walking and reflex studies. *Brain Research. Brain Research Reviews*, *40*(1-3), 274–291.

Bareyre, F. M., Kerschensteiner, M., Raineteau, O., Mettenleiter, T. C., Weinmann, O., & Schwab, M. E. (2004). The injured spinal cord spontaneously forms a new intraspinal circuit in adult rats. *Nature Neuroscience*, *7*(3), 269–277.

Beck, K. D., Nguyen, H. X., Galvan, M. D., Salazar, D. L., Woodruff, T. M., & Anderson, A. J. (2010). Quantitative analysis of cellular inflammation after traumatic spinal cord injury: evidence for a multiphasic inflammatory response in the acute to chronic environment. *Brain: A Journal of Neurology*, *133*(Pt 2), 433–447.

Bellver-Landete, V., Bretheau, F., Mailhot, B., Vallières, N., Lessard, M., Janelle, M.-E., … Lacroix, S. (2019). Microglia are an essential component of the neuroprotective scar that forms after spinal cord injury. *Nature Communications*, *10*(1), 518.

Bennett, D. J., Hultborn, H., Fedirchuk, B., & Gorassini, M. (1998). Synaptic activation of plateaus in hindlimb motoneurons of decerebrate cats. *Journal of Neurophysiology*, *80*(4), 2023–2037.

Bethea, J. R., Nagashima, H., Acosta, M. C., Briceno, C., Gomez, F., Marcillo, A. E., … Dietrich, W. D. (1999). Systemically administered interleukin-10 reduces tumor necrosis factor-alpha production and significantly improves functional recovery following traumatic spinal cord injury in rats. *Journal of Neurotrauma*, *16*(10), 851–863.

Blight, A. R. (1983). Axonal physiology of chronic spinal cord injury in the cat: intracellular recording in vitro. *Neuroscience*, *10*(4), 1471–1486.

Blight, A. R. (1992). Macrophages and inflammatory damage in spinal cord injury. *Journal of Neurotrauma*, *9 Suppl 1*, S83–S91.

Bours, M. J. L., Swennen, E. L. R., Di Virgilio, F., Cronstein, B. N., & Dagnelie, P. C. (2006). Adenosine 5’-triphosphate and adenosine as endogenous signaling molecules in immunity and inflammation. *Pharmacology & Therapeutics*, *112*(2), 358–404.

Brundula, V., Rewcastle, N. B., Metz, L. M., Bernard, C. C., & Yong, V. W. (2002). Targeting leukocyte MMPs and transmigration: minocycline as a potential therapy for multiple sclerosis. *Brain: A Journal of Neurology*, *125*(Pt 6), 1297–1308.

Burrows, M. (1996). Neurotransmitters, neuromodulators and neurohormones Neurotransmitters, neuromodulators and neurohormones. In M. Burrows (Ed.), *The Neurobiology of an Insect Brain* (pp. 168–228). Oxford University Press.

Carlsson, A., Magnusson, T., & Rosengren, E. (1963). 5-HYDROXYTRYPTAMINE OF THE SPINAL CORD NORMALLY AND AFTER TRANSECTION. *Experientia*, *19*, 359.

Casha, S., Zygun, D., McGowan, M. D., Bains, I., Yong, V. W., & Hurlbert, R. J. (2012). Results of a phase II placebo-controlled randomized trial of minocycline in acute spinal cord injury. *Brain: A Journal of Neurology*, *135*(Pt 4), 1224–1236.

Chen, M., Ona, V. O., Li, M., Ferrante, R. J., Fink, K. B., Zhu, S., … Friedlander, R. M. (2000). Minocycline inhibits caspase-1 and caspase-3 expression and delays mortality in a transgenic mouse model of Huntington disease. *Nature Medicine*, *6*(7), 797–801.

Cooper, J. R., Bloom, F. E., & Roth, R. H. (2003). *The Biochemical Basis of Neuropharmacology*. Oxford University Press.

Courtine, G., Bunge, M. B., Fawcett, J. W., Grossman, R. G., Kaas, J. H., Lemon, R., … Edgerton, V. R. (2007). Can experiments in nonhuman primates expedite the translation of treatments for spinal cord injury in humans? *Nature Medicine*, *13*(5), 561–566.

Cragg, J. J., Scott, A. L., & Ramer, M. S. (2010). Depletion of spinal 5-HT accelerates mechanosensory recovery in the deafferented rat spinal cord. *Experimental Neurology*, *222*(2), 277–284.

Crutcher, K. A., Gendelman, H. E., Kipnis, J., Perez-Polo, J. R., Perry, V. H., Popovich, P. G., & Weaver, L. C. (2006). Debate: "is increasing neuroinflammation beneficial for neural repair?" *Journal of Neuroimmune Pharmacology: The Official Journal of the Society on NeuroImmune Pharmacology*, *1*(3), 195–211.

Dahlstroem, A., & Fuxe, K. (1965). Evidence for the existence of monoamine neurons in the central nervous system. II. experimentally induced changes in the intraneuronal amine levels of bulbospinal neuron systems. *Acta Physiologica Scandinavica. Supplementum*, SUPPL 247:1–36.

Dai, X., Noga, B. R., Douglas, J. R., & Jordan, L. M. (2005). Localization of spinal neurons activated during locomotion using the c-fos immunohistochemical method. *Journal of Neurophysiology*, *93*(6), 3442–3452.

D'Amico, J. M., Condliffe, E. G., Martins, K. J. B., Bennett, D. J., & Gorassini, M. A. (2014). Recovery of neuronal and network excitability after spinal cord injury and implications for spasticity. *Frontiers in Integrative Neuroscience*, *8*, 36.

David, S., & Kroner, A. (2011). Repertoire of microglial and macrophage responses after spinal cord injury. *Nature Reviews. Neuroscience*, *12*(7), 388–399.

Díaz-Ruiz, A., Ibarra, A., Pérez-Severiano, F., Guízar-Sahagún, G., Grijalva, I., & Ríos, C. (2002). Constitutive and inducible nitric oxide synthase activities after spinal cord contusion in rats. *Neuroscience Letters*, *319*(3), 129–132.

Dürk, T., Panther, E., Müller, T., Sorichter, S., Ferrari, D., Pizzirani, C., … Idzko, M. (2005). 5-Hydroxytryptamine modulates cytokine and chemokine production in LPS-primed human monocytes via stimulation of different 5-HTR subtypes. *International Immunology*, *17*(5), 599–606.

Eggen, B. J. L., Raj, D., Hanisch, U.-K., & Boddeke, H. W. G. M. (2013). Microglial phenotype and adaptation. *Journal of Neuroimmune Pharmacology: The Official Journal of the Society on NeuroImmune Pharmacology*, *8*(4), 807–823.

El Manira, A. (2014). Dynamics and plasticity of spinal locomotor circuits. *Current Opinion in Neurobiology*, *29*, 133–141.

El Oussini, H., Scekic-Zahirovic, J., Vercruysse, P., Marques, C., Dirrig-Grosch, S., Dieterlé, S., … Dupuis, L. (2017). Degeneration of serotonin neurons triggers spasticity in amyotrophic lateral sclerosis. *Annals of Neurology*, *82*(3), 444–456.

Faden, A. I., Gannon, A., & Basbaum, A. I. (1988). Use of serotonin immunocytochemistry as a marker of injury severity after experimental spinal trauma in rats. *Brain Research*, *450*(1-2), 94–100.

Fehlings, M. G., & Tator, C. H. (1995). The relationships among the severity of spinal cord injury, residual neurological function, axon counts, and counts of retrogradely labeled neurons after experimental spinal cord injury. *Experimental Neurology*, *132*(2), 220–228.

Festoff, B. W., Ameenuddin, S., Arnold, P. M., Wong, A., Santacruz, K. S., & Citron, B. A. (2006). Minocycline neuroprotects, reduces microgliosis, and inhibits caspase protease expression early after spinal cord injury. *Journal of Neurochemistry*, *97*(5), 1314–1326.

Filli, L., Engmann, A. K., Zörner, B., Weinmann, O., Moraitis, T., Gullo, M., … Schwab, M. E. (2014). Bridging the gap: a reticulo-propriospinal detour bypassing an incomplete spinal cord injury. *The Journal of Neuroscience: The Official Journal of the Society for Neuroscience*, *34*(40), 13399–13410.

Fouad, K., Pedersen, V., Schwab, M. E., & Brösamle, C. (2001). Cervical sprouting of corticospinal fibers after thoracic spinal cord injury accompanies shifts in evoked motor responses. *Current Biology: CB*, *11*(22), 1766–1770.

Fouad, K., Rank, M. M., Vavrek, R., Murray, K. C., Sanelli, L., & Bennett, D. J. (2010). Locomotion after spinal cord injury depends on constitutive activity in serotonin receptors. *Journal of Neurophysiology*, *104*(6), 2975–2984.

Fouad, K., Schnell, L., Bunge, M. B., Schwab, M. E., Liebscher, T., & Pearse, D. D. (2005). Combining Schwann cell bridges and olfactory-ensheathing glia grafts with chondroitinase promotes locomotor recovery after complete transection of the spinal cord. *The Journal of Neuroscience: The Official Journal of the Society for Neuroscience*, *25*(5), 1169–1178.

Francos-Quijorna, I., Santos-Nogueira, E., Gronert, K., Sullivan, A. B., Kopp, M. A., Brommer, B., … López-Vales, R. (2017). Maresin 1 Promotes Inflammatory Resolution, Neuroprotection, and Functional Neurological Recovery After Spinal Cord Injury. *The Journal of Neuroscience: The Official Journal of the Society for Neuroscience*, *37*(48), 11731–11743.

Franzen, R., Schoenen, J., Leprince, P., Joosten, E., Moonen, G., & Martin, D. (1998). Effects of macrophage transplantation in the injured adult rat spinal cord: a combined immunocytochemical and biochemical study. *Journal of Neuroscience Research*, *51*(3), 316–327.

Freria, C. M., Hall, J. C. E., Wei, P., Guan, Z., McTigue, D. M., & Popovich, P. G. (2017). Deletion of the Fractalkine Receptor, CX3CR1, Improves Endogenous Repair, Axon Sprouting, and Synaptogenesis after Spinal Cord Injury in Mice. *The Journal of Neuroscience: The Official Journal of the Society for Neuroscience*, *37*(13), 3568–3587.

Fuxe, K. (1965). Evidence for the existence of monoamine neurons in the central nervous system. *Zeitschrift Für Zellforschung Und Mikroskopische Anatomie*, *65*(4), 573–596.

Gaudet, A. D., & Fonken, L. K. (2018). Glial Cells Shape Pathology and Repair After Spinal Cord Injury. *Neurotherapeutics: The Journal of the American Society for Experimental NeuroTherapeutics*, *15*(3), 554–577.

Gensel, J. C., Nakamura, S., Guan, Z., van Rooijen, N., Ankeny, D. P., & Popovich, P. G. (2009). Macrophages promote axon regeneration with concurrent neurotoxicity. *The Journal of Neuroscience: The Official Journal of the Society for Neuroscience*, *29*(12), 3956–3968.

Ghosh, A., Sydekum, E., Haiss, F., Peduzzi, S., Zörner, B., Schneider, R., … Schwab, M. E. (2009). Functional and anatomical reorganization of the sensory-motor cortex after incomplete spinal cord injury in adult rats. *The Journal of Neuroscience: The Official Journal of the Society for Neuroscience*, *29*(39), 12210–12219.

Ghosh, M., & Pearse, D. D. (2014). The role of the serotonergic system in locomotor recovery after spinal cord injury. *Frontiers in Neural Circuits*, *8*, 151.

Giulian, D., & Robertson, C. (1990). Inhibition of mononuclear phagocytes reduces ischemic injury in the spinal cord. *Annals of Neurology*, *27*(1), 33–42.

Gladwin, M. T., & Ofori-Acquah, S. F. (2014). [Review of *Erythroid DAMPs drive inflammation in SCD*]. *Blood*, *123*(24), 3689–3690.

Guth, L., Zhang, Z., & Roberts, E. (1994). Key role for pregnenolone in combination therapy that promotes recovery after spinal cord injury. *Proceedings of the National Academy of Sciences of the United States of America*, *91*(25), 12308–12312.

Hansen, C. N., Fisher, L. C., Deibert, R. J., Jakeman, L. B., Zhang, H., Noble-Haeusslein, L., … Basso, D. M. (2013). Elevated MMP-9 in the lumbar cord early after thoracic spinal cord injury impedes motor relearning in mice. *The Journal of Neuroscience: The Official Journal of the Society for Neuroscience*, *33*(32), 13101–13111.

Harrison, M., O'Brien, A., Adams, L., Cowin, G., Ruitenberg, M. J., Sengul, G., & Watson, C. (2013). Vertebral landmarks for the identification of spinal cord segments in the mouse. *NeuroImage*, *68*, 22–29.

Harvey, P. J., Li, X., Li, Y., & Bennett, D. J. (2006). 5-HT2 receptor activation facilitates a persistent sodium current and repetitive firing in spinal motoneurons of rats with and without chronic spinal cord injury. *Journal of Neurophysiology*, *96*(3), 1158–1170.

Hashimoto, T., & Fukuda, N. (1991). Contribution of serotonin neurons to the functional recovery after spinal cord injury in rats. *Brain Research*, *539*(2), 263–270.

Hauben, E., Butovsky, O., Nevo, U., Yoles, E., Moalem, G., Agranov, E., … Schwartz, M. (2000). Passive or active immunization with myelin basic protein promotes recovery from spinal cord contusion. *The Journal of Neuroscience: The Official Journal of the Society for Neuroscience*, *20*(17), 6421–6430.

Hauben, E., Nevo, U., Yoles, E., Moalem, G., Agranov, E., Mor, F., … Schwartz, M. (2000). Autoimmune T cells as potential neuroprotective therapy for spinal cord injury. *The Lancet*, *355*(9200), 286–287.

Heckmann, C. J., Gorassini, M. A., & Bennett, D. J. (2005). Persistent inward currents in motoneuron dendrites: implications for motor output. *Muscle & Nerve*, *31*(2), 135–156.

He, Y., Yu, W., & Baas, P. W. (2002). Microtubule Reconfiguration during Axonal Retraction Induced by Nitric Oxide. *The Journal of Neuroscience: The Official Journal of the Society for Neuroscience*, *22*(14), 5982–5991.

Hines, D. J., Hines, R. M., Mulligan, S. J., & Macvicar, B. A. (2009). Microglia processes block the spread of damage in the brain and require functional chloride channels. *Glia*, *57*(15), 1610–1618.

Hoek, R. M., Ruuls, S. R., Murphy, C. A., Wright, G. J., Goddard, R., Zurawski, S. M., … Sedgwick, J. D. (2000). Down-regulation of the macrophage lineage through interaction with OX2 (CD200). *Science*, *290*(5497), 1768–1771.

Horn, K. P., Busch, S. A., Hawthorne, A. L., van Rooijen, N., & Silver, J. (2008). Another barrier to regeneration in the CNS: activated macrophages induce extensive retraction of dystrophic axons through direct physical interactions. *The Journal of Neuroscience: The Official Journal of the Society for Neuroscience*, *28*(38), 9330–9341.

Houle, J. D., & Ye, J. H. (1999). Survival of chronically-injured neurons can be prolonged by treatment with neurotrophic factors. *Neuroscience*, *94*(3), 929–936.

Hounsgaard, J. (2002). [Review of *Motoneurons do what motoneurons have to do*]. *The Journal of physiology*, *538*(Pt 1), 4.

Hounsgaard, J., Hultborn, H., Jespersen, B., & Kiehn, O. (1988). Bistability of alpha-motoneurones in the decerebrate cat and in the acute spinal cat after intravenous 5-hydroxytryptophan. *The Journal of Physiology*, *405*(1), 345–367.

Howat,

William J., and Beverley A. Wilson. 2014. "Tissue Fixation and the Effect of Molecular Fixatives on Downstream Staining Procedures." *Methods* 70

(1): 12–19.

Husch, A., Van Patten, G. N., Hong, D. N., Scaperotti, M. M., Cramer, N., & Harris-Warrick, R. M. (2012). Spinal cord injury induces serotonin supersensitivity without increasing intrinsic excitability of mouse V2a interneurons. *The Journal of Neuroscience: The Official Journal of the Society for Neuroscience*, *32*(38), 13145–13154.

Joks, Rauno, and Helen G. Durkin. 2011. "Non-Antibiotic Properties of Tetracyclines as Anti-Allergy and Asthma Drugs." *Pharmacological Research: The Official Journal of the Italian Pharmacological Society* 64 (6): 602–9.

Jones, T. B., Basso, D. M., Sodhi, A., Pan, J. Z., Hart, R. P., MacCallum, R. C., … Popovich, P. G. (2002). Pathological CNS autoimmune disease triggered by traumatic spinal cord injury: implications for autoimmune vaccine therapy. *The Journal of Neuroscience: The Official Journal of the Society for Neuroscience*, *22*(7), 2690–2700.

Jordan, L. M., Liu, J., Hedlund, P. B., Akay, T., & Pearson, K. G. (2008). Descending command systems for the initiation of locomotion in mammals. *Brain Research Reviews*, *57*(1), 183–191.

Kigerl, K. A., de Rivero Vaccari, J. P., Dietrich, W. D., Popovich, P. G., & Keane, R. W. (2014). Pattern recognition receptors and central nervous system repair. *Experimental Neurology*, *258*, 5–16.

Kigerl, K. A., Gensel, J. C., Ankeny, D. P., Alexander, J. K., Donnelly, D. J., & Popovich, P. G. (2009). Identification of two distinct macrophage subsets with divergent effects causing either neurotoxicity or regeneration in the injured mouse spinal cord. *The Journal of Neuroscience: The Official Journal of the Society for Neuroscience*, *29*(43), 13435–13444.

Kigerl, K. A., McGaughy, V. M., & Popovich, P. G. (2006). Comparative analysis of lesion development and intraspinal inflammation in four strains of mice following spinal contusion injury. *The Journal of Comparative Neurology*, *494*(4), 578–594.

Kotaka, K., Nagai, J., Hensley, K., & Ohshima, T. (2017). Lanthionine ketimine ester promotes locomotor recovery after spinal cord injury by reducing neuroinflammation and promoting axon growth. *Biochemical and Biophysical Research Communications*, *483*(1), 759–764.

Krabbe, G., Matyash, V., Pannasch, U., Mamer, L., Boddeke, H. W. G. M., & Kettenmann, H. (2012). Activation of serotonin receptors promotes microglial injury-induced motility but attenuates phagocytic activity. *Brain, Behavior, and Immunity*, *26*(3), 419–428.

Kroner, A., Greenhalgh, A. D., Zarruk, J. G., Passos Dos Santos, R., Gaestel, M., & David, S. (2014). TNF and increased intracellular iron alter macrophage polarization to a detrimental M1 phenotype in the injured spinal cord. *Neuron*, *83*(5), 1098–1116.

Kwon, B. K., Okon, E., Hillyer, J., Mann, C., Baptiste, D., Weaver, L. C., … Tetzlaff, W. (2011). A systematic review of non-invasive pharmacologic neuroprotective treatments for acute spinal cord injury. *Journal of Neurotrauma*, *28*(8), 1545–1588.

Leech, K. A., Kinnaird, C. R., & Hornby, T. G. (2014). Effects of serotonergic medications on locomotor performance in humans with incomplete spinal cord injury. *Journal of Neurotrauma*, *31*(15), 1334–1342.

Lee, R. H., & Heckman, C. J. (1998). Bistability in spinal motoneurons in vivo: systematic variations in rhythmic firing patterns. *Journal of Neurophysiology*, *80*(2), 572–582.

Lee, S. M., Yune, T. Y., Kim, S. J., Park, D. W., Lee, Y. K., Kim, Y. C., … Oh, T. H. (2003). Minocycline reduces cell death and improves functional recovery after traumatic spinal cord injury in the rat. *Journal of Neurotrauma*, *20*(10), 1017–1027.

Lee, T. T., Green, B. A., Dietrich, W. D., & Yezierski, R. P. (1999). Neuroprotective effects of basic fibroblast growth factor following spinal cord contusion injury in the rat. *Journal of Neurotrauma*, *16*(5), 347–356.

Li, Q., & Barres, B. A. (2018). Microglia and macrophages in brain homeostasis and disease. *Nature Reviews. Immunology*, *18*(4), 225–242.

Li, Y., & Bennett, D. J. (2003). Persistent sodium and calcium currents cause plateau potentials in motoneurons of chronic spinal rats. *Journal of Neurophysiology*, *90*(2), 857–869.

Madriaga, M. A., McPhee, L. C., Chersa, T., Christie, K. J., & Whelan, P. J. (2004). Modulation of locomotor activity by multiple 5-HT and dopaminergic receptor subtypes in the neonatal mouse spinal cord. *Journal of Neurophysiology*, *92*(3), 1566–1576.

Mahé, C., Loetscher, E., Dev, K. K., Bobirnac, I., Otten, U., & Schoeffter, P. (2005). Serotonin 5-HT7 receptors coupled to induction of interleukin-6 in human microglial MC-3 cells. *Neuropharmacology*, *49*(1), 40–47.

Marlier, L., F. Sandillon, P. Poulat, N. Rajaofetra, M. Geffard, and A. Privat. 1991. "Serotonergic Innervation of the Dorsal Horn of Rat Spinal Cord: Light and Electron Microscopic Immunocytochemical Study." *Journal of Neurocytology* 20 (4): 310–22.

Martinez, M., & Rossignol, S. (2011). Chapter 14 - Changes in CNS structures after spinal cord lesions: implications for BMI. In J. Schouenborg, M. Garwicz, & N. Danielsen (Eds.), *Progress in Brain Research* (Vol. 194, pp. 191–202). Elsevier.

Maxwell, D. J., C. Leranth, and A. A. Verhofstad. 1983. "Fine Structure of Serotonin-Containing Axons in the Marginal Zone of the Rat Spinal Cord." *Brain Research* 266 (2): 253–59.

McPhail, L. T., Stirling, D. P., Tetzlaff, W., Kwiecien, J. M., & Ramer, M. S. (2004). The contribution of activated phagocytes and myelin degeneration to axonal retraction/dieback following spinal cord injury. *The European Journal of Neuroscience*, *20*(8), 1984–1994.

Millan, M. J. (2002). Descending control of pain. *Progress in Neurobiology*, *66*(6), 355–474.

Miron, V. E., Boyd, A., Zhao, J.-W., Yuen, T. J., Ruckh, J. M., Shadrach, J. L., … French-Constant, C. (2013). M2 microglia and macrophages drive oligodendrocyte differentiation during CNS remyelination. *Nature Neuroscience*, *16*(9), 1211–1218.

Moalem, G., Leibowitz-Amit, R., Yoles, E., Mor, F., Cohen, I. R., & Schwartz, M. (1999). Autoimmune T cells protect neurons from secondary degeneration after central nervous system axotomy. *Nature Medicine*, *5*(1), 49–55.

Mogil, Jeffrey S. 2012. "Sex Differences in Pain and Pain Inhibition: Multiple Explanations of a Controversial Phenomenon." *Nature Reviews. Neuroscience* 13 (12): 859–66.

Murray, K. C., Nakae, A., Stephens, M. J., Rank, M., D'Amico, J., Harvey, P. J., … Fouad, K. (2010). Recovery of motoneuron and locomotor function after spinal cord injury depends on constitutive activity in 5-HT2C receptors. *Nature Medicine*, *16*(6), 694–700.

Nardone, R., Höller, Y., Thomschewski, A., Höller, P., Lochner, P., Golaszewski, S., … Trinka, E. (2015). Serotonergic transmission after spinal cord injury. *Journal of Neural Transmission* , *122*(2), 279–295.

Noble, L. J., & Wrathall, J. R. (1989). Correlative analyses of lesion development and functional status after graded spinal cord contusive injuries in the rat. *Experimental Neurology*, *103*(1), 34–40.

Noble, P. W. (2002). Hyaluronan and its catabolic products in tissue injury and repair. *Matrix Biology: Journal of the International Society for Matrix Biology*, *21*(1), 25–29.

Oudega, M., Vargas, C. G., Weber, A. B., Kleitman, N., & Bunge, M. B. (1999). Long-term effects of methylprednisolone following transection of adult rat spinal cord. *The European Journal of Neuroscience*, *11*(7), 2453–2464.

Pajoohesh-Ganji, A., & Byrnes, K. R. (2011). Novel neuroinflammatory targets in the chronically injured spinal cord. *Neurotherapeutics: The Journal of the American Society for Experimental NeuroTherapeutics*, *8*(2), 195–205.

Paolicelli, R. C., Bolasco, G., Pagani, F., Maggi, L., Scianni, M., Panzanelli, P., … Gross, C. T. (2011). Synaptic pruning by microglia is necessary for normal brain development. *Science*, *333*(6048), 1456–1458.

Pearlstein, E., Ben Mabrouk, F., Pflieger, J. F., & Vinay, L. (2005). Serotonin refines the locomotor-related alternations in the in vitro neonatal rat spinal cord. *The European Journal of Neuroscience*, *21*(5), 1338–1346.

Perrier, J.-F., & Hounsgaard, J. (2003). 5-HT2 receptors promote plateau potentials in turtle spinal motoneurons by facilitating an L-type calcium current. *Journal of Neurophysiology*, *89*(2), 954–959

Plemel, J. R., Wee Yong, V., & Stirling, D. P. (2014). Immune modulatory therapies for spinal cord injury--past, present and future. *Experimental Neurology*, *258*, 91–104.

Popovich, P. G., Guan, Z., Wei, P., Huitinga, I., van Rooijen, N., & Stokes, B. T. (1999). Depletion of hematogenous macrophages promotes partial hindlimb recovery and neuroanatomical repair after experimental spinal cord injury. *Experimental Neurology*, *158*(2), 351–365.

Popovich, P. G., & Wei P And Stokes. (1998). Cellular Inflammatory Response After Spinal Cord Injury in Sprague-Dawley and Lewis Rats. *Journal of Comparative Neurology*, *377*, 443–464.

Prewitt, C. M., Niesman, I. R., Kane, C. J., & Houlé, J. D. (1997). Activated macrophage/microglial cells can promote the regeneration of sensory axons into the injured spinal cord. *Experimental Neurology*, *148*(2), 433–443.

Prüss, H., Kopp, M. A., Brommer, B., Gatzemeier, N., Laginha, I., Dirnagl, U., & Schwab, J. M. (2011). Non-resolving aspects of acute inflammation after spinal cord injury (SCI): indices and resolution plateau. *Brain Pathology* , *21*(6), 652–660.

Rabchevsky, A. G., & Streit, W. J. (1997). Grafting of cultured microglial cells into the lesioned spinal cord of adult rats enhances neurite outgrowth. *Journal of Neuroscience Research*, *47*(1), 34–48.

Raineteau, O., & Schwab, M. E. (2001). Plasticity of motor systems after incomplete spinal cord injury. *Nature Reviews. Neuroscience*, *2*(4), 263–273.

Ransohoff, R. M., & Perry, V. H. (2009). Microglial physiology: unique stimuli, specialized responses. *Annual Review of Immunology*, *27*, 119–145.

Rapalino, O., Lazarov-Spiegler, O., Agranov, E., Velan, G. J., Yoles, E., Fraidakis, M., … Schwartz, M. (1998). Implantation of stimulated homologous macrophages results in partial recovery of paraplegic rats. *Nature Medicine*, *4*(7), 814–821.

(Rick Hansen Institute and Urban Futures). (2010). *The Incidence and Prevalence of Spinal Cord Injury in Canada Overview and estimates based on current evidence*. Retrieved from http://fecst.inesss.qc.ca/fileadmin/documents/photos/LincidenceetlaprevalencedestraumamedullaireauCanada.pdf

Rossignol, S., Dubuc, R., & Gossard, J.-P. (2006). Dynamic sensorimotor interactions in locomotion. *Physiological Reviews*, *86*(1), 89–154.

Rossignol, S., & Frigon, A. (2011). Recovery of locomotion after spinal cord injury: some facts and mechanisms. *Annual Review of Neuroscience*, *34*, 413–440.

Ruan, Chunsheng, Linlin Sun, Alexandra Kroshilina, Lien Beckers, Philip De Jager, Elizabeth M. Bradshaw, Samuel A. Hasson, Guang Yang, and Wassim Elyaman. 2019. "A Novel Tmem119-tdTomato Reporter Mouse Model for Studying Microglia in the Central Nervous System." *Brain, Behavior, and Immunity*, October. https://doi.org/10.1016/j.bbi.2019.10.009.

Sanchez Mejia, R. O., Ona, V. O., Li, M., & Friedlander, R. M. (2001). Minocycline reduces traumatic brain injury-mediated caspase-1 activation, tissue damage, and neurological dysfunction. *Neurosurgery*, *48*(6), 1393–1399; discussion 1399–1401.

Schmidt, B. J., & Jordan, L. M. (2000). The role of serotonin in reflex modulation and locomotor rhythm production in the mammalian spinal cord. *Brain Research Bulletin*, *53*(5), 689–710.

Schwab, M. E., & Bartholdi, D. (1996). Degeneration and regeneration of axons in the lesioned spinal cord. *Physiological Reviews*, *76*(2), 319–370.

Serhan, C. N. (2007). Resolution phase of inflammation: novel endogenous anti-inflammatory and proresolving lipid mediators and pathways. *Annual Review of Immunology*, *25*, 101–137.

Silver, J., Schwab, M. E., & Popovich, P. G. (2014). Central nervous system regenerative failure: role of oligodendrocytes, astrocytes, and microglia. *Cold Spring Harbor Perspectives in Biology*, *7*(3), a020602.

Skaper, Stephen D., and Laura Facci. 2012. "Mast Cell-Glia Axis in Neuroinflammation and Therapeutic Potential of the Anandamide Congener Palmitoylethanolamide." *Philosophical Transactions of the Royal Society of London. Series B, Biological Sciences* 367 (1607): 3312–25.

Spinal cord injury. (n.d.). Retrieved April 24, 2019, from https://www.who.int/news-room/fact-sheets/detail/spinal-cord-injury

Springer, J. E., Azbill, R. D., & Knapp, P. E. (1999). Activation of the caspase-3 apoptotic cascade in traumatic spinal cord injury. *Nature Medicine*, *5*(8), 943–946.

Stevens, B., Allen, N. J., Vazquez, L. E., Howell, G. R., Christopherson, K. S., Nouri, N., … Barres, B. A. (2007). The classical complement cascade mediates CNS synapse elimination. *Cell*, *131*(6), 1164–1178.

Stirling, D. P., Khodarahmi, K., Liu, J., McPhail, L. T., McBride, C. B., Steeves, J. D., … Tetzlaff, W. (2004). Minocycline treatment reduces delayed oligodendrocyte death, attenuates axonal dieback, and improves functional outcome after spinal cord injury. *The Journal of Neuroscience: The Official Journal of the Society for Neuroscience*, *24*(9), 2182–2190.

Stirling, D. P., & Yong, V. W. (2008). Dynamics of the inflammatory response after murine spinal cord injury revealed by flow cytometry. *Journal of Neuroscience Research*, *86*(9), 1944–1958.

Tan, A. M., Stamboulian, S., Chang, Y.-W., Zhao, P., Hains, A. B., Waxman, S. G., & Hains, B. C. (2008). Neuropathic pain memory is maintained by Rac1-regulated dendritic spine remodeling

after spinal cord injury. *The Journal of Neuroscience: The Official Journal of the Society for Neuroscience*, *28*(49), 13173–13183.

Tanaka, T., Narazaki, M., & Kishimoto, T. (2014). IL-6 in inflammation, immunity, and disease. *Cold Spring Harbor Perspectives in Biology*, *6*(10), a016295.

Teng, Y. D., Choi, H., Onario, R. C., Zhu, S., Desilets, F. C., Lan, S., … Friedlander, R. M. (2004). Minocycline inhibits contusion-triggered mitochondrial cytochrome c release and mitigates functional deficits after spinal cord injury. *Proceedings of the National Academy of Sciences of the United States of America*, *101*(9), 3071–3076.

Thomas, S. L., & Gorassini, M. A. (2005). Increases in corticospinal tract function by treadmill training after incomplete spinal cord injury. *Journal of Neurophysiology*, *94*(4), 2844–2855.

Tikka, T. M., & Koistinaho, J. E. (2001). Minocycline provides neuroprotection against N-methyl-D-aspartate neurotoxicity by inhibiting microglia. *Journal of Immunology* , *166*(12), 7527–7533.

Ung, R.-V., Landry, E. S., Rouleau, P., Lapointe, N. P., Rouillard, C., & Guertin, P. A. (2008). Role of spinal 5-HT2 receptor subtypes in quipazine-induced hindlimb movements after a low-thoracic spinal cord transection. *The European Journal of Neuroscience*, *28*(11), 2231–2242.

Vavrek, R., Girgis, J., Tetzlaff, W., Hiebert, G. W., & Fouad, K. (2006). BDNF promotes connections of corticospinal neurons onto spared descending interneurons in spinal cord injured rats. *Brain: A Journal of Neurology*, *129*(Pt 6), 1534–1545.

Veasey, S. C., C. A. Fornal, C. W. Metzler, and B. L. Jacobs. 1995. “Response of Serotonergic Caudal Raphe Neurons in Relation to Specific Motor Activities in Freely Moving Cats.” *The Journal of Neuroscience: The Official Journal of the Society for Neuroscience* 15 (7 Pt 2): 5346–59.

Wang, X., Jung, J., Asahi, M., Chwang, W., Russo, L., Moskowitz, M. A., … Lo, E. H. (2000). Effects of matrix metalloproteinase-9 gene knock-out on morphological and motor outcomes after traumatic brain injury. *The Journal of Neuroscience: The Official Journal of the Society for Neuroscience*, *20*(18), 7037–7042.

Wang, X., Zhu, S., Drozda, M., Zhang, W., Stavrovskaya, I. G., Cattaneo, E., … Friedlander, R. M. (2003). Minocycline inhibits caspase-independent and -dependent mitochondrial cell death pathways in models of Huntington's disease. *Proceedings of the National Academy of Sciences of the United States of America*, *100*(18), 10483–10487.

Watson C., Paxinos G., & Kayalinoglu. (2008). The spinal cord (1st ed), *Academic Press, 1-408*

Weidner, N., Ner, A., Salimi, N., & Tuszynski, M. H. (2001). Spontaneous corticospinal axonal plasticity and functional recovery after adult central nervous system injury. *Proceedings of the National Academy of Sciences of the United States of America*, *98*(6), 3513–3518.

Wells, J. E. A., Hurlbert, R. J., Fehlings, M. G., & Yong, V. W. (2003). Neuroprotection by minocycline facilitates significant recovery from spinal cord injury in mice. *Brain: A Journal of Neurology*, *126*(Pt 7), 1628–1637.

Yin, Y., Henzl, M. T., Lorber, B., Nakazawa, T., Thomas, T. T., Jiang, F., … Benowitz, L. I. (2006). Oncomodulin is a macrophage-derived signal for axon regeneration in retinal ganglion cells. *Nature Neuroscience*, *9*(6), 843–852.

Yong, V. Wee, Jennifer Wells, Fabrizio Giuliani, Steven Casha, Christopher Power, and Luanne M. Metz. 2004. "The Promise of Minocycline in Neurology." *Lancet Neurology* 3 (12): 744–51.

Yrjänheikki, J., Keinänen, R., Pellikka, M., Hökfelt, T., & Koistinaho, J. (1998). Tetracyclines inhibit microglial activation and are neuroprotective in global brain ischemia. *Proceedings of the National Academy of Sciences of the United States of America*, *95*(26), 15769–15774

Yune, T. Y., Lee, J. Y., Jung, G. Y., Kim, S. J., Jiang, M. H., Kim, Y. C., … Oh, T. H. (2007). Minocycline alleviates death of oligodendrocytes by inhibiting pro-nerve growth factor production in microglia after spinal cord injury. *The Journal of Neuroscience: The Official Journal of the Society for Neuroscience*, *27*(29), 7751–7761.

Zhou, Xiang, Xijing He, and Yi Ren. 2014. "Function of Microglia and Macrophages in Secondary Damage after Spinal Cord Injury." *Neural Regeneration Research*, 9 (20): 1787–95.